

Université de Montréal

Molécules anti-facteurs de virulence : étude de l'efficacité et de l'amélioration d'une molécule inhibitrice du système de sécrétion de type IV de *Helicobacter pylori*

Par Claire Morin

Département de biochimie et Médecine moléculaire, Faculté de Médecine

Thèse réalisée en cotutelle avec Christian Baron, présentée en vue de l'obtention du grade de
Docteurat en Biochimie et Médecine Moléculaire

Aout 2023

Université de Montréal

Département de biochimie et Médecine moléculaire, Faculté de Médecine

Ce mémoire intitulé

Molécules anti-facteurs de virulence : étude de l'efficacité et de l'amélioration
d'une molécule inhibitrice du système de sécrétion de type IV de *Helicobacter*
pylori

Présenté par

Claire Morin

A été évalué par un jury composé des personnes suivantes

Nathalie Grandvaux

Président-rapporteur

Christian Baron

Directeur de recherche

Marylise Duperthuy

Membre du jury

Carole Creuzenet

Examineur externe

Frédéric A. Mallette

Représentant du doyen

Table des matières

Résumé	5
Abstract	7
Abréviations	9
I. Introduction	11
<i>A. Helicobacter pylori</i>	11
i. Une bactérie isolée de biopsies gastriques	11
ii. Une bactérie responsable d'une inflammation chronique de l'estomac	12
iii. <i>H. pylori</i> est impliqué dans les maladies gastriques sévères	13
iv. Une bactérie capable de coloniser l'estomac de l'hôte	14
v. Le système de sécrétion de type 4 : une seringue impliquée dans la translocation d'une oncoprotéine bactériale	17
<i>B. Campagne d'éradication de H. pylori</i>	21
i. Prévalence de <i>H. pylori</i> dans le monde	21
ii. Hypothèse de la bactérie commensale	21
iii. Traitement d'éradication de <i>H. pylori</i>	23
iv. Résistance aux antibiotiques : un problème global	25
<i>C. Nouvelles approches pour les traitements des infections à H. pylori</i>	25
i. Développement de vaccins	25
ii. L'utilisation des phages	26
iii. Recherche de nouvelles sources de traitement via les remèdes ancestraux	27
<i>D. Problématique de thèse.</i>	27
II. Justification de la méthodologie	30

<i>A. Etude in vitro</i>	30
i. Mutation dirigée et purification de protéines	30
ii. Fluorimétrie différentielle à balayage (<i>Differential Scanning Fluorimetry :DSF</i>)	30
iii. Test de l'activité ATPase	30
<i>B. Etudes sur modèle d'infection cellulaire</i>	31
i. Modèle d'infection cellulaire	31
ii. Quantification des IL-8 par test ELISA	31
iii. Observation des protéines Cag par Western Blot	31
iv. Visualisation du SST4 par microscopie électronique	31
III. Publications	32
<i>A. Papier #1 : Inhibition du système de sécrétion de type IV des isolats cliniques d'Helicobacter pylori résistants aux antibiotiques soutient le potentiel de CagA en tant que cible anti-virulence.</i>	32
i. Abstract	33
ii. Introduction	34
iii. Materials and Methods	37
iv. Results	40
v. Discussion	48
vi. Study materials	50
vii. Funding and Acknowledgments:	50
viii. Declaration of interests:	50
ix. Author contributions:	50
x. References	51
xi. Tables	57
xii. Supplementary materials	59
<i>B. Papier #2 : Conception basée sur la structure de petits inhibiteurs de molécules de l'ATPase CagA du système de sécrétion de type IV (cagT4SS) d'Helicobacter pylori.</i>	66

i. Abstract	67
ii. Introduction	68
iii. Materials and Methods	70
iv. Results	76
v. Discussion	89
vi. Acknowledgements	91
vii. Author Contributions	91
viii. References	93
ix. Supplementary information	101
IV. Conclusion et discussion	117
V. Références	122
Remerciements	140
Sources et Permission d'utilisation des figures	141
<i>A. Figure 1</i>	<i>141</i>
<i>B. Figure 3</i>	<i>141</i>
<i>C. Figure 4</i>	<i>141</i>

Résumé

Helicobacter pylori est une bactérie à Gram négatif qui colonise plus de 50% de la population humaine. Cette bactérie est l'un des pathogènes les plus présents dans la population et la colonisation se fait dans l'enfance et l'adolescence. *H. pylori* est responsable de l'apparition de maladies gastriques chez l'humain comme des ulcères gastriques, mais aussi des cancers gastriques. Plusieurs mécanismes contribuent aux maladies gastriques dont une infection chronique à long terme ainsi que des facteurs de virulence comme le système de sécrétion de type 4 (SST4). Le SST4 forme une seringue protéique utilisée par la bactérie pour injecter la protéine CagA dans les cellules humaines. Cette protéine a été la première protéine bactérienne classifiée comme une oncoprotéine par sa capacité à interférer et modifier de nombreuses fonctions et signaux métaboliques des cellules épithéliales gastriques. Afin d'éradiquer *Helicobacter*, une antibiothérapie est utilisée, cependant depuis les 10 dernières années plus de 50% des bactéries isolées de patients ont été identifiées comme étant porteuses de résistances contre aux moins un antibiotique de première ligne. L'utilisation de petites molécules organiques capables d'interférer avec les facteurs de virulence est une alternative intéressante à la thérapie aux antibiotiques. L'utilisation de ces molécules possède des avantages dont la faible pression de sélection de résistance parce qu'elles n'impactent pas des fonctions vitales des bactéries.

Le SST4 de *H. pylori* est composé de nombreuses protéines essentielles qui pourraient être de potentielles cibles pour des molécules inhibitrices. Nous avons choisi la cible Cag α , une ATPase homologue à VirB11 de *Agrobacterium tumefaciens*. Cette protéine est essentielle pour l'injection de CagA. Précédemment, notre laboratoire a identifié une petite molécule nommée 1G2 qui était capable d'interagir avec Cag α et de diminuer l'induction de l'interleukine 8 produit par les cellules gastriques lors de l'infection par des souches de *H. pylori* possédant un SST4 fonctionnel. A partir d'une structure cristallographique de Cag α liée à 1G2 et nous avons créé des protéines Cag α avec des mutations aux site de liaison de 1G2. En utilisant la fluorimétrie différentielle à balayage (DSF) nous avons pu identifier les acides aminés qui contribuent à la liaison de 1G2 (K41, R73 et F39). Basé sur cette information nous avons utilisé la chimie médicinale pour créer une librairie de molécules dérivées de 1G2 dans le but d'identifier des inhibiteurs plus puissants. Après avoir

éliminé les molécules ayant un effet toxique sur les cellules gastriques et *H. pylori*, nous avons sélectionné cinq molécules (1313, 1338, 2886, 2889 et 2902) qui inhibent la production d'IL-8 plus que 1G2 dans notre modèle d'infection cellulaire. Nous avons montré par DSF que les molécules interagissent toujours avec Cag α et 1338, 2889 et 2902 sont des inhibiteurs plus puissants de son activité d'ATPase. Avec le modèle d'infection, nous avons déterminé que les cinq molécules n'affectent pas la présence de CagA dans le lysat de l'infection. Cependant, nous avons observé par microscopie électronique à balayage que le SST4 pilus n'était pas présent en présence des inhibiteurs. En plus, nous avons testé les effets de 1G2 sur des souches de *H. pylori* résistantes, à un ou plusieurs antibiotiques de première ligne, isolées de biopsie gastriques de patients. Comme dans le cas de la bactérie modèle de laboratoire, nous avons observé une diminution de l'induction des IL-8 lors de l'infection ainsi qu'une inhibition de la formation du SST4 pilus. Nous avons aussi identifié que le gène de la protéine Cag α d'une des bactéries résistantes à 1G2 (souche #3822) porte un remplacement de R73 à K ce qui pourrait expliquer la résistance à 1G2.

Pour conclure, nous avons dans cette étude caractérisé le site de liaison de 1G2 à Cag α et nous avons identifié des molécules qui sont plus puissantes comme inhibiteurs que 1G2.

Mots clé : *Helicobacter pylori*, cagPAI, Cag α , VirB11, ATPase, anti-virulence, système de sécrétion de type IV, pili, inhibiteurs

Abstract

Helicobacter pylori is a Gram-negative bacterium that colonizes more than 50% of the human population. This bacterium is one of the most common pathogens in the population and colonization occurs in childhood and adolescence. *H. pylori* is implicated in the manifestation of gastric diseases in humans such as gastric ulcers and also gastric cancer. Several mechanisms are involved in the formation of gastric diseases including long-term chronic infection as well as virulence factors such as the type 4 secretion system (T4SS). The T4SS forms a protein syringe used by the bacteria to inject the protein CagA into mammalian cells. This protein is the first bacterial protein classified as an oncoprotein by its ability to interact with numerous metabolic functions of gastric epithelial cells. To eradicate *Helicobacter*, antibiotic therapy is used, but for the last 10 years more than 50% of the bacteria isolated from patients have been identified as carrying resistance against at least one first-line antibiotic. The use of small molecules capable of interfering with virulence factors is being studied as an alternative to antibiotic therapy. The use of these molecules has many advantages, and they may cause lower selection pressure for resistance than antibiotics.

The *H. pylori* T4SS is composed of many essential proteins that could be potential targets for inhibitory molecules. We chose the target Cag α , an ATPase homologous to the model VirB11 from *Agrobacterium tumefaciens*. This protein is essential for the injection of CagA. Previously, our laboratory identified a small molecule coined 1G2 that interacts with Cag α and decreases the induction of interleukin-8 produced by gastric cells upon infection with *H. pylori* strains with functional T4SS. Based on a crystallographic study of Cag α bound to 1G2, we created Cag α proteins with mutations at the 1G2 binding site. Using differential scanning fluorimetry, we identified amino acids that contribute to 1G2 binding (K41, R73 and F39). Based on these observations, we used medicinal chemistry to create a library of molecules derived from 1G2 to create more potent inhibitors. After eliminating the molecules with a toxic effect on gastric cells and *H. pylori* growth, we selected five molecules with stronger effects than 1G2 on IL8 induction in our cell infection model (1313, 1338, 2886, 2889 and 2902). We observed by DSF that the molecules interact with Cag α and 1338, 2889 and 2902 are stronger inhibitors of the ATPase

activity than 1G2. With our infection model, we determined that the five molecules do not affect the presence of CagA. However, by scanning electron microscopy we observed that the T4SS pilus was not present. In addition to the tests on a laboratory model bacterium, we evaluated 1G2 on resistant strains of *H. pylori* isolated from gastric biopsy from patients. Similar to the laboratory model bacterium, 1G2 decreased IL-8 induction and inhibited T4SS pilus formation. We have also identified that strain #3822 that is resistant to 1G2 carries a R73 to K mutation in the Cag α gene, which could explain the 1G2 resistance.

To conclude, we have here characterized the 1G2 binding site on Cag α and we created inhibitors that are more potent than 1G2.

Keywords: *Helicobacter pylori*, cagPAI, Cag α , VirB11, ATPase, anti-virulence, type IV secretion system, pili, inhibitors

Abréviations

Helicobacter pylori: *H. pylori*

MCPs: *methyl-accepting chemotaxis proteins*

VacA: *vacuolating cytotoxin A*

Lymphocytes T : LT

Lymphocytes B : LB

Système de sécrétion du type 4 : SST4

ADN: acide désoxyribonucléique

cag: *cytotoxin-associated gene*

cagPAI: *cytotoxin-associated gene pathogenicity island*

Motif EPIYA: motif Glu-Pro-Ile-Tyr-Ala

Crk: *CT10 regulator of kinase*

PI3K: *phosphoinositide 3-kinase*

MAPK: *mitogen-activated protein kinases*

ATP: Adénosine triphosphate

ATPase : Adénosine triphosphate hydrolase

LPS : lipopolysaccharide

IL-1 β : interleukine-1 bêta

TNF- α : facteur de nécrose tumorale alpha

IL-8 : interleukine-8

ROS : *reactive oxygen species*

RNS : *reactive nitrogen species*

COX-2 : cyclooxygenase-2

iNOS : *inducible nitric oxide synthase*

IPP : inhibiteurs de la pompe à protons

C : clarithromycine

A : amoxicilline

M : métronidazole

T : tétracycline

PME : protéines de la membrane externe

PCR : *polymerase chain reaction*, réaction en chaîne par polymérase

SEM : *scanning electron microscopy*, microscopie électronique à balayage

DSF : *differential scanning fluorimetry*, Fluorimétrie différentielle à balayage

F : phénylalanine

K: lysine

R: arginine

ELISA: *enzyme-linked immunosorbent assay*

Cryo-EM: *cryo electron microscopy*

Cryo-TEM: *cryo transmission electron microscopy*

DMF: *Dimethylformamide*

LCMS: *liquid chromatography mass spectrometry*

Cryo-TEM : microscopie électronique en transmission cryogénique

I. Introduction

A. Helicobacter pylori

i. Une bactérie isolée de biopsies gastriques

Pendant des siècles, il était largement considéré que l'estomac était stérile dû à sa forte acidité. Cependant, dans les années 80, Warren et Marshall, ont réussi à isoler une bactérie à partir de biopsies gastriques. Cette bactérie appelée *Helicobacter pylori*, a été identifiée comme étant capable de coloniser l'estomac de façon durable. Warren et Marshall ont aussi démontré que *H. pylori* était impliquée dans l'apparition d'ulcères gastriques (1). Aujourd'hui, *H. pylori* est reconnue pour son implication dans l'apparition des maladies gastriques sévères comme les ulcères, mais aussi différents types cancers gastriques (2).

Depuis sa découverte, *H. pylori* a été caractérisée comme étant une bactérie à Gram négative faisant partie du phylum des *Proteobacteria*, de la classe des *Epsilonproteobacteria*, de l'ordre des *Campylobacterales*, de la famille des *Helicobacteraceae* et du genre *Helicobacter*. *H. pylori* possède une forme hélicoïdale d'environ 4 micromètres de longueur (**figure 1 A**) présentant quatre flagelles au pôle lui permettant de pénétrer le mucus gastrique grâce à sa forme hélicoïdale.

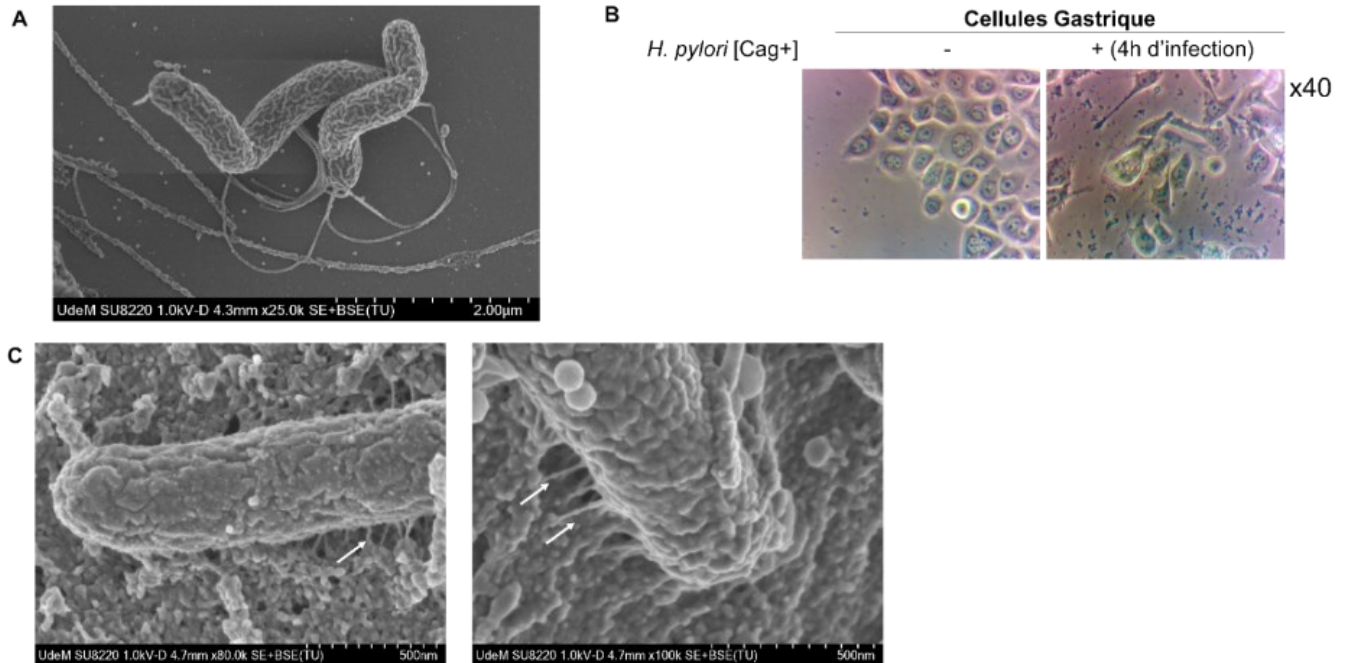


Figure 1 : Morphologie et image de microscopie de *Helicobacter pylori*.

A) Image de microscopie électronique à balayage de la souche sauvage de laboratoire de *H. pylori* 26695, B) image de microscopie confocale de cellules gastriques humaines (AGS) avant et après infection avec la souche 26695, C) Image de microscopie électronique à balayage de cellules AGS infectées par la souche 26695, les cagSST4 pili sont indiqués par des flèches blanches

ii. Une bactérie responsable d'une inflammation chronique de l'estomac

Malgré sa capacité à résister au système immunitaire de l'hôte, *H. pylori* induit une inflammation des tissus gastriques, qui devient chronique si l'infection n'est pas traitée. Au début de l'infection, l'immunité innée est activée avec la prolifération des neutrophiles, macrophages et cellules dendritiques après la reconnaissance de lipopolysaccharide (LPS) et des flagelles de *H. pylori*. Dans le même temps, des cytokines pro-inflammatoires telles que l'interleukine-1 bêta (IL-1 β), le facteur de nécrose tumorale alpha (TNF- α) et l'interleukine-8 (IL-8) sont sécrétées. Après l'activation de la réponse immunitaire innée, la réponse adaptative est déclenchée. La production des cellules spécifiques comme les lymphocytes B (LB) et T (LT) qui vont reconnaître

spécifiquement *H. pylori* se met en place ainsi que la production d'anticorps qui reconnaissent les protéines de la surface de *H. pylori*, CagA ou encore les flagellines (3–6). Malgré les différents mécanismes immunitaires mis en place par les cellules hôtes, *H. pylori* a pu s'adapter et créer des mécanismes d'échappement au système immunitaire. Par exemple, *H. pylori* est capable de modifier ses récepteurs membranaires, comme les lipides A des LPS, afin qu'ils ne soient pas reconnus par les anticorps (7–9). Cette capacité à échapper au système immunitaire entraîne une constante inflammation des tissus gastriques générant une inflammation chronique.

iii. *H. pylori* est impliqué dans les maladies gastriques sévères

a. *Les maladies gastriques communes causées par Helicobacter pylori*

La colonisation par *H. pylori* induit une inflammation chronique chez les individus. Il est maintenant bien établi qu'une inflammation chronique sur le long terme peut aboutir au développement de cancer (10). La colonisation de l'estomac par *H. pylori* conduit au développement de gastrites asymptomatiques ou symptomatiques. Il s'agit d'une inflammation des tissus gastriques causant un inconfort notable jusqu'à des vomissements et saignements (11).

La gastrite peut se développer en ulcère gastrique dont l'origine est un affaiblissement de la protection de la paroi gastrique. Cela entraîne une plus forte sensibilité aux acides gastriques générant des dommages et lésions des tissus (12). Dans les cas les plus graves, l'infection par *H. pylori* est impliquée dans l'apparition de cancers gastriques.

b. *L'implication de H. pylori dans l'apparition du cancer de l'estomac*

En Amérique du Nord, la prévalence de *H. pylori* est plus faible qu'en Asie de l'Est et les cas de cancer de l'estomac sont aussi moins courants (13). Cependant, le cancer de l'estomac est le 3ème cancer le plus mortel, en raison d'un diagnostic le plus souvent tardif (14–16). L'infection à *H. pylori* mène à une inflammation chronique qui sur le long terme et endommage sévèrement de la muqueuse gastrique.

Un des effets d'une inflammation chronique est l'induction de dommages de l'ADN. En effet, l'infection par *H. pylori* induit la production de ROS (*reactive oxygen species*) et RNS (*reactive nitrogen species*) engendrant un stress oxydatif dans les cellules gastriques. Une expression excessive ainsi qu'une exposition prolongée des cellules aux ROS et RNS lors de l'infection à *H. pylori*, est connu pour provoquer des cassures de l'ADN, des modifications de bases ou encore des réticulations de l'ADN (17,18). Lors de la réponse immunitaire adaptative, des cytokines pro-inflammatoires sont produites. L'induction des cytokines pro-inflammatoires a aussi un effet négatif sur l'ADN car leur activation entraîne également la production d'enzymes capables d'endommager l'ADN comme les COX-2 (cyclooxygenase-2) ou encore les iNOS (*inducible nitric oxide synthase*) (5,18).

En plus de l'inflammation chronique induite par *H. pylori*, l'implication des facteurs de virulence joue un rôle majeur dans l'évolution des gastrites. CagA interagit avec de nombreuses voies métaboliques entraînant une désorganisation des cellules épithéliales gastriques (19,20), déclenche une dépolarisation des cellules épithéliales, la perte de l'adhésion entre cellules, une augmentation de leur mobilité ainsi qu'une régulation de l'apoptose. Tous ces mécanismes entraînent une prolifération incontrôlée des cellules épithéliales, créant des tumeurs qui peuvent évoluer en cancer (7,21).

iv. Une bactérie capable de coloniser l'estomac de l'hôte

H. pylori utilise de nombreux mécanismes afin de coloniser l'estomac et de s'établir de façon durable. *H. pylori* possède un grand nombre de facteurs de virulence utilisés à différents stades de l'infection et encore aujourd'hui de nouveaux facteurs de virulence sont caractérisés (**figure 2**).

L'une des premières étapes de l'infection à *H. pylori* est l'échappement à l'acidité des sucs gastriques. En effet, *H. pylori*, n'étant pas une bactérie acidophile, doit échapper à l'acidité de l'estomac afin de pouvoir s'installer. *H. pylori* utilise un système complexe de chimiotaxie impliquant de nombreux récepteurs et autres protéines. Ces systèmes permettent à *H. pylori* de détecter l'acidité du milieu et d'y échapper en activant son système de mobilité via ses flagelles. Les facteurs majeurs reconnus sont l'histidine Kinase CheA, le régulateur de réponse CheY ainsi que les MCPs (*methyl-accepting chemotaxis proteins*) qui sont des détecteurs de stimuli chimiques.

H. pylori possède aussi des récepteurs capables d'identifier le pH d'un milieu comme TlpB qui interagit avec CheA permettant la régulation de la chaîne de chimiotaxie et induisant la mobilité de *H. pylori* afin d'échapper au milieu acide (22–26).

L'un des autres systèmes majeurs connu chez *H. pylori* pour échapper à l'acidité du milieu est le système de production d'urée. Il s'agit d'un système crucial pour la survie de *H. pylori* impliquant la neutralisation du milieu acide pour la production d'ammonium via la métabolisation de l'urée (24,27–31). L'uréase est utilisée par *H. pylori* pour neutraliser l'acidité du milieu. Pour cela, l'uréase hydrolyse l'urée gastrique, en utilisant le nickel comme cofacteur, en ammonium. La neutralisation de l'acidité du milieu gastrique aide *H. pylori* à naviguer jusqu'au mucus gastrique et les cellules gastriques entre lesquelles *H. pylori* peut s'installer. Ce système de l'uréase est essentiel pour l'installation durable de *H. pylori* dans l'estomac (32).

Une fois que *H. pylori* a atteint les cellules gastriques, elle doit s'établir durablement. *H. pylori* emploie plusieurs systèmes de toxines afin de créer des ouvertures entre les cellules épithéliales gastriques (29,33). Une toxine particulièrement étudiée est une toxine polyvalente aux multiples fonctions : VacA (*Vacuolating cytotoxin A*). VacA, une fois internalisée dans les cellules, forme des vacuoles notamment dans des organites comme des endosomes, les lysosomes et encore les mitochondries. VacA possède un effet cytotoxique sur les cellules, mais induit aussi une altération des membranes cellulaires, altère des voies de signalisation cellulaire et surtout induit l'apoptose des cellules infectées. VacA est aussi impliquée dans l'échappement du système immunitaire de l'hôte. En effet, VacA est capable d'inhiber la prolifération des lymphocytes T (LT) en interférant avec l'intégrité des endosomes ce qui, une fois internalisée dans les LT, interfère avec l'environnement acide et la maturation des endosomes (34–37).

Enfin, chez toutes les espèces bactériennes, on retrouve l'implication des LPS. Chez *H. pylori*, les LPS jouent un rôle crucial dans l'adhérence aux cellules gastriques ainsi que dans l'induction de l'inflammation. Les LPS sont exprimés à la surface des bactéries favorisant les interactions avec les récepteurs présents à la surface des cellules épithéliales gastriques. Les LPS de *H. pylori* ont la capacité de reconnaître et de se lier spécifiquement à l'antigène Lewis b. Les antigènes Lewis sont des glycoprotéines présentes à la surface des cellules humaines y compris les cellules épithéliales

gastriques et font partie du système de groupes sanguins humains. Ces antigènes sont divisés en deux principaux : Lewis a (Lea) et Lewis b (Leb). Les LPS sont aussi impliqués dans la réponse immunitaire innée chez l'hôte. Ils sont reconnus par les récepteurs tels que le récepteur Toll-like 4 (TLR4) et activent la voie de signalisation inflammatoire, déclenchant la libération de cytokines pro-inflammatoires telles que l'interleukine-1 (IL-1), l'interleukine-6 (IL-6) et le facteur de nécrose tumorale alpha (TNF- α). Afin de continuer à persister dans l'estomac, *H. pylori* a développé des mécanismes de régulation des LPS régulant ainsi la réponse immunitaire. Un exemple de mécanisme d'échappement est la variabilité de l'antigène O. Cet antigène possède une structure très diversifiée et porte un antigène de Lewis. La présence de l'antigène de Lewis permet à la bactérie d'imiter la surface protéique des cellules de l'hôte et d'ainsi échapper au système immunitaire (38–43).

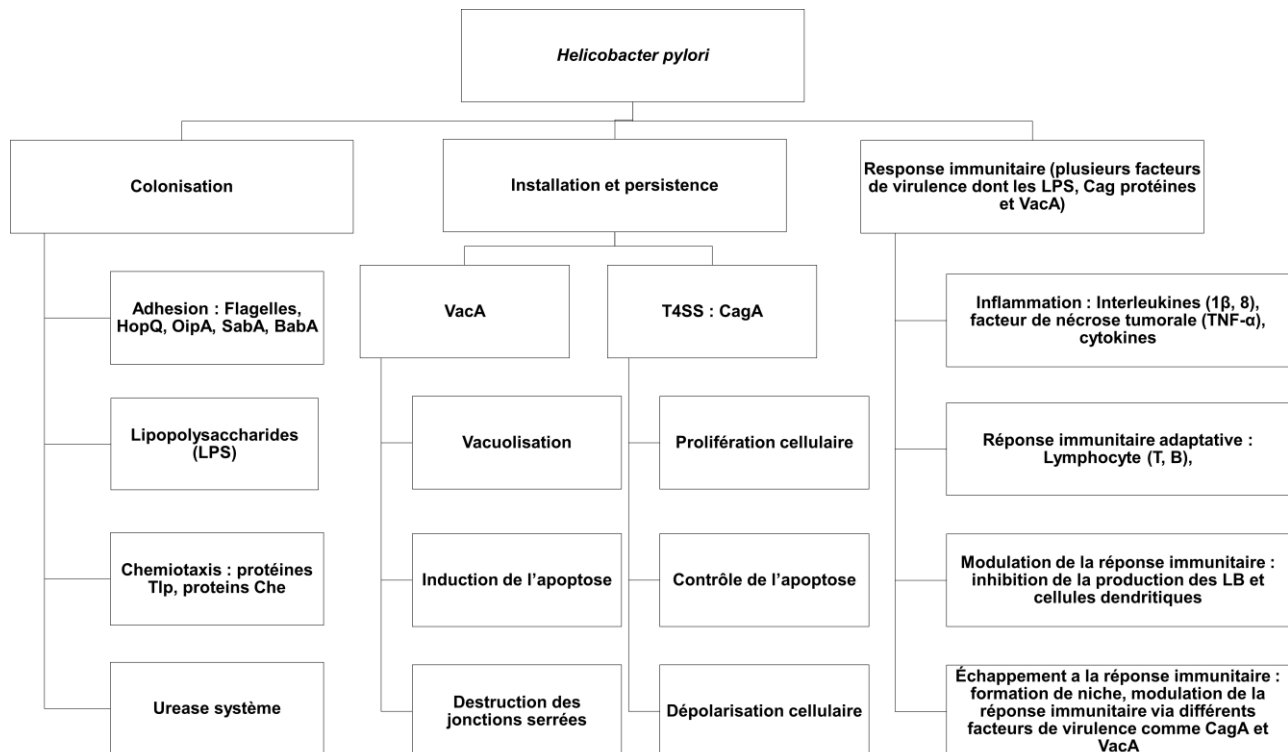


Figure 2 : Principales étapes de l'infection à *Helicobacter pylori* avec les facteurs de virulence majeurs associés ainsi que les principales réponses immunitaires

Résumé des différents facteurs de virulence majeurs de *H. pylori* et leurs fonctions lors de l'infection ainsi que les différentes réponses immunitaires induites par l'infection.

v. Le système de sécrétion de type 4 : une seringue impliquée dans la translocation d'une oncoprotéine bactériale

Le système de sécrétion du type 4 (SST4) est un système protéique complexe présent chez de nombreuses bactéries. Ce système permet la sécrétion de protéines ou d'ADN dans le cytoplasme des cellules cibles. Le modèle original pour le SST4 provient de la bactérie *Agrobacterium tumefaciens* responsable de l'apparition de tumeurs chez les plantes. La figure 3 présente les diversités retrouvées dans la structure des SST4. Les SST4 portés par le plasmide pKM101 isolé chez *Klebsiella pneumoniae* et F isolé chez *Escherichia coli*, *H. pylori* et *L. pneumophila* sont décrits en utilisant la microscopie électronique en transmission cryogénique (cryo-TEM). La structure du SST4 diffère selon les espèces, il peut être très simple avec peu de composants (*minimised* ou minimaliste) ou être très complexe (*expanded* ou étendu), mais il est toujours composé de trois parties : un pilus, une partie intermembranaire appelée le cœur et une partie cytoplasmique composée de la machinerie énergétique et de protéines de translocation (**figures 3 et 4**)(44–46).

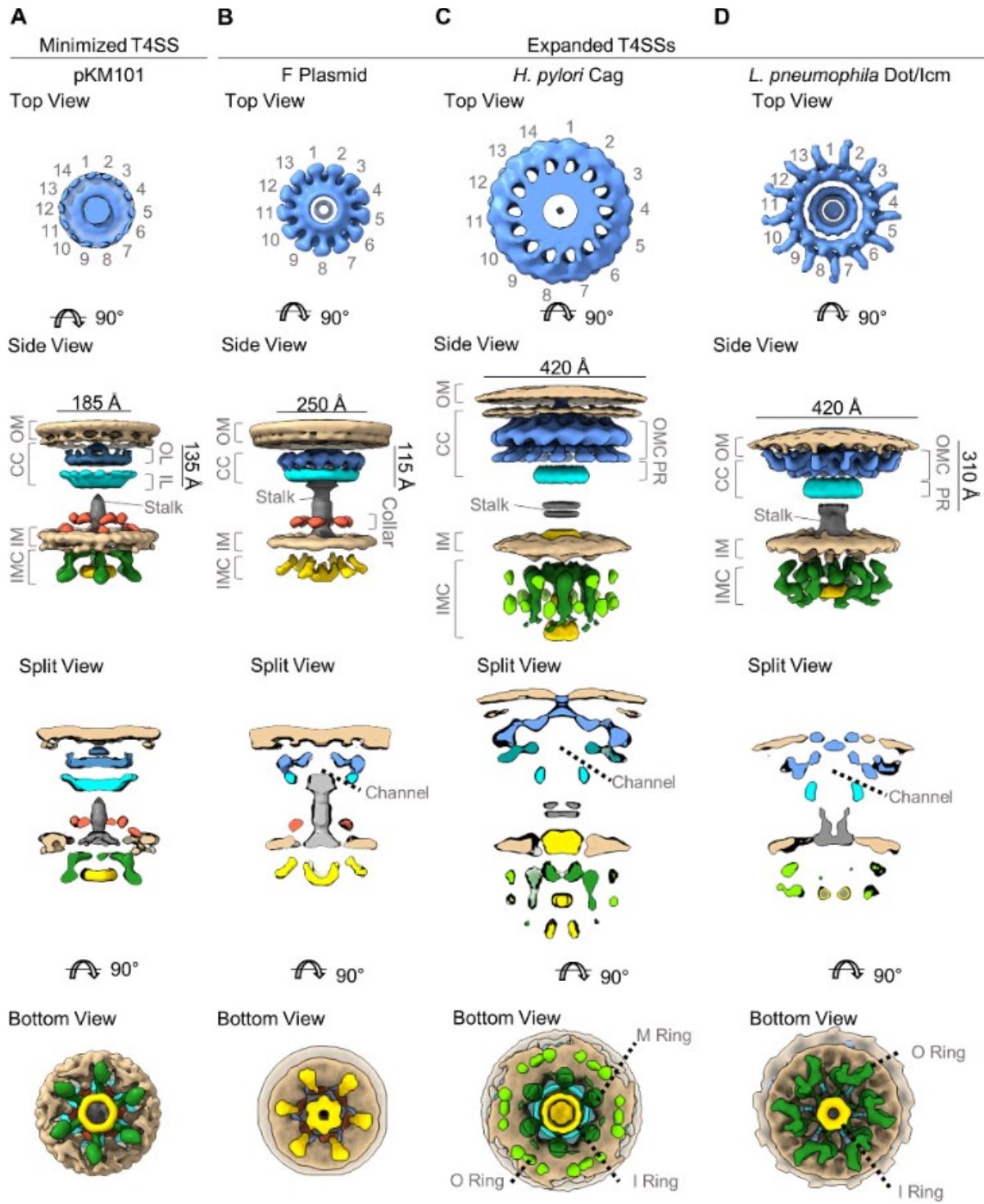


Figure 3 : Comparaison de la structure en cryo-TEM de différents SST4 décrite dans la publication de Sheedlo *et al*, 2022.

Différentes structures de SST4 trouvées dans différentes espèces bactériennes par cryo-TEM. Différentes vues sont montrées : « top view » de dessus relative à la membrane externe ; « bottom view » du bas relative à la membrane interne. IL, couche interne ; IM, membrane interne ; IMC, complexe de membrane interne ; M, milieu ; O, extérieur ; OL, couche externe ; OM, membrane externe ; OMC, capuchon à membrane externe ; PR, anneau périplasmique » (46)

Chez *H. pylori*, le SST4 est codé par un îlot de pathogénicité *cagPAI* (*cytotoxin-associated gene pathogenicity island*). Le *cagPAI* comprend 28 à 30 gènes *cag* (*cytotoxin-associated gene*) qui codent pour des protéines qui font partie du *cagSST4*. Le *cagSST4* effectue l'injection de la première oncoprotéine bactérienne caractérisée, CagA (19,47,48).

CagA est une protéine de 120-150kDa transloquée dans les cellules épithéliales gastriques après l'attachement de *H. pylori*. Une fois dans le cytoplasme, CagA interagit avec de nombreuses voies métaboliques induisant des changements drastiques chez les cellules infectées. CagA possède une séquence répétée en C-terminal : EPIYA (Glu-Pro-Ile-Tyr-Ala). Ces motifs EPIYA sont associés à la capacité de CagA d'interférer avec les voies de signalisation cellulaires dans les cellules hôtes. Le motif EPIYA est phosphorylé sur la tyrosine par les kinases Src et Abl. Il existe à ce jour 4 types de motif EPIYA retrouvés dans différentes régions géographiques, caractériser par l'acide aminé suivant directement le motif. Nous trouvons dans les pays occidentaux les motifs EPIYA-A, EPIYA-B et EPIYA-C alors qu'en Asie de l'Est, ce sont les motifs EPIYA-A, EPIYA-B et EPIYA-D qui prédominent. Il y a aussi une à plusieurs copies du motif EPIYA-C, ce qui impacte le niveau de phosphorylation de CagA et son interaction avec les protéines des cellules hôtes. Il a été démontré que la présence des motifs EPIYA-C et D était associée à un plus grand risque de développer des maladies gastriques sévères (19,49–51). Une fois phosphorylée, CagA perturbe de nombreuses voies métaboliques. Par exemple, CagA réarrange le cytosquelette en interagissant avec la protéine adaptatrice Crk (*CT10 regulator of kinase*) qui est impliquée dans la voie de signalisation de l'adhésion, la mobilité et la prolifération cellulaire. CagA interagit aussi avec les voies des E-cadherin/ β -catenin, les phosphoinositide 3-kinase (PI3K)/Akt, et les *mitogen-activated protein kinases* (MAPK). Toutes ces interactions induisent de nombreuses modifications du

métabolisme cellulaire. CagA est aussi impliquée dans la régulation de l'apoptose cellulaire, ainsi que la polarité et la sécrétion d'acide gastrique. Enfin, CagA active également l'élongation ainsi que la mobilité cellulaire (19,46,52–54). Un phénotype typique d'une cellule infectée par *H. pylori*, associé à CagA, est l'élongation de la cellule. Il s'agit d'un phénotype appelé *Hummingbird* par sa similarité avec le bec du colibri (**figure 1 B**) (55,56).

Afin d'énergiser ce grand complexe protéique qu'est le cagSST4, des ATPases sont nécessaires. Parmi les ATPases du cagSST4 se trouve l'ATPase Cag α , un homologue à l'ATPase modèle VirB11 d'*A. tumefaciens*. Cag α est une protéine hexamérique localisée au niveau de la membrane interne de la bactérie. Les protéines homologues à VirB11 sont très bien caractérisées et Cag α est essentielle à l'assemblage et à la fonction du cagSST4 (**figure 4**) (57–60).

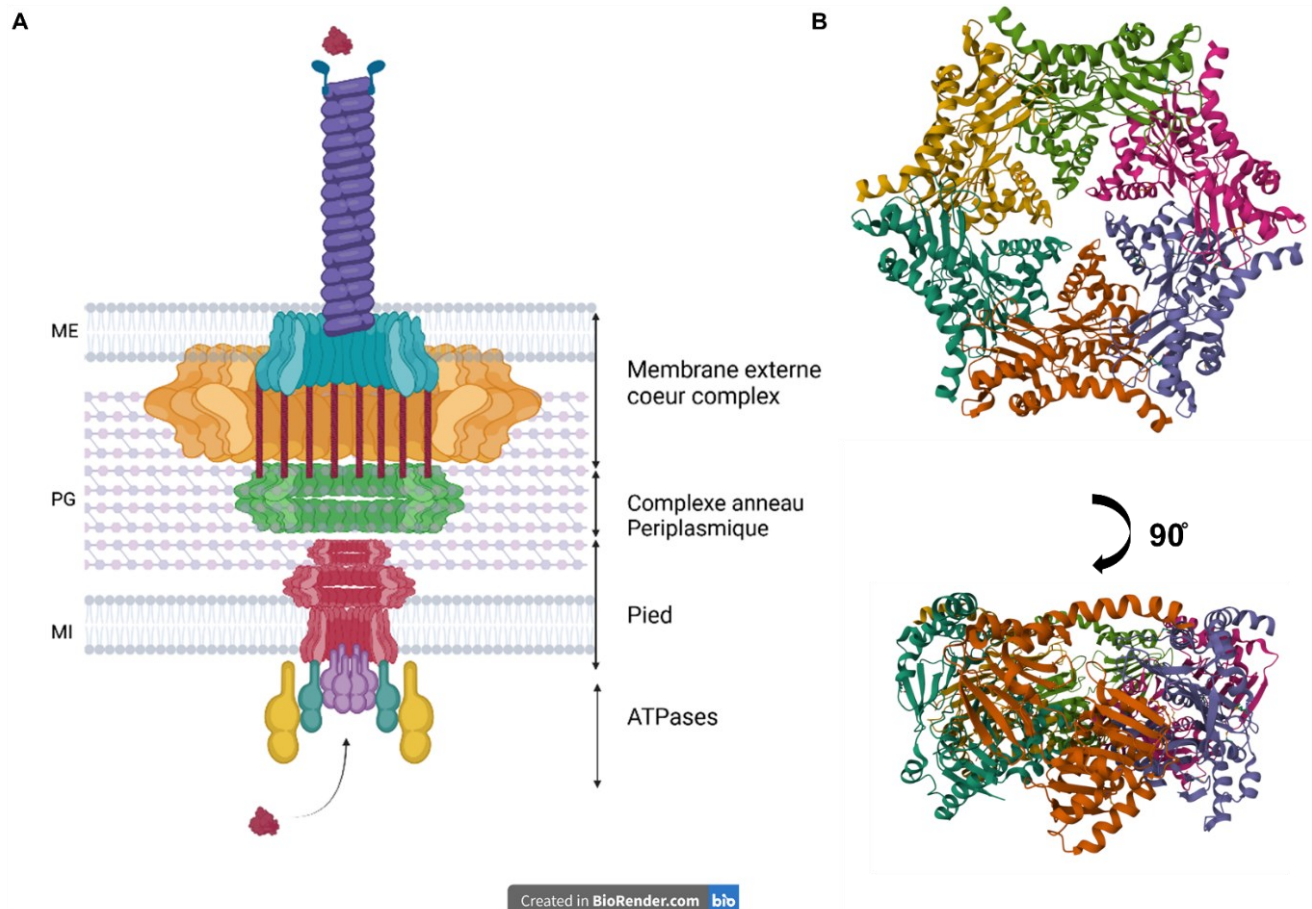


Figure 4 : Schéma simplifié de la structure du cagT4SS et de la cible Caga

A) Schéma simplifié de la structure du cagSST4 dans l'enveloppe de cellules bactériennes, cagPilus : CagC, H, I, L et Y ; complexe cœur : CagH, M, N, T, U, V, W, X, Y et δ ; ATPases : CagE, β et Cag α (violet) ; Substrat : CagA. B) Structure cristallographique de l'ATPase Cag α basée sur la publication de Yeo *et al*, 2001, (<https://doi.org/10.2210/pdb1G6O/pdb>). ME : membrane externe; PG : peptidoglycane ; MI : membrane interne

B. Campagne d'éradication de *H. pylori*

i. Prévalence de *H. pylori* dans le monde

Le mécanisme de transmission d'*H. pylori* n'est pas bien compris et plusieurs voies semblent être impliquées. Tout d'abord, *H. pylori* est une bactérie communautaire dont la transmission est effectuée par la voie orale-fécale (61,62). La colonisation s'effectuerait dans l'enfance ou l'adolescence d'un individu et diffère selon l'ethnicité et les zones géographiques. Un exemple frappant de la colonisation par *H. pylori* est lié à la différence de prévalence qu'on trouve dans les pays de l'Asie de l'Est comparée aux pays d'Amérique du Nord. En effet, en Amérique du Nord, la prévalence de *H. pylori* est d'environ 50% tandis que chez les individus de l'Asie de l'Est la colonisation peut atteindre les 90% (13,63,64). Cette différence pourrait être expliquée par différents facteurs comme des facteurs génétiques, le statut socioéconomique, environnemental ou encore la densité de population (65).

ii. Hypothèse de la bactérie commensale

Il est intéressant de noter qu'*H. pylori* semble coexister avec l'espèce humaine depuis plusieurs millénaires, comme en témoigne l'identification récente d'un génome très similaire aux souches de *H. pylori* sur une momie âgée de plus de 5000 ans. Cette observation n'est pas un cas isolé puisque d'autres recherches ont montrées des observations similaires. Ces différentes observations ont conduit à l'hypothèse que *H. pylori* pourrait faire partie intégrale du microbiome humain (66). Malgré sa forte présence dans la population humaine, seulement un faible pourcentage d'individus colonisés par *H. pylori* vont, au cours de leur vie, développer une maladie gastrique sévère (67,68). Une observation importante de ces dernières années concerne la diversité de souches variantes retrouvées chez *H. pylori*. En effet, il a été observé que l'association entre l'origine géographique

du variant de *H. pylori* et de son hôte peut influencer grandement le risque de développer des maladies gastriques. Une étude sur plusieurs décennies de populations isolées en Colombie a montré que le risque de développer une maladie gastrique est plus faible si les variants de *H. pylori* correspondaient à la même région géographique que son hôte (2,69–72).

En plus de la variation génétique des souches de *H. pylori*, un autre facteur important à prendre en compte est la composition du microbiome gastrique de l'hôte. Plusieurs études sur le microbiome gastrique ont pu être réalisées. Toutefois, l'obtention d'échantillons provenant d'individus sains représente un défi majeur, car la méthode la plus appropriée pour obtenir une idée précise de la composition du microbiome gastrique est d'étudier des cultures issues de biopsies gastriques, ce qui n'est pas une procédure anodine. Par conséquent, la collecte de données à long terme en vue d'établir une base de données sur les variations du microbiote demeure complexe. Par ailleurs, l'obtention de données fiables est complexe en raison de la nature de l'estomac en tant que lieu de transit pour de nombreuses espèces microbiennes, qu'il s'agisse de bactéries, de virus ou de champignons provenant de l'environnement. Néanmoins, les données récoltées apportent un début de réponse par rapport quant à la composition du microbiome gastrique. Il a été observé par exemple, que *H. pylori* a un effet sur la composition du microbiome gastrique quand on compare individu colonisés et non colonisés (73,74). En effet, chez un individu non colonisé par *H. pylori*, on observe majoritairement des bactéries bénéfiques comme des *Lactobacillus* qui promeuvent une balance digestive et supportent le système immunitaire ; des *Bifidobacterium* qui réduisent l'inflammation et supportent une bonne digestion ; des *Streptococcus* qui produisent, entre autres, des acides lactiques ; des *Prevotella* qui permettent la dissociation des carbohydrates ainsi que des *Faecalibacterium* qui possèdent des caractéristiques anti-inflammatoires et produisent des acides gras bénéfiques pour la santé gastrique (74–80). En comparaison, chez un individu colonisé par *H. pylori*, on observe une prolifération des *Proteobacteria*, des *Fusobacterium*, des *Enterococcus* ou encore des *Campylobacter*. Ces phyla sont associés à une augmentation de l'inflammation gastrique et sont mis en cause dans l'apparition de maladies gastriques. Il est important de noter que ces données reflètent l'ensemble du système gastrique comprenant plusieurs compartiments avec des conditions de milieux différents. Par exemple, les *Campylobacter*, qui sont plus associées

au microbiome intestinal, pourraient plus être localisées au niveau du duodénum qui est à la limite entre l'estomac et les intestins (74–81).

iii. Traitement d'éradication de *H. pylori*

Pour limiter la propagation de *H. pylori* dans les communautés et traiter les cas graves de gastrite associée à cette bactérie, une campagne d'éradication a été mise en place. En Amérique du Nord, la première ligne de traitement consiste en une quadrithérapie utilisant des antibiotiques à spectre large avec des compléments comme des inhibiteurs de la pompe à protons (IPP) ainsi que des sels de bismuth. Cette thérapie inclut la clarithromycine (C), un antibiotique macrolide à spectre large qui cible la synthèse protéique ; l'amoxicilline (A), une pénicilline à spectre large inhibant la synthèse du peptidoglycane ; le métronidazole (M), un antibiotique de type nitroimidazole qui est spécifique aux bactéries anaérobiques et parasites protozoaires; et enfin la tétracycline (T), un antibiotique à spectre large qui cible la synthèse protéique (82–88).

En complément des antibiotiques, des inhibiteurs de pompes à proton (IPP) sont utilisés pour inhiber l'activité des pompes à proton gastriques et ainsi réduire l'acidité de l'estomac et améliorer l'efficacité des antibiotiques. Des sels de bismuth sont aussi inclus dans les thérapies et leur fonction n'est pas bien comprise. Cependant il a été démontré que les sels de bismuth possèdent de nombreuses activités comme des effets anti-inflammatoires ou encore offrent une protection contre la cytotoxicité cellulaire (89,90).

Habituellement, la thérapie de première ligne est composée des IPPs ainsi que de la combinaison de C et A ou M. La durée de la thérapie peut varier selon les antibiotiques utilisés, mais se situe habituellement entre 10 et 14 jours (87). Dans le cas d'une modification de la thérapie, le patient peut recevoir jusqu'à 21 jours de thérapie entraînant dans le même temps une forte pression de sélection de résistances (**tableau 1**).

Antibiotiques	Famille ; fonction ; Spectre ; mécanisme d'inhibition et de résistance	Administration	Utilisation	Références
Clarithromycine	Macrolide ; bactériostatique Large Interaction avec le peptide synthase de la sous-unité 23S du ribosome Mutation sur la région V de la peptide synthase, système de Pompes à efflux, l'expression des protéines de la membrane externe OMPs, HopT (adhésive), OMP31 (porines), and HofC (protéine de surface) est augmentée	O	Première ligne	(84,91–94)
Amoxicilline	Semi synthétique pénicilline ; bactéricide Large Attachement au pénicilline binding protein (PBPs) empêchant la synthèse du peptidoglycane Mutation sur les PBPs, production de β -lactamase, mutation des porines et pompes a efflux (HopB, HopC, HefA, HefC, et HofH)	O		(85,95–97)
Métronidazole	Nitroimidazole ; bactéricide ; Bactéries anaérobiques et parasite protozoaire Production de nitro anion radicaux, de dérivé des nitroso, et d'hydroxylamine via la nitro réductase, ces chaines de réaction cause la destruction de l'hélice de l'ADN Mutation sur le gene RdxA codant pour la nitroreductase oxygène sensible NADPH, OMPs, hp1165 and HefA	O ou IV		(83,98–102)
Tétracycline	Cycline ; bactériostatique Large Inhibition de la synthèse protéique en se liant à l'animoacyl-ARNt du ribosome Mutation ponctuelle sur l'ARN 16S et pompe a proton	O ou P ou L		(103–106)
Rifamycine	Rifampicine ; Bactéricide Gram-positive et antituberculeux Inhibe l'and dépendantes ARN polymérase Mutation ponctuelle au niveau de l'and-dépendante ARN polymérase	O	Seconde ligne	(107)
Doxycycline	Cycline ; bactériostatique Large Inhibition de la synthèse protéique en se liant à l'animoacyl-ARNt du ribosome Mutation ponctuelle sur l'ARN 16S et pompe a proton	O ou P ou L		(108)
Ornidazole	Nitroimidazole ; bactéricide Bactéries anaérobiques et parasite protozoaire Production de nitro anion radicaux, de dérivé des nitroso, et d'hydroxylamine via la nitro réductase, ces chaines de réaction cause la destruction de l'hélice de l'ADN	O ou IV		(109,110)
Tinidazole	Mutation sur le gene RdxA codant pour la nitroreductase oxygène sensible NADPH, OMPs, hp1165 and HefA			

Tableau 1 : Récapitulatif des antibiotiques majeurs utilisés contre l'infection à *Helicobacter pylori*, O : oral ; IV : intraveineux ; P : parentéral ; L : local.

iv. Resistance aux antibiotiques : un problème global

L'antibiothérapie contre *H. pylori* exerce une forte pression de sélection de résistance (**tableau 1**). En effet, l'utilisation d'antibiotiques à spectre large sur une longue période peut induire une pression de sélection sur la bactérie ciblée, mais aussi sur le microbiome humain. Un aspect à considérer chez *H. pylori* est sa capacité à acquérir facilement du matériel génétique dans son environnement (111–114). En effet, *H. pylori* est naturellement transformable, lui permettant d'acquérir de l'ADN dans son environnement, facilitant l'acquisition de résistances dans un milieu soumis à une forte pression de sélection, de plus *H. pylori* est capable de transférer du matériel génétique via conjugaison (115–118). Un exemple de résistance est celle contre le métronidazole où *H. pylori* perd la fonction de plusieurs gènes impliqués dans la métabolisation du métronidazole qui perd donc son efficacité (99). On retrouve comme résistance acquise la mutation sur le ribosome pour contrer les effets de la clarithromycine. Depuis la dernière décennie, plus de 50% des souches isolées de patients présentaient au moins une résistance contre les antibiotiques de première ligne. Les différents mécanismes de transfert de matériel génétique, que ce soit horizontal ou vertical, amènent une grande capacité d'adaptation de *H. pylori* causant un problème majeur pour le traitement des patients, mais aussi entraînent une prolifération des résistances dans les communautés (113,119–121).

C. Nouvelles approches pour les traitements des infections à *H. pylori*

Avec la montée de la résistance aux antibiotiques de *H. pylori*, de nouvelles voies thérapeutiques sont en cours d'étude (122,123).

i. Développement de vaccins

En raison de sa prévalence élevée dans la population humaine, il semble judicieux de considérer la vaccination systématique contre *H. pylori* (124). De nombreuses études sont en cours mais aucun vaccin n'a encore été mis sur le marché. Parmi les cibles envisagées pour la vaccination, on trouve les protéines de la membrane externe (PME). Les PME sont des protéines exprimées à la surface de *H. pylori* qui sont impliquées dans l'adhésion aux cellules épithéliales. Leur accessibilité en fait des cibles potentielles pour un vaccin. Cependant, *H. pylori* exprime plusieurs types de PME en fonction des souches, et la variabilité génétique de celles-ci rend l'élaboration d'un vaccin universel

peu faisable. D'autres cibles potentielles envisagées seraient l'uréase ainsi que CagA, mais l'uréase n'est pas spécifique à *H. pylori* et CagA n'est pas présent chez toutes les souches de *H. pylori*. L'élaboration de vaccins semble pour le moment très limitée, les variabilités génétiques et la disponibilité de la cible, vu que *H. pylori* colonise en profondeur les tissus gastriques, sont des facteurs limitants majeurs (119,124–131).

ii. L'utilisation des phages

Une autre option pour combattre les infections bactériennes est l'utilisation des phages. La phagothérapie est étudiée depuis des décennies, mais n'a jamais vraiment été mise en place à grande échelle à cause de nombreux obstacles liés à l'application clinique et de la dominance de l'utilisation des antibiotiques (132,133). Malgré tout, l'utilisation des phages présente de nombreux avantages par rapport aux antibiotiques. Par exemple, contrairement aux antibiotiques, l'action des phages est généralement spécifique à l'espèce, diminuant le risque d'effets indésirables sur le microbiome humain. Il existe plusieurs bactériophages ciblant *H. pylori* et ceux-ci pourraient être utilisés en thérapie, en principe (134,135). Par exemple, au Portugal, on retrouve le phage lytique HPy1R isolé d'une souche de *H. pylori* provenant d'un patient. Ce phage a démontré sa capacité à interagir avec un grand nombre de souches provenant de biopsies chez différents patients (134). D'autres phages lytiques ont été isolés chez des patients, cependant à ce jour peu d'étude sur leur possible utilisation en clinique n'ont été élaboré (135). On retrouve plusieurs limites pour l'utilisation des phages en thérapie. En effet, pour obtenir des résultats probants, il faudrait traiter chaque patient individuellement en fonction de la souche de *H. pylori* impliquée, de l'évaluation de la colonisation (stade d'infection) ou encore des dommages déjà causés au niveau de la muqueuse gastrique (134–138). Ces différents critères rendent l'utilisation de phagothérapie compliquée à mettre en place de façon routinière en milieu hospitalier. De plus, l'utilisation de phages en thérapie reste à être définie dans les réglementations des médicaments et aura aussi un coût non négligeable à cause de son application personnalisée pour chaque patient. En complément, comme pour les antibiotiques, les bactéries ont la capacité de développer des résistances contre les bactériophages, comme par exemple un changement de la cible induisant une perte d'affinité (139–141).

iii. Recherche de nouvelles sources de traitement via les remèdes ancestraux

De nombreuses études de remèdes ancestraux sont aussi en cours. La plupart de ces études se concentrent sur le traitement des symptômes et non sur l'éradication de *H. pylori*. En plus, il est reconnu que les remèdes dits ancestraux possèdent des composants antibiotiques. L'extraction de ses composants reste encore aujourd'hui une piste étudiée dans la communauté scientifique. Un exemple de produit naturel identifié comme efficace contre *H. pylori* est l'allicine, un composant extrait de l'ail. L'allicine possède des caractéristiques antibactériennes, mais aussi des effets anti-inflammatoire et antioxydant (142–148).

D. Problématique de thèse.

De nouvelles idées pour lutter contre les infections bactériennes émergent de plus en plus dans la communauté scientifique. Une voie à explorer est l'inhibition des facteurs de virulence des bactéries. Ces facteurs sont importants pour l'infection de l'hôte et on trouve typiquement des facteurs de virulence spécifiques à chaque espèce bactérienne. L'utilisation de molécules capables d'inhiber des facteurs de virulence présente de nombreux avantages par rapport aux antibiotiques. Tout d'abord, en ciblant un facteur de virulence spécifique à une bactérie, nous réduisons le spectre d'action du traitement, diminuant ainsi l'impact sur le microbiome. De plus, en visant des fonctions non essentielles à la survie bactérienne, le risque d'acquisition de résistance est restreint. Enfin, les facteurs de virulence sont impliqués dans l'apparition de symptômes de la maladie, donc en ciblant ceux-ci, les symptômes sont limités (149–159). Ces points soulignent les avantages par rapport au traitement aux antibiotiques. En effet, les antibiotiques présentent le plus souvent un spectre d'action large qui ne discrimine pas entre le pathogène et les bactéries du microbiome, causant alors des dysbioses qui peuvent avoir des effets nocifs pour le patient. En plus, la pression de sélection des antibiotiques engendre l'apparition de résistances qui peuvent ensuite être propagées dans la communauté (160–163).

Dans notre laboratoire, nous nous intéressons aux SST4s, un système utilisé pour injecter des protéines effectrices et/ou des molécules d'ADN. Chez *Helicobacter pylori*, ce système est utilisé pour injecter une oncoprotéine, CagA, qui est capable de déréguler la croissance de cellules épithéliales provoquant, dans certains cas, l'apparition de tumeurs malignes conduisant à un cancer

de l'estomac(164). Le SST4 transporte aussi du peptidoglycane ou encore de l'ADN. Parmi les protéines qui composent le SST4 de *H. pylori*, une ATPase, CagA a été bien caractérisée (58). Cette protéine est essentielle pour le fonctionnement du SST4 et sa délétion entraîne une perte de l'injection de CagA dans les cellules épithéliales gastriques réduisant le risque de développer une maladie gastrique sévère. CagA est donc une cible potentielle pour le design de molécules anti-facteur de virulence.

L'inhibition des ATPases a fait l'objet d'études approfondies depuis plusieurs années. Cependant, les progrès ont été limités jusqu'à présent en raison de l'absence d'observation du site de liaison molécule/cible, rendant ainsi difficile l'identification de la spécificité de la cible (165–170). De plus, les ATPases ciblées sont le plus souvent utilisées pour des fonctions essentielles à la bactérie, telles que la topoisomérase IV ou l'ADN Gyrase (165), ou ciblent des domaines très conservés, tels que les sous-unités de la F1Fo ATP synthase présentes chez de nombreuses espèces (166,171). Ces inhibitions présentent donc un risque accru d'acquisition de résistances et ne sont pas très spécifiques.

L'étude de l'inhibition des systèmes de sécrétion est en cours, mais elle se concentre très peu sur le SST4. Des inhibiteurs ont été développés, par exemple, pour les systèmes de sécrétion de type III, et des approches ont été explorées pour les SST4, mais elles ne visent pas spécifiquement le cagSST4 (172–175). L'étude de l'inhibition de CagA a déjà été entreprise, mettant en évidence la molécule CHIR-1 capable d'inhiber l'activité ATPase de CagA. Cette molécule a démontré la capacité de réduire l'induction des IL-8 et de diminuer la translocation de CagA dans les cellules gastriques. Cependant, aucune mise à jour sur cette molécule n'a été effectuée depuis 2006 (169).

Précédemment, Arya *et al*, ont identifié une petite molécule, 1G2, comme étant capable de se lier à CagA sans entrer en compétition avec son substrat, l'ATP. La quantification de l'induction des IL-8 dans des cellules humaines en contact avec *H. pylori* a montré que la présence de 1G2 réduit l'induction d'environ 30-40%, montrant l'inhibition du SST4 (176).

Dans mes travaux de thèse, nous avons cherché à comprendre le mécanisme d'inhibition de 1G2 en créant des mutants du site de liaison de 1G2 sur CagA. De plus, nous avons créé une librairie de

petites molécules dérivées de 1G2 pour augmenter l'efficacité de l'inhibition de Cag α . Nous avons aussi analysé le potentiel clinique de 1G2 en testant son efficacité sur des souches issues de biopsies gastriques résistantes aux antibiotiques de première ligne.

La combinaison d'une étude *in vitro* sur la cible purifiée avec le modèle cellulaire d'infection nous permettra de mieux appréhender le potentiel d'une nouvelle voie thérapeutique contre *H. pylori*. Cette approche a le potentiel d'ouvrir les portes pour une application à plus grande échelle sur des bactéries du microbiome connues pour leur potentiel opportuniste.

II. Justification de la méthodologie

Afin d'étudier le potentiel des petites molécules inhibitrices, deux types d'approches ont été utilisées. Pour comprendre les interactions entre la cible Cag α et les molécules, des expériences *in vitro* sur la cible purifiée ont été réalisées.

En parallèle, des tests sur des cellules gastriques humaines en culture ont été effectués afin d'appréhender les effets sur le SST4 dans son ensemble.

A. Etude *in vitro*

i. Mutation dirigée et purification de protéines

A partir de la structure de l'interaction entre Cag α et 1G2 présentée dans le papier #2, le site de liaison de 1G2 sur Cag α a été identifié (176). Des mutations dirigées sur un plasmide inducible porteur du gène de Cag α sauvage ont été réalisées. Pour chaque acide aminé impliqué au site de liaison, le codon a été remplacé par le codon de l'alanine. Cette méthode nous a permis de produire et purifier des protéines Cag α mutantes afin de tester les affinités de nos molécules et de confirmer le site de liaison de 1G2 et ses molécules dérivées.

ii. Fluorimétrie différentielle à balayage (*Differential Scanning Fluorimetry :DSF*)

La DSF permet d'observer les changements de conformation d'une protéine en déterminant la température de fusion de celle-ci. Une interaction physique peut être identifiée avec cette approche, car la fixation d'une molécule à une protéine change la conformation de celle-ci et donc change la température de fusion de la protéine. En utilisant le DSF, nous pouvons déterminer si les molécules interagissent avec notre cible.

iii. Test de l'activité ATPase

Cag α est une ATPase et la mesure de son activité lors de l'ajout de molécules permet de connaître le type d'interaction entre celles-ci. Arya *et al*, ont déjà caractérisé 1G2 comme étant une molécule non-compétitrice avec le ligand de Cag α , l'ATP (176). Ici, nous avons testé l'activité de Cag α afin de connaître le niveau d'inhibition de l'activité de nos molécules.

B. Etudes sur modèle d'infection cellulaire

i. Modèle d'infection cellulaire

L'utilisation de cellules gastriques humaines (AGS), qui sont une lignée cellulaire d'adénocarcinome gastrique humain largement utilisée comme modèle pour l'étude des cancers gastriques et de l'infection à *H. pylori*, permet d'avoir un aperçu de l'effet des molécules sur les tissus gastriques de l'estomac (177–180). La visualisation par microscopie (confocale et électronique) ainsi que la réponse cellulaire peuvent être analysées en utilisant ce modèle. Les cellules gastriques sont infectées par *H. pylori* pré-incubées avec les molécules. Le milieu de culture de l'infection a été utilisé pour quantifier l'induction des IL-8, le lysat de l'infection (cellules et bactéries) a été utilisé pour identifier la présence des protéines Cag, et en parallèle, un duplicata des infections a été traité pour une visualisation en microscopie électronique.

ii. Quantification des IL-8 par test ELISA

Lors de l'infection cellulaire, les cellules produisent des marqueurs d'inflammation, dont IL-8 qui est spécifiquement induit par le SST4 et CagA (20,180,181). La quantification d'IL-8, dans le milieu de culture, permet de d'identifier indirectement si le SST4 est fonctionnel et donc nous indique le niveau d'efficacité de molécules inhibitrices.

iii. Observation des protéines Cag par Western Blot

Afin de comprendre l'influence des molécules sur les protéines Cag, des western blots du lysat des infections ont été réalisés. La présence de CagA total (dans les cellules gastriques et les bactéries) et Cag α a été observée en utilisant des anticorps spécifiques.

iv. Visualisation du SST4 par microscopie électronique

Afin de voir si l'inhibition de Cag α affecte directement le SST4, la microscopie électronique a été utilisée. Cette technique permet de visualiser directement les SST4 pili qui interagissent avec les cellules et d'identifier l'effet global des inhibiteurs sur le SST4.

III. Publications

- A. Papier #1 : Inhibition du système de sécrétion de type IV des isolats cliniques d'*Helicobacter pylori* résistants aux antibiotiques soutient le potentiel de Cag α en tant que cible anti-virulence.

Inhibition of the type IV secretion system from antibiotic-resistant *Helicobacter pylori* clinical isolates supports the potential of Cag α as an anti-virulence target

¹Flore Oudouhou[#], ¹Claire Morin[#], ²Mickael Bouin, ³Christiane Gaudreau and ¹Christian Baron*

¹Department of Biochemistry and Molecular Medicine, Faculty of Medicine,

Université de Montréal, Québec, Canada

²Department of Medicine, Faculty of Medicine,

Université de Montréal and Centre Hospitalier de l'Université de Montréal (CHUM)

³Department of Microbiology, Infectiology and Immunology, Faculty of Medicine,

Université de Montréal and Centre Hospitalier de l'Université de Montréal (CHUM)

*Corresponding author : christian.baron@umontreal.ca

#Author names in bold designate shared co-first authorship

DOI: [10.1139/cjm-2023-0168](https://doi.org/10.1139/cjm-2023-0168)

This is the last version after peer review.

i. Abstract

Helicobacter pylori resistance to antibiotics is a growing problem and it increasingly leads to treatment failure. While the bacterium is present worldwide, the severity of clinical outcomes is highly dependent on the geographical origin and genetic characteristics of the strains. One of the major virulence factors identified in *H. pylori* is the *cag* pathogenicity island (*cagPAI*), which encodes a type IV secretion system used to translocate effectors into human cells. Here, we investigated the genetic variability of the *cagPAI* among 13 antibiotic-resistant *H. pylori* strains that were isolated from patient biopsies in Québec. Seven of the clinical strains carried the *cagPAI*, but only four could be readily cultivated under laboratory conditions. We observed variability of the sequences of CagA and CagL proteins that are encoded by the *cagPAI*. All clinical isolates induce interleukin-8 secretion and morphological changes upon co-incubation with gastric cancer cells and two of them produce extracellular T4SS pili. Finally, we demonstrate that molecule 1G2, a small molecule inhibitor of the Cag α protein from the model strain *H. pylori* 26695, reduces interleukin-8 secretion in one of the clinical isolates. Co-incubation with 1G2 also inhibits the assembly of T4SS pili, suggesting a mechanism for its action on T4SS function.

Keywords: *Helicobacter pylori*, *cagPAI*, CagA, CagL, Cag α , interleukin-8, antibiotic resistance, anti-virulence

ii. Introduction

Helicobacter pylori is a human pathogen that colonizes the stomach of about half of the world's population. While the infection usually leads to asymptomatic gastritis, more severe outcomes such as peptic ulceration and adenocarcinoma are observed in a subset of subjects (Covacci *et al.*, 1999; Cover and Blaser, 1999). Different treatment regimens have been established to eradicate the infection, but due to increasing resistance to antibiotics, failure of *H. pylori* eradication therapy is becoming a growing problem (Gatta *et al.*, 2013). *H. pylori* strains that carry the *cag* pathogenicity island (*cagPAI*), a 40 kb chromosomal region, and have potential to cause severe gastric diseases (Hatakeyama, 2014; Yong *et al.*, 2015; Cover, 2016). The *cagPAI* comprises 28-30 genes and encodes a type IV-secretion system (T4SS), a macromolecular complex that spans across the double membrane of the bacterium enabling the injection of effectors directly into host cells. Several molecules are translocated through the *H. pylori* T4SS such as the cytotoxin CagA, bacterial peptidoglycan, chromosomal DNA and heptose-1,7-bisphosphate (HBP), a metabolic precursor of lipopolysaccharide synthesis (Odenbreit, 2000; Viala *et al.*, 2004; Varga *et al.*, 2016; Gall *et al.*, 2017). While all these effectors are known to contribute to pro-inflammatory responses in epithelial gastric cells via activation of the NF- κ B transcription factor, CagA is recognized as the major virulence factor.

CagA is a 120-145 kDa protein encoded by the *cagPAI* that is associated with increased risk of gastric cancer and is considered an oncoprotein (Hatakeyama, 2014; Cover, 2016). Following bacterial attachment and CagA translocation into epithelial cells, CagA can interact with more than 25 host cell proteins, and it hijacks cellular signaling pathways. CagA induces actin-based cytoskeletal rearrangements, cell motility and proliferation, it affects cell polarity, cell adhesion, the cell cycle, the apoptosis pathway and it also induces inflammatory pathways (Tegtmeyer *et al.*, 2017). The interaction of CagA with some of its partners depends on its phosphorylation status. Following its translocation, CagA undergoes phosphorylation by Src and Abl kinases on tyrosine sites of the EPIYA (Glu-Pro-Ile-Tyr-Ala) motifs that are present in its C-terminus (Selbach *et al.*, 2002; Hatakeyama and Higashi, 2005; Tammer *et al.*, 2007; Backert *et al.*, 2008). Based on the flanking sequences, four specific EPIYA motifs have been described. The EPIYA-A, -B and -C

motifs are usually found in *H. pylori* isolates from Western countries while EPIYA-A, -B and -D are present in East Asian strains (Higashi *et al.*, 2002). The EPIYA-C site occurs in different numbers; it is typically present in one to three copies and these differences are directly related to the levels of CagA tyrosine phosphorylation and binding to host proteins like SHP-2 (Src homology 2 phosphatase) (Higashi *et al.*, 2002). A larger number of EPIYA-C motifs and the presence of EPIYA-D are associated with increased virulence and carcinogenicity (Hatakeyama and Higashi, 2005). In strains from Western countries it was observed that CagA can carry a specific A/T polymorphism, called the EPIYT motif, which presents an alternative binding site for phosphatidylinositol 3-kinase (PI3-kinase), influencing cancer risk (Zhang *et al.*, 2015). In addition, the C-terminal domain includes another repeated sequence motif that was originally designated as the CagA multimerization (CM) motif enabling multimerization via this 16 amino-acid region (Ren *et al.*, 2006). Differences between five typical amino-acid residues enable the distinction between Western and East Asian CagA CM motifs. Whereas Western species contain multiple CM motifs located within each EPIYA-C region plus one distal to the last EPIYA-C, East Asian CagA proteins comprise a single CM motif that is located distally to the EPIYA-D segment.

The injection of effectors into the host cell cytoplasm requires bacterial adhesion to the gastric epithelium. CagL that locates at the tip of pilus-like structures (T4SS pili) is one of the *cagPAI*-encoded proteins that contribute to this process. CagL binds to many host integrins, such as the integrins $\alpha 5\beta 1$, $\alpha V\beta 3$, $\alpha V\beta 5$, $\alpha V\beta 6$ and $\alpha V\beta 8$, notably via the conserved RGD (Arg-Gly-Asp) motif (Kwok *et al.*, 2007; Wiedemann *et al.*, 2012; Barden and Niemann, 2015). Its binding to host integrins can activate the NF- κ B pathway leading to the production of several pro-inflammatory cytokines. It has been shown that several variations of the CagL sequence are associated with higher risk of gastric cancer, e.g. the CagL-Y58E59 variant induces higher integrin $\alpha 5\beta 1$ expression levels and increases inflammation (Yeh *et al.*, 2011; Ogawa *et al.*, 2017). Several other variations at different amino acid residues (Thr30; Asn101; Ala141; Glu142; Asn201; Ile234) are proposed to occur in higher rates in gastric cancer patients, but the mechanism on their contribution requires further investigation (Ogawa *et al.*, 2017).

In *H. pylori*, T4SS pilus biogenesis and translocation of effectors are energized by three ATPases (Fischer *et al.*, 2002; Hilleringmann *et al.*, 2006; Kutter *et al.*, 2008; Jurik *et al.*, 2010). Among them, Cag α is a VirB11-like ATPase. VirB11-like proteins are present in all T4SSs and they have been extensively characterized (Krause *et al.*, 2000; Yeo *et al.*, 2000; Machón *et al.*, 2002; Savvides, 2003; Hare *et al.*, 2007). Because of its importance for T4SS functions, Cag α is a target for T4SS inhibitors. We have previously identified the small molecule 1G2 that binds Cag α and reduces its ATPase activity *in vitro* (Arya *et al.*, 2019). We also showed that 1G2 significantly reduces the production of proinflammatory cytokines secreted by gastric adenocarcinoma (AGS) cells in response to *H. pylori* infection, suggesting that it may have potential for development as an anti-virulence drug that attenuates the pathogenicity of the pathogen (Arya *et al.*, 2019).

Here, we describe the genetic and biochemical variability of antibiotic-resistant *H. pylori* strains isolated from patient biopsies in Québec (Canada) and two *H. pylori* control strains. Seven of the 13 analyzed strains carry the *cagPAI*. We characterized the CagA EPIYA and CM motifs as well as the amino-acid variations in the CagL protein showing considerable variability. We also analyzed the effects of co-cultivation with the *H. pylori* strains on IL-8 production, on cytoskeletal changes in epithelial gastric cells and on the production of extracellular T4SS pili. Finally, we demonstrated the effects of the 1G2 molecule on the strains suggesting that this molecule may have potential for development as an anti-virulence treatment.

iii. Materials and Methods

a. *Bacterial strains, cell lines and culture conditions*

H. pylori strains 26695 (ATCC700392) and ATCC43504 were used as positive controls, and the previously described (Fischer et al., 2002; Arya et al., 2019) Δ cagV (hp0530) mutant recreated in our laboratory was used as a negative control. *H. pylori* strains that were isolated from biopsies of 13 patients at the CHUM (Centre Hospitalier de l'Université de Montréal, Québec, Canada) (Table S1). All the strains were cultivated on Columbia agar base (BD) containing 10% (v/v) horse serum (Wisent Inc.), 5% (v/v) laked horse Blood (Wisent Inc.) with β -cyclodextrin (2 mg/ml), vancomycin (10 μ g/ml) and amphotericin B (10 μ g/ml). Chloramphenicol (34 μ g/ml) was added in case of the Δ cagV strain to select for the chloramphenicol (cam) gene cassette used to disrupt the gene. For liquid cultures, brain heart infusion (BHI) media (Oxoid) was supplemented with 10% fetal bovine serum (FBS) and appropriate antibiotics. Bacteria were cultivated at 37°C in an incubation container under microaerophilic conditions (5% oxygen, 10% CO₂, GasPak™ EZ Gas BD). AGS cells (CRL-1739) were grown at 37°C in F12K media (Wisent Inc.) with 10% (v/v) FBS (Wisent Inc.) in a 5% CO₂-containing atmosphere.

Antimicrobial susceptibility testing for *H. pylori* was done using metronidazole and clarithromycin Etest strips. *H. pylori* clinical strains and control strain, cultured on blood agar plates, were suspended in NaCl 0.45% 2 ml for a McFarland no. 2 standard, these suspensions were inoculated on 5% sheep blood agar plates with sterile swabs. The plates on which Etest strips were added, one strip by plate, were incubated at 37°C, in a microaerobic atmosphere (5% O₂, 10% CO₂, and 85% N₂) for 72 h. The minimal inhibitory concentration (MIC) was the one at the intersection of *H. pylori* growth on the strip. The susceptible, intermediate and resistant criteria for clarithromycin were those of CLSI (Clinical and Laboratory Standards Institute) guidelines. The susceptible and resistant criteria for metronidazole were those of EUCAST (European Committee on Antimicrobial Susceptibility Testing) guidelines (Best *et al.*, 2003; Wayne, 2016; *euca*st: *Clinical breakpoints and dosing of antibiotics*, no date).

b. Extraction of bacterial genomic DNA and analysis of the sequences

The extraction of bacterial genomic DNA was performed using the GenElute Bacterial Genomic DNA kit (Sigma Aldrich), according to the instructions of the manufacturer and sequenced using the Sanger sequencing on an ABI 3730 sequencer. The sequences has been analysed using the SnapGene Viewer 5.3.2 and aligned using <https://www.genome.jp/tools-bin/clustalw> (with protein alignment default setting).

c. Infection of AGS cells with H. pylori strains

AGS cells cultivated at 7×10^5 cells/well density in 6-well plates were infected for 4h with *H. pylori* at a multiplicity of infection (MOI) of 1:100. *H. pylori* were first pre-incubated for 1h in F12K media with 10% FBS with or without 1G2 at a concentration of 200 μ M at 37°C in a 5% CO₂-containing atmosphere.

d. Imaging the AGS cell “Hummingbird” phenotype by interference contrast microscopy

AGS cells cultivated at a density of 6×10^5 cells/well in 6-well plates were infected with overnight cultures of *H. pylori* at a MOI of 100:1. After 4h of incubation under microaerophilic conditions, the media was removed, and the wells were washed twice with cold PBS. AGS cells were fixed with 2.5% glutaraldehyde and visualized with a Nikon Eclipse TE2000U microscope.

e. Analysis of IL-8 secretion by AGS cells

After 4h of infection, supernatants were sampled and centrifuged at 15,000 g to remove cells and debris and frozen at -20°C. The level of IL-8 in cell culture supernatants was determined using a Human IL-8 Uncoated ELISA kit (Invitrogen, ThermoFisher Scientific Inc.).

f. Sample preparation and western blotting

After 4h of infection, the cells were wash with phosphate-buffered saline (Wisent Inc.) and lysed in RIPA Buffer (50 mM Tris-HCl pH 8.0, 150 mM sodium chloride, 1.0% Igepal CA-630 NP-40,

0.5% sodium deoxycholate, 0.1% sodium dodecyl sulfate), complemented with a protease inhibitor cocktail for mammalian tissues (Sigma Aldrich) and a phosphatase inhibitor cocktail for tyrosine protein phosphatases, acid and alkaline phosphatases (Sigma Aldrich). The cells were harvested, incubated at 95°C for 5 min with SDS-PAGE sample buffer and centrifuged for 10 min at 10,000 rpm, followed by SDS-PAGE and western blotting. The production of proteins was assessed with monoclonal mouse anti-*Helicobacter pylori* CagA (Cat.# 3HE70ccm, HP-1811cc, HyTest Ltd.) and rabbit Cag α antiserum (Abcam). The actin has been identified using the Antibody Anti- β -Actin Antibody (C4): m-IgG Fc BP-HRP (Santa Cruz, sc-528515). The secondary antibodies (rabbit and mouse) were purchased from Biorad and the HRP signal was developed using Clarity Western ECL Substrate (Biorad).

g. Sample preparation and scanning electron microscopic analysis

AGS cells were cultivated on round cover glasses (Fisherbrand) at 6×10^5 cells/well density in 6-well plates. The cells were infected with *H pylori* for 4h as explained above, washed with cold phosphate buffer (PB 0.1 M), fixed in 4% paraformaldehyde/0.1% glutaraldehyde for 30 min at 4°C, followed by another wash in PB. The samples were then incubated in osmium tetroxide 4% (0.1%) for 1 hour at 4°C, followed by washing with PB. The samples were then dehydrated using a series of ethanol dilutions for 15 min each (30%, 50%, 70%, 80%, 90%, 95%, 100%, 100%), followed by drying using critical point dryer using the Leica EM CPD300. Then cells were then coated with 5 nm of carbon using the Leica EM ACE600. The sample were visualised using a Hitachi Regulus 8220 scanning electron Microscope. The length and number of T4SS pili was measured using ImageJ software.

h. Statistical analysis

All the statistical analyses were performed using GraphPad Prism.

iv. Results

a. *Analysis of the cagPAI in H. pylori clinical isolates*

We studied 13 *H. pylori* strains isolated from patient biopsies from 2017 to 2018 at the CHUM (Centre Hospitalier de l'Université de Montréal) presenting a resistance to clarithromycin and/or metronidazole, and two ATCC control strains, strain 26695 and ATCC43504 (Table S1). After extraction of bacterial genomic DNA, PCR amplification of the *cagA* and *cagL* genes was performed to determine the presence of the *cagPAI* (Figure S1, Table S2). The *vacA* gene, which encodes for the vacuolating cytotoxin and is present in virtually all *H. pylori* strains (Cover and Blanke, 2005), was used as a control for PCR amplifications to confirm the identity of *H. pylori*; all strains were *vacA* positive (data not shown). Among the 13 clinical *H. pylori* strains, seven are *cagPAI*-positive as were the two reference strains from the ATCC (Table 1). Out of the seven *cagPAI*-positive strains, four (#3793, #3813, #3822 and #3830) are readily cultivatable under laboratory conditions and we selected them for the rest of this study.

b. *Analysis of the variability of the CagA and CagL sequences*

CagA displays C-terminal variability, which involves different types and/or numbers of EPIYA repeat sequences, and this diversity may correlate with differences of their virulence and distinct clinical outcomes (Hatakeyama and Higashi, 2005; Zhang *et al.*, 2015). The *cagA* PCR products of the *cagPAI* positive strains were sequenced, followed by comparative analysis of the EPIYA motifs, CM types and A/T polymorphisms (Table 2 and Figure S2). Most of the strains comprise a Western CagA type (EPIYA-ABC) with two CM motifs, one inside the EPIYA-C and one distal to the EPIYA-C segment. Interestingly, the clinical isolate #3793 carries both the Western CM motif (CM^W) and the East Asian CM motif (CM^{EA}). The clinical strain #3830 contains an East Asian type (EPIYA-ABD) with one CM^{EA} motif distal to the EPIYA-C segment. Finally, the A/T polymorphism is present in the EPIYA-B motifs of the clinical strain #3822 and in the reference strain 26695.

Next, we PCR-amplified the upstream regions of *cagL* gene, followed by sequencing and alignment to the CagL sequences from the *H. pylori* reference strain 26695 (Figure S3). The alignment shows that only two clinical strains (#3793 and #3822) do not contain the characteristic Glu59 residue but a Lysine, and that all of them contain the residues Asn201 and Ile234. These residues were previously reported to occur at higher rates in strains from gastric cancer patients (Ogawa *et al.*, 2017). We also observe other sequence variations supporting that the strains have diverse origins.

c. Effect of infection with H. pylori on co-cultivated AGS cells

CagA translocation into epithelial cells induces dysregulation of cellular signaling leading to the so-called “Hummingbird” phenotype, characterized by spreading and elongation of the cells (Segal *et al.*, 1999). We co-cultivated AGS cells with the *H. pylori* strains, followed by interference contrast microscopy to monitor cell shape and counting of the proportion of cells displaying the Hummingbird phenotype (Figure 1). No morphological changes are observed in AGS cells alone and the number was low (up to 3%) in the case of cells incubated with the avirulent $\Delta cagV$ strain. Incubation with strains 26695, #3793 and #3813 induces the Hummingbird phenotype in 13% to 14% of the cells, respectively. In the case of strain #3822 and #3830, we observe that a larger number of cells (23% and 29%) display the characteristic morphological changes (Figure 1).

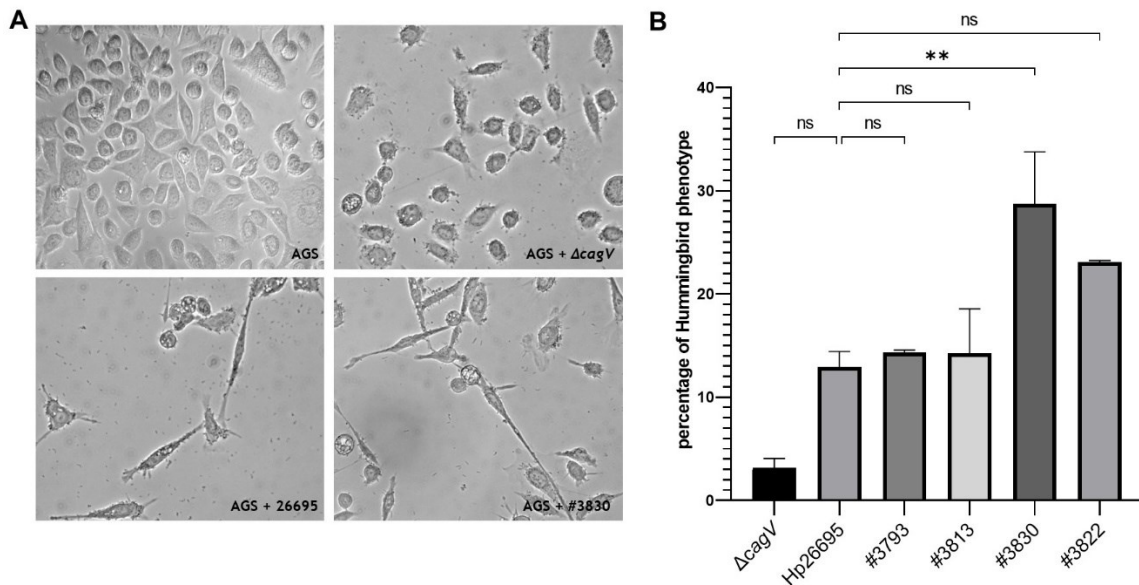


Figure 1. Hummingbird phenotype induced by *H. pylori* infection. (A) AGS cells were infected for four hours with *H. pylori* strains at MOI 100, followed by washing and the adherent cells were fixed and observed using interference contrast microscopy. Negative controls (AGS) and elongated cells induced by the infection with Δ cagV, Hp26695 and #3830 strains are shown as examples; each image represents a representative example for each condition. (B) Elongated cells were counted, and the results are represented as a percentage of total cells. The data represent means and standard deviations of duplicate experiments with at least 500 cells for each condition. **: $p < 0.05$, Anova test.

We next analyzed the levels of IL-8 produced by the AGS cells in response to infection with the *H. pylori* strains. We observed that infection with the #3813 strains induces lower levels of IL-8 production than the 26695 reference strain. In contrast, strains #3793, #3822 and #3830 strains induce IL-8 production to comparable levels as 26695 (Figure 2).

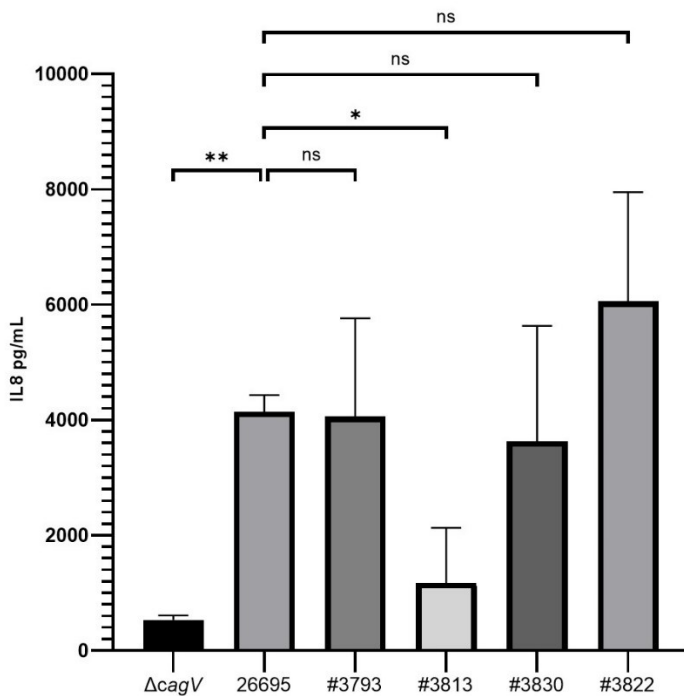


Figure 2. Interleukin-8 production by AGS cells infected with *H. pylori* strains. AGS cells were infected for 24h with the different *H. pylori* strains and the amounts of secreted

IL-8 were measured by ELISA (n=4). ** p<0.005, * p< 0.01, One-way ANOVA, ns: non-significant.

d. Molecule 1G2 reduces IL-8 secretion of some H. pylori clinical isolates

We previously described the 1G2 molecule that inhibits Cag α ATPase activity and significantly reduces the pro-inflammatory response induced by infection with *H. pylori* strain 26695 (Arya *et al.*, 2019). To assess whether this molecule has potential for application as inhibitor of the virulence of clinical strains we tested the impact on strains #3793, #3813, #3822 and #3830. We observed that co-incubation with 1G2 at 200 μ M concentration significantly decreases the production IL-8 in the case of strain #3793 as well as in the 26695 control. In contrast, in the case of strains #3813, #3830 and #3822, we do not observe a significant difference of IL8 induction in the presence of 1G2 (Figure 3A). Since the inhibitor 1G2 may also affect the stability of its target, we also monitored levels of the oncoprotein CagA and of Cag α using western blotting (Figure 3B). We do not observe differences of the levels of CagA in the presence or in the absence of 1G2. In strain #3830 the protein is not detected by the antibody used, suggesting a different epitope localised between the Asp562 and Gln795, epitope recognised by the antibody used. Similarly, 1G2 has no effect on the levels of Cag α suggesting that it does not negatively impact the stability of Cag proteins (Arya *et al.*, 2019).

(figure S5) (B). The results of the IL-8 quantification were analyzed by pairs comparing the non-treated result (100% induction) with the treated results. The Δ cagV strain was used as negative control and analyzed using the strain 26695 as 100%. (n=6). Lad : molecular weight Ladder ** p<0.005, * p< 0.01, one-way ANOVA, ns: non-significant.

e. Molecule 1G2 affects the formation of T4SS pili

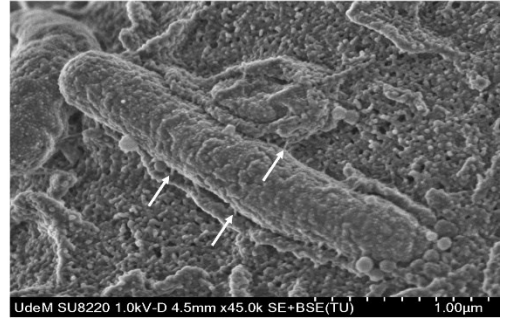
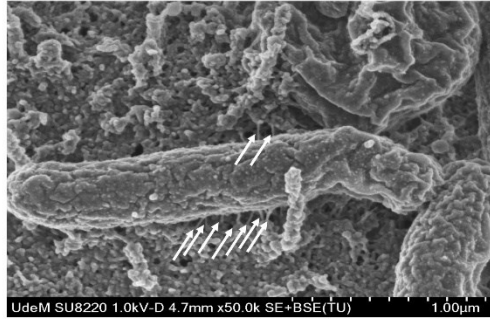
As an alternative approach to measure the activity of the T4SS, we monitored the formation of T4SS pili during the infection of AGS cells using scanning electron microscopy (SEM) in the presence or in the absence of 1G2 (Figure 4A). We observe an average of 14-15 T4SS pili per bacterium for the strains 26695 and #3793 in the absence of 1G2 (Figure 4B). In the presence of 1G2, the number of pili is drastically reduced, and we observe on average three T4SS pili per cell in both strains (Figure 4B). We do not observe any T4SS pili in strains #3813 and #3830 in the presence or in the absence of 1G2, suggesting that those strains are not capable of forming a T4SS pili. Finally, in strain #3822 1G2 does not have an impact on the number of T4SS pili (12/cell), which correlates with the absence of an effect on IL8 induction (Figure 4B, Figure 3A).

A 1G2

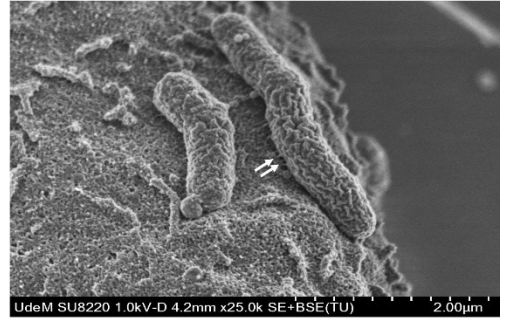
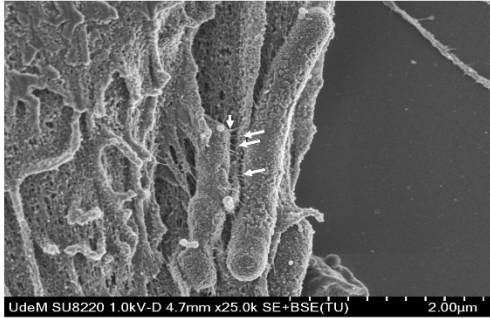
-

+

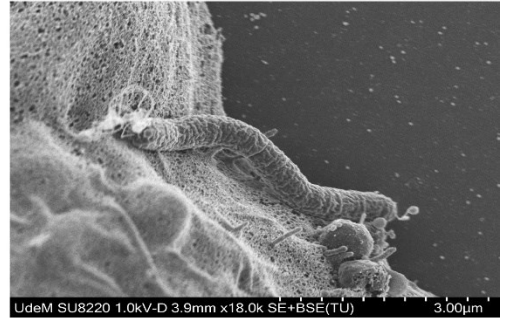
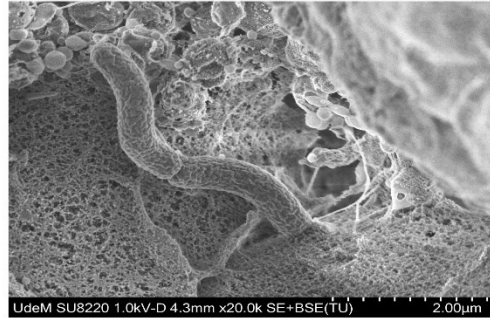
26695



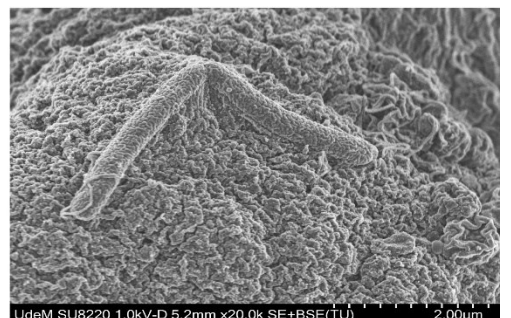
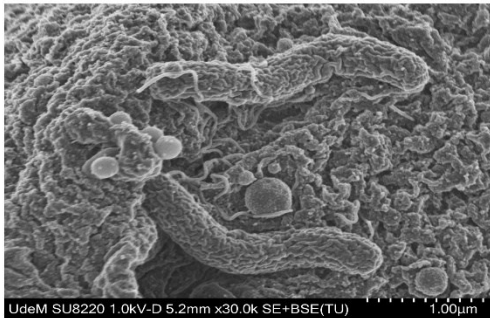
#3793



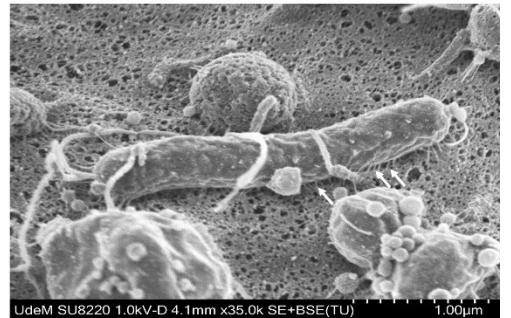
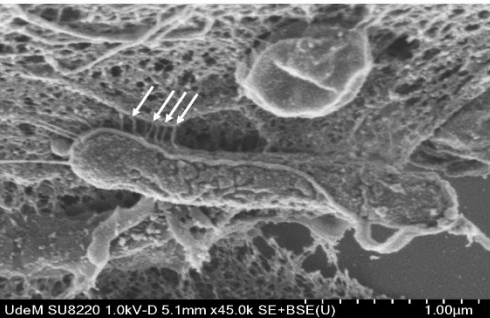
#3813



#3830



46 #3822



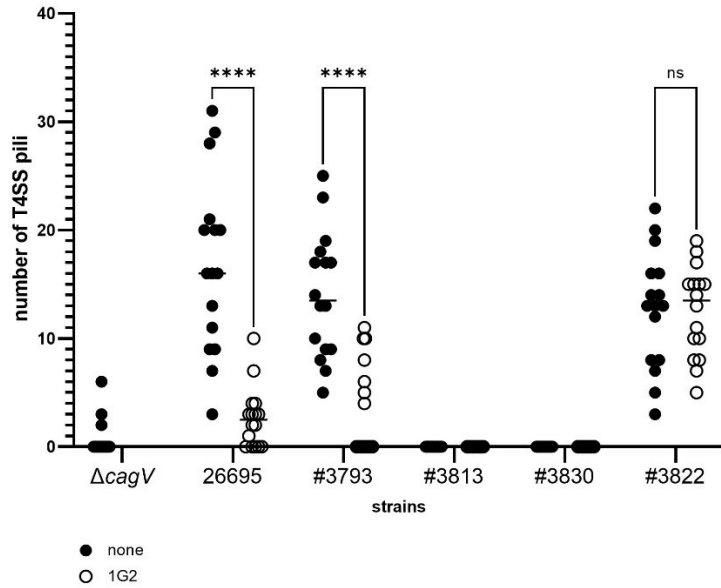
B

Figure 4. 1G2 affects the number of T4SS pili during AGS infection. *H. pylori* strains were pre-incubated without (-) or with (+) 200 μ M of 1G2, followed by co-cultivation with AGS cells for 4h and the samples were then fixed and analyzed using scanning electron microscopy. T4SS pili are identified with arrows (A) and the T4SSpili were counted using ImageJ (B) (n = 16 images from 2 infection). The $\Delta cagV$ strain was used as negative control. ****: $p < 0.001$, Student's T-test, ns: non-significant

v. Discussion

The presence of a functional *cag* pathogenicity island (*cagPAI*) in *H. pylori* strains has been demonstrated to increase the risk for the development of more severe forms of gastric diseases (Hatakeyama and Higashi, 2005; Hatakeyama, 2014; Yong *et al.*, 2015; Cover, 2016). Here, we characterized 13 antibiotic-resistant *H. pylori* strains isolated from patient biopsies in Québec. We showed that seven of the strains carry the *cagA* and *cagL* genes and were thus considered as *cagPAI* positive and we further characterized the virulence phenotype of four strains (#3793, #3813, #3822 and #3830) that could be readily cultivated in laboratory conditions. To assess the virulence of *H. pylori* strains we monitored the production of Cag proteins, the induction of IL-8 production, the induction of changes of the cytoskeleton (“hummingbird” phenotype) and the formation of T4SS pili. The clinical strains induce a hummingbird phenotype in AGS cells that is similar to the 26695 control and the cytoskeletal changes are even more pronounced in strain #3830. Similarly, all clinical strains induce IL-8 production in AGS cells. These data suggest that all the clinical strains carry functional T4SSs and that their effects can be monitored using the established AGS cell infection assay.

We also monitored the production of T4SS pili after co-incubation with AGS cells by scanning electron microscopy and this constitutes a novel quantifiable assay for T4SS function. We observe between 12 and 15 T4SS pili per cell in the 26995 strain and in the clinical strains #3793 and #3822. In contrast, we do not observe any T4SS pili in strains #3813, #3830. Both strains induce IL-8 production and cytoskeletal changes after co-incubation with AGS cells suggesting that they do not need elaborate extracellular structures to translocate virulence factors. This constitutes a marked difference to previously characterized *H. pylori* strains even if we cannot exclude that these strains assemble very short T4SS pili that can not be detected by SEM. In addition, the imaging was done using only one angle, limiting the observation of the interaction between the bacteria and cells.

Comparative analysis of the CagA C-terminal domains showed significant variability among the *H. pylori* strains. Interestingly, strain #3793 carries both eastern and western CM motifs (CM^W/CM^{EA}). The CM motif has been demonstrated to serve as a binding site for PAR1b and this

interaction is highly influenced by the nature of the motif and its numbers of repetition (Nishikawa *et al.*, 2016). The presence of this combination of CM motifs may therefore influence the virulence of strain #3793, but differences are not apparent when IL-8 production or effects on cytoskeletal changes are monitored. Similarly, the differences between the CagL sequences of the different strain do not correlate with effects on AGS cells, but they may impact the pathogenicity in patients.

Finally, we tested the effects of the previously characterized 1G2 molecule on the antibiotic resistant *H. pylori* strains (Arya *et al.*, 2019). We showed that 1G2 significantly decreases T4SS activity in strains 26695 and #3793 as measured by IL-8 production of AGS cells and assembly of T4SS pili. In contrast, 1G2 has no effect on the production of IL-8 in strains #3813, #3830 and #3822 or on the production of T4SS pili in strain #3822.

Interestingly, the strain #3813 and #3830, considered as T4SS positives, didn't present T4SS pili using SEM imaging. The images and the low level of IL-8 induced suggests that the strain #3813 does not carry a functional T4SS. As for the strain #3830, the high level of IL-8 induced, and the high Hummingbird phenotype induced suggest that there is a CagA effect. As suggested previously, this strain could carry very short T4SS pili not visible using only SEM imaging or could possess another delivery system. The observation for the strain #3822 can be explain as the strain carry a mutation on one amino acid identified as important for 1G2 binding with Cag α that would explain the results (figure S4) (Morin *et al.*, 2023).

These results suggest that 1G2 may have potential for the development of treatments against some clinical strains, but that more potent derivatives would have to be developed to have broad clinical impact. 1G2 has no effect on the levels of CagA or of the target Cag α showing that it does not destabilize its target (Arya *et al.*, 2019). Interestingly, 1G2 inhibits the formation of T4SS pili in strains 26695 and #3793 suggesting that this is the primary mechanism for the effect of this molecule on *H. pylori* virulence.

vi. Study materials

Data, analytic methods, and study materials will be made available to other researchers upon request addressed to the corresponding author.

vii. Funding and Acknowledgments:

This work was supported by grants from the Cancer Research Society, the Charles Bowers Memorial Fund, the Bergeron-Jetté Foundation (CRS, #23404 and #25102) and the Natural Sciences and Engineering Research Council (NSERC, #RGPIN-2017-05123) to C.B. We grateful to Dr. Dainelys Guadarrama Bell and Dr. Nanci at the Université de Montréal electron microscopy facility for technical support and assistance.

viii. Declaration of interests:

The authors declare no competing interests.

ix. Author contributions:

F.O. designed and carried out experiments and analyzed data for the genomic part and the primary design of the infection protocol. (manuscript draft and revisions, genomic part and the primary design of the infection protocol)

C.M. designed the infection part and carried out experiments and analyzed data. (Manuscript draft, improvement of the infection protocol and infection assays)

M.B. contributed resources, analyzed data

C.G. contributed resources, analyzed data

C.B. designed experiments, analyzed data and wrote the manuscript with input from all the co-authors. All co-authors have approved the final version of this manuscript.

x. References

- Arya, T. *et al.* (2019) 'Fragment-based screening identifies inhibitors of ATPase activity and of hexamer formation of Cag α from the *Helicobacter pylori* type IV secretion system', *Scientific Reports*, 9(1), p. 6474. Available at: <https://doi.org/10.1038/s41598-019-42876-6>.
- Backert, S. *et al.* (2008) 'Phosphorylation of tyrosine 972 of the *Helicobacter pylori* CagA protein is essential for induction of a scattering phenotype in gastric epithelial cells: Function of the *H. pylori* CagA protein', *Molecular Microbiology*, 42(3), pp. 631–644. Available at: <https://doi.org/10.1046/j.1365-2958.2001.02649.x>.
- Barden, S. and Niemann, H.H. (2015) 'Adhesion of Several Cell Lines to *Helicobacter pylori* CagL Is Mediated by Integrin α V β 6 via an RGDLXXL Motif', *Journal of Molecular Biology*, 427(6), pp. 1304–1315. Available at: <https://doi.org/10.1016/j.jmb.2015.01.006>.
- Best, L.M. *et al.* (2003) 'Multilaboratory Comparison of Proficiencies in Susceptibility Testing of *Helicobacter pylori* and Correlation between Agar Dilution and E Test Methods', *Antimicrobial Agents and Chemotherapy*, 47(10), pp. 3138–3144. Available at: <https://doi.org/10.1128/AAC.47.10.3138-3144.2003>.
- Covacci, A. *et al.* (1999) '*Helicobacter pylori* Virulence and Genetic Geography', *Science*, 284(5418), pp. 1328–1333. Available at: <https://doi.org/10.1126/science.284.5418.1328>.
- Cover, T.L. (2016) '*Helicobacter pylori* Diversity and Gastric Cancer Risk', *mBio*, 7(1), pp. e01869-15, [/mbio/7/1/e01869-15.atom](https://doi.org/10.1128/mBio.01869-15). Available at: <https://doi.org/10.1128/mBio.01869-15>.
- Cover, T.L. and Blanke, S.R. (2005) '*Helicobacter pylori* VacA, a paradigm for toxin multifunctionality', *Nature Reviews Microbiology*, 3(4), pp. 320–332. Available at: <https://doi.org/10.1038/nrmicro1095>.
- Cover, T.L. and Blaser, M.J. (1999) '*Helicobacter pylori* factors associated with disease', *Gastroenterology*, 117(1), pp. 257–260. Available at: [https://doi.org/10.1016/S0016-5085\(99\)70575-5](https://doi.org/10.1016/S0016-5085(99)70575-5).

eucast: Clinical breakpoints and dosing of antibiotics (no date). Available at: https://www.eucast.org/clinical_breakpoints (Accessed: 19 July 2023).

Fischer, W. *et al.* (2002) ‘Systematic mutagenesis of the *Helicobacter pylori* *cag* pathogenicity island: essential genes for CagA translocation in host cells and induction of interleukin-8: Functional dissection of the *H. pylori* type IV secretion system’, *Molecular Microbiology*, 42(5), pp. 1337–1348. Available at: <https://doi.org/10.1046/j.1365-2958.2001.02714.x>.

Gall, A. *et al.* (2017) ‘TIFA Signaling in Gastric Epithelial Cells Initiates the *cag* Type 4 Secretion System-Dependent Innate Immune Response to *Helicobacter pylori* Infection’, *mBio*. Edited by M.J. Blaser, 8(4), pp. e01168-17, [/mbio/8/4/e01168-17.atom](https://doi.org/10.1128/mBio.01168-17). Available at: <https://doi.org/10.1128/mBio.01168-17>.

Gatta, L. *et al.* (2013) ‘Global eradication rates for *Helicobacter pylori* infection: systematic review and meta-analysis of sequential therapy’, *BMJ*, 347(aug07 1), pp. f4587–f4587. Available at: <https://doi.org/10.1136/bmj.f4587>.

Hare, S. *et al.* (2007) ‘Identification, structure and mode of action of a new regulator of the *Helicobacter pylori* HP0525 ATPase’, *The EMBO Journal*, 26(23), pp. 4926–4934. Available at: <https://doi.org/10.1038/sj.emboj.7601904>.

Hatakeyama, M. (2014) ‘*Helicobacter pylori* CagA and Gastric Cancer: A Paradigm for Hit-and-Run Carcinogenesis’, *Cell Host & Microbe*, 15(3), pp. 306–316. Available at: <https://doi.org/10.1016/j.chom.2014.02.008>.

Hatakeyama, M. and Higashi, H. (2005) ‘*Helicobacter pylori* CagA: a new paradigm for bacterial carcinogenesis’, *Cancer Science*, 96(12), pp. 835–843. Available at: <https://doi.org/10.1111/j.1349-7006.2005.00130.x>.

Higashi, H. *et al.* (2002) ‘Biological activity of the *Helicobacter pylori* virulence factor CagA is determined by variation in the tyrosine phosphorylation sites’, *Proceedings of the National*

Academy of Sciences, 99(22), pp. 14428–14433. Available at: <https://doi.org/10.1073/pnas.222375399>.

Hilleringmann, M. *et al.* (2006) ‘Inhibitors of *Helicobacter pylori* ATPase CagA block CagA transport and cag virulence’, *Microbiology*, 152(10), pp. 2919–2930. Available at: <https://doi.org/10.1099/mic.0.28984-0>.

Jurik, A. *et al.* (2010) ‘The Coupling Protein Cag β and Its Interaction Partner CagZ Are Required for Type IV Secretion of the *Helicobacter pylori* CagA Protein’, *Infection and Immunity*, 78(12), pp. 5244–5251. Available at: <https://doi.org/10.1128/IAI.00796-10>.

Krause, S. *et al.* (2000) ‘Sequence-related protein export NTPases encoded by the conjugative transfer region of RP4 and by the *cag* pathogenicity island of *Helicobacter pylori* share similar hexameric ring structures’, *Proceedings of the National Academy of Sciences*, 97(7), pp. 3067–3072. Available at: <https://doi.org/10.1073/pnas.97.7.3067>.

Kutter, S. *et al.* (2008) ‘Protein Subassemblies of the *Helicobacter pylori* Cag Type IV Secretion System Revealed by Localization and Interaction Studies’, *Journal of Bacteriology*, 190(6), pp. 2161–2171. Available at: <https://doi.org/10.1128/JB.01341-07>.

Kwok, T. *et al.* (2007) ‘*Helicobacter* exploits integrin for type IV secretion and kinase activation’, *Nature*, 449(7164), pp. 862–866. Available at: <https://doi.org/10.1038/nature06187>.

Machón, C. *et al.* (2002) ‘TrwD, the Hexameric Traffic ATPase Encoded by Plasmid R388, Induces Membrane Destabilization and Hemifusion of Lipid Vesicles’, *Journal of Bacteriology*, 184(6), pp. 1661–1668. Available at: <https://doi.org/10.1128/JB.184.6.1661-1668.2002>.

Morin, C. *et al.* (2023) *Structure-based design of small molecule inhibitors of the cagT4SS ATPase CagA of Helicobacter pylori*. preprint. *Biochemistry*. Available at: <https://doi.org/10.1101/2023.11.06.565890>.

- Nishikawa, H. *et al.* (2016) 'Impact of structural polymorphism for the *Helicobacter pylori* CagA oncoprotein on binding to polarity-regulating kinase PAR1b', *Scientific Reports*, 6(1), p. 30031. Available at: <https://doi.org/10.1038/srep30031>.
- Odenbreit, S. (2000) 'Translocation of *Helicobacter pylori* CagA into Gastric Epithelial Cells by Type IV Secretion', *Science*, 287(5457), pp. 1497–1500. Available at: <https://doi.org/10.1126/science.287.5457.1497>.
- Ogawa, H. *et al.* (2017) 'Genetic variants of *Helicobacter pylori* type IV secretion system components CagL and CagI and their association with clinical outcomes', *Gut Pathogens*, 9(1), p. 21. Available at: <https://doi.org/10.1186/s13099-017-0165-1>.
- Ren, S. *et al.* (2006) 'Structural Basis and Functional Consequence of *Helicobacter pylori* CagA Multimerization in Cells', *Journal of Biological Chemistry*, 281(43), pp. 32344–32352. Available at: <https://doi.org/10.1074/jbc.M606172200>.
- Savvides, S.N. (2003) 'VirB11 ATPases are dynamic hexameric assemblies: new insights into bacterial type IV secretion', *The EMBO Journal*, 22(9), pp. 1969–1980. Available at: <https://doi.org/10.1093/emboj/cdg223>.
- Segal, E.D. *et al.* (1999) 'Altered states: Involvement of phosphorylated CagA in the induction of host cellular growth changes by *Helicobacter pylori*', *Proceedings of the National Academy of Sciences*, 96(25), pp. 14559–14564. Available at: <https://doi.org/10.1073/pnas.96.25.14559>.
- Selbach, M. *et al.* (2002) 'Src Is the Kinase of the *Helicobacter pylori* CagA Protein in Vitro and in Vivo', *Journal of Biological Chemistry*, 277(9), pp. 6775–6778. Available at: <https://doi.org/10.1074/jbc.C100754200>.
- Tammer, I. *et al.* (2007) 'Activation of Abl by *Helicobacter pylori*: A Novel Kinase for CagA and Crucial Mediator of Host Cell Scattering', *Gastroenterology*, 132(4), pp. 1309–1319. Available at: <https://doi.org/10.1053/j.gastro.2007.01.050>.

- Tegtmeier, N. *et al.* (2017) ‘Subversion of host kinases: a key network in cellular signaling hijacked by *Helicobacter pylori* CagA: Host kinases hijacked by CagA’, *Molecular Microbiology*, 105(3), pp. 358–372. Available at: <https://doi.org/10.1111/mmi.13707>.
- Varga, M.G. *et al.* (2016) ‘Pathogenic *Helicobacter pylori* strains translocate DNA and activate TLR9 via the cancer-associated cag type IV secretion system’, *Oncogene*, 35(48), pp. 6262–6269. Available at: <https://doi.org/10.1038/onc.2016.158>.
- Viala, J. *et al.* (2004) ‘Nod1 responds to peptidoglycan delivered by the *Helicobacter pylori* cag pathogenicity island’, *Nature Immunology*, 5(11), pp. 1166–1174. Available at: <https://doi.org/10.1038/ni1131>.
- Wayne, P. (2016) *Methods for Antimicrobial Dilution and Disk Susceptibility Testing of Infrequently Isolated or Fastidious Bacteria*. (Clinical and Laboratory Standards Institute). Available at: https://webstore.ansi.org/preview-pages/CLSI/preview_CLSI+M45-Ed3.pdf.
- Wiedemann, T. *et al.* (2012) ‘*Helicobacter pylori* CagL dependent induction of gastrin expression via a novel $\alpha\beta 5$ -integrin–integrin linked kinase signalling complex’, *Gut*, 61(7), pp. 986–996. Available at: <https://doi.org/10.1136/gutjnl-2011-300525>.
- Yeh, Y.-C. *et al.* (2011) ‘*H. pylori* cagL amino acid sequence polymorphism Y58E59 induces a corpus shift of gastric integrin $\alpha 5\beta 1$ related with gastric carcinogenesis: *H. pylori* cagL & GASTRIC INTEGRIN’, *Molecular Carcinogenesis*, 50(10), pp. 751–759. Available at: <https://doi.org/10.1002/mc.20753>.
- Yeo, H.-J. *et al.* (2000) ‘Crystal Structure of the Hexameric Traffic ATPase of the *Helicobacter pylori* Type IV Secretion System’, *Molecular Cell*, 6(6), pp. 1461–1472. Available at: [https://doi.org/10.1016/S1097-2765\(00\)00142-8](https://doi.org/10.1016/S1097-2765(00)00142-8).
- Yong, X. *et al.* (2015) ‘*Helicobacter pylori* virulence factor CagA promotes tumorigenesis of gastric cancer via multiple signaling pathways’, *Cell Communication and Signaling*, 13(1), p. 30. Available at: <https://doi.org/10.1186/s12964-015-0111-0>.

Zhang, X.-S. *et al.* (2015) 'A Specific A/T Polymorphism in Western Tyrosine Phosphorylation B-Motifs Regulates *Helicobacter pylori* CagA Epithelial Cell Interactions', *PLOS Pathogens*. Edited by S.R. Blanke, 11(2), p. e1004621. Available at: <https://doi.org/10.1371/journal.ppat.1004621>.

xi. Tables

Table 1. *cagPAI* positive and negative *H. pylori* strains

<i>cagPAI</i> positive strains	<i>cagPAI</i> negative strains
26695	3800
ATCC 43504	3811
3723	3834
3763	3838
3783	3855
3793	3859
3813	
3822	
3830	

Table 2. Characteristics of the CagA isoforms from the *cagPAI* positive *H. pylori* strains.

<i>H. pylori</i> isolates	EPIYA motif type	EPIYA-B polymorphism	Number of CM motifs	CM motif types	CM motif 1	CM motif 2
26695	ABC	EPIYT	2	CM ^W	FPLKRHDKVDDLKVG	FPLKRHDKVDDLKVG
3793	ABC		2	CM^W/CM^{EA}	<i>id.</i>	FPLRRSAKVEDLKVG
3813	ABC		2	CM ^W	FPLKRHSKVDDLKVG	<i>id.</i>
3822	ABC	EPIYT	2	CM ^W	<i>id.</i>	<i>id.</i>
3830	ABD		1	CM^{EA}		FPLRRSAAVNDLKVG

id : sequence identical to the reference strain ATCC26695 ; amino acid variation in the CM sequence are bolded; CM^W: Western CM motif ; CM^{EA}: East Asian CM motif

xii. Supplementary materials

Table S1. *H. pylori* strains and resistance to antibiotics

<i>H. pylori</i> Strain	Resistance	
	Metronidazole (MIC mg/L)	Clarithromycin (MIC mg/L)
3723	R (256)	R (256)
3763	R (> 256)	R (> 256)
3783	S (0.06)	R (8)
3793	R (> 256)	R (256)
3800	R (128)	S (<= 0.03)
3811	R (> 256)	R (1)
3813	R (128)	R (256)
3822	R (> 256)	R(> 256)
3830	S (0.06)	S (<= 0.03)
3834	R (> 256)	R (32)
3838	R (> 256)	R (16)
3855	R (> 256)	R (32)
3859	R (64)	S (<= 0.03)
ATCC 43504	R	S
26695	S	S

S : susceptible, R : resistant

Table S2. Primers used for PCR amplification and sequencing

vacA-F1	5'-ATGGAAATACAACAAACACACCGCAA-3'
vacA-R1	5'-CATTTTTACTGCTAGTAATCCCTTCTGAA-3'
cagL-F1	5'-AATCTTGAAAAAAAAAAGCCGAC-3'
cagL-R1	5'-TAGCGTCATTAATCAAATAG-3'
cagA-F1	5'-TCAAATACACCAACGCCTCCAA-3'
cagA-R1	5'-CACATTATGCGCAACTATCTTATCA-3'
cagα-F1	5'-GAGCAAAAATAAGACTTATCTCACTTCTTT-3'
cagα-R1	5'-TAACCCTATGAAACTAAAAATAACAACCAA-3'

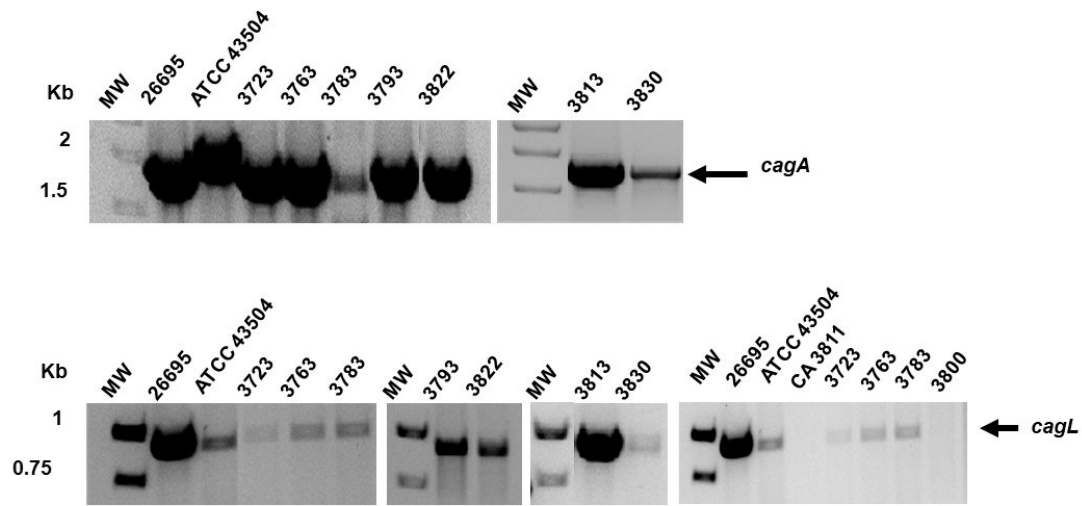


Figure S1. PCR amplification of *cagA* and *cagL* genes from *H. pylori* isolates. PCR amplifications with *cagA*- and *cagL*- specific primers were performed from genomic DNA isolated from the *H. pylori* strains followed by agarose gel analysis. Kb: Kilobases, MW : molecular weight

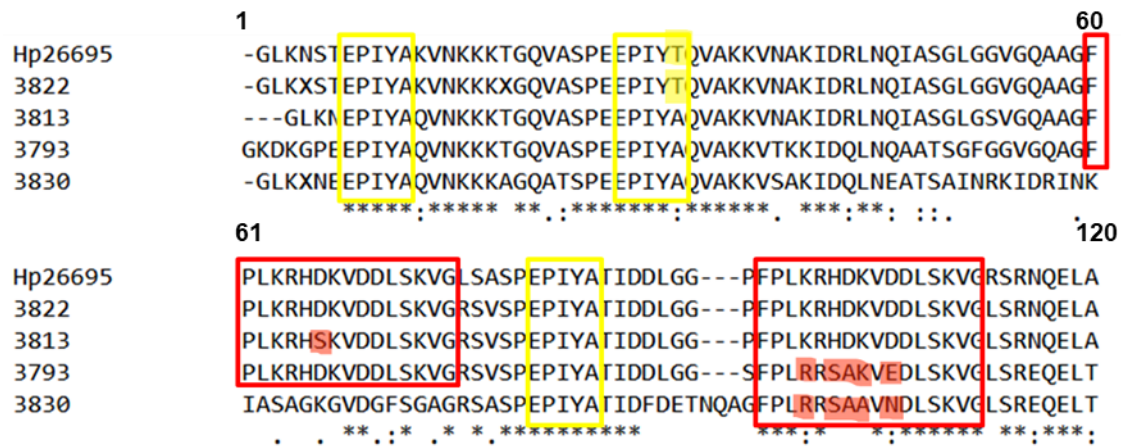


Figure S2. Alignment of the sequences of CagA comprising the three EPIYA motifs. The EPIYA motifs are labelled with yellow boxes and the CM motifs are marked with red boxes; variations inside the sequence are highlighted in the same colors. “*” indicates positions which have a single, fully conserved residue; “:.” indicates that one of the 'strong' groups is fully conserved:-STA, NEQK, NHQK, NDEQ, QHRK, MILV, MILF, HY, FYW; “..” indicates that one of the 'weaker' groups is fully conserved:- CSA, ATV, SAG, STNK, STPA, SGND, SNDEQK, NDEQHK, NEQHRK, FVLIM, HFY ; These are all the positively scoring groups that occur in the Gonnet Pam250 matrix. The strong and weak groups are defined as strong score >0.5 and weak score =<0.5 respectively. https://www.genome.jp/tools/clustalw/clustalw_readme.html

```

1 60
3813 MKTLVKNTIYSFLLL SVLMAEDITSGLKQLDNNTYQETNQQVLKNLDEIFSTTSPSANNEI
3830 MKTLVKNTISSFLLL SVLMAEDITSGLKQLDSTYQETNQQVLKNLDEIFSTTSPSANNEI
Hp26695 MKTLVKNTISSFLLL SVLMAEDITSGLKQLDSTYQETNQQVLKNLDEIFSTTSPSANNEM
3793 MKTLVKNTIFSFLLL SVLMAEDITSGLKQLDSTYQETNQQALKNLDEIFSTTSPSANDKM
3822 MKTLVKNTILSFLLL SVLMAEDITSGLKQLDSTYQETNQQVLKNLDEIFSTTSPSANDKM
*****:*****:*****:*****:*****:
61 120
3813 GQEDALNIKKAAIALRGD.ALLKANFEANELFFISEDVIFKTYMSSPELLLLTYMKINPLD
3830 GXEDALNIKKAAIALRGD.ALLKANFEANELFFISEDVIFKTYMSSPELLLLTYMKINPLD
Hp26695 GEEDALNIKKAAIALRGD.ALLKANFEANELFFISEDVIFKTYMSSPELLLLTYMKINPLD
3793 GEEDALNIKKAAMALRGD.ALLKANFEANELFFISEDVIFKTYMSSPELLLLTYMKINPLD
3822 GEEDALNIKKAAMALRGD.ALLKANFEANELFFISEDVIFKTYMSSPELLLLTYMKINPLD
* *****:*****:*****:*****:*****:
121 180
3813 QNTAEQQCGISDKVLVLYCEGKLEIEQEKQNIRERLETSLKAYQSNIGGTASLITASQTL
3830 QXTAEQQCGISDKVLVLYCEGKLEIEQEKQNIRERLETSLKAYQSNIGGTASLITASQTL
Hp26695 QNTAEQQCGISDKVLVLYCEGKLEIEQEKQNIRERLETSLKAYQSNIGGTASLITASQTL
3793 QKTAEQQCGISDKILVLYCGGGKLEIEQEKQNIRERLEASLKAYQSNIGGTASLIIASQTL
3822 QKTAEQQCGISDKILVLYCEGKLEIEQEKQNIRERLETSLKTYQSNIGGTASLITASQTL
* *****:*****:*****:*****:*****:
181 237
3813 VESLKNKNFIKGIRKLMLAHNKIFLNLYLEELDALERSLEQSKRQYLQERQSSKIIVK
3830 VESLXNKNFIKGIRKLMLAHNKVFLNLYLEELDALERSLEQXKRQYLQERQSSKIIVK
Hp26695 VESLKNKNFIKGIRKLMLAHNKVFLNLYLEELDALERSLEQSKRQYLQERQSSKIIVK
3793 VESLKNKNFIKGIRKLMLAHNKVFLNLYLEELDALERSLEQNKRQYLQERQSSKIIVK
3822 VESLKNKNFIKGIRKLMLAHNKVFLNLYLEELDALERSLEQSKRQYLQERQSSKIIVK
**** *****:*****:*****:*****:

```

Figure S3. Alignment of the CagL sequences from the *cagPAI* positive *H. pylori* strains.

Amino acid residues that occur at a significantly higher rate in isolates from patients with gastric cancer are highlighted in red, all the other variations identified within the alignment are highlighted in yellow. The highly conserved RGD motif that is involved in the interaction with host cell integrins is indicated by a red box. “*” indicates positions which have a single, fully conserved residue; “.” indicates that one of the 'strong' groups is fully conserved: -STA, NEQK, NHQK, NDEQ, QHRK, MILV, MILF, HY, FYW; These are all the positively scoring groups that occur in the Gonnet Pam250 matrix. The strong and weak groups are defined as strong score >0.5 and weak score =<0.5 respectively. https://www.genome.jp/tools/clustalw/clustalw_readme.html


```

1                               60
26695  MTEDRLSAEDKKFLEVERALKEAALNPLRHATEELFGDFLKMENITEICYNGNKVWVWLK
3822   MTEDRLSAEDKKFLEVERALKEAALNPLRHATEELFGDFLKMENITEICYNGNKVWVWLK
*****
61                               120
26695  NNGEWQPFVDRDRKAFSLSRMLMHFARCCASFKKKTIDNYENPILSSNLANGERVQIVLSP
3822   NNGEWQPFVDRDKKAFSLSRMLMHFARCCASFKKKTIDNYENPILSSNLANGERVQIVLSP
*****
121                               180
26695  VTVNDETIISIRIPSKTTYPHSFEEQGFYNLLDNKEQAISAIKDGIAIGKNVIVCGGT
3822   VTVNDETIISIRIPSKTTYPHSFEEQGFYNLLDNKEQAISAIKDGIAIGKNVIVCGGT
*****
181                               240
26695  GSGKTTYIKSIMEFIPKEERIISIEDTEEIVFKHHKNYQLFFGGNITSADCLKSCLRMR
3822   GSGKTTYIKSIMEFIPKEERIISIEDTEEIVFKHHKNYQLFFGGNITSADCLKSCLRMR
*****
241                               300
26695  PDR IILGELRSSEAYDFYNVLCSGHGKTLTTLHAGSSEEAFIRLANMSSNSAARNIKFE
3822   PDR IILGELRSSEAYDFYNVLCSGHGKTLTTLHAGSSEEAFIRLANMSSNSAARNIKFE
*****

```

Figure S4. Alignment of the Caga sequences from the strain 26695 (ATCC700392) and #3822 show a mutation of the Arginine 73 in Lysine.

“*” indicates positions which have a single, fully conserved residue.

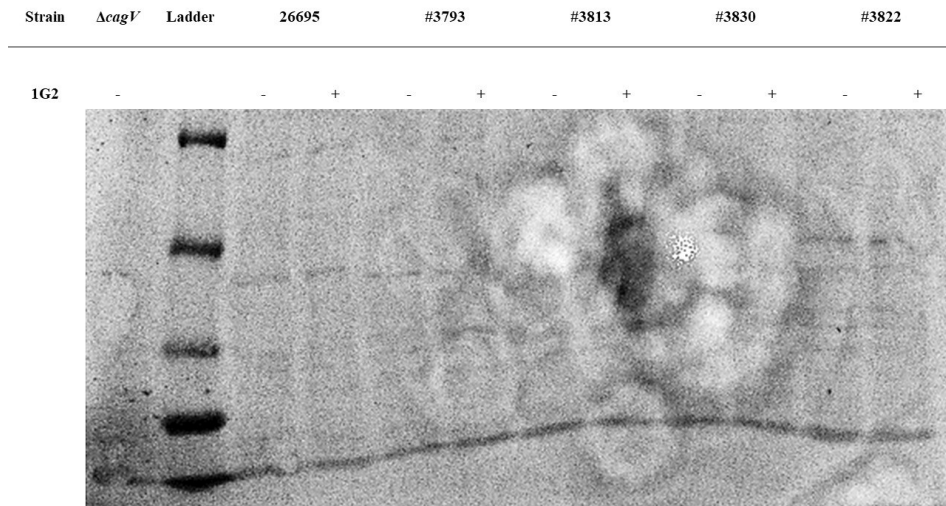


Figure S5. Ponceau coloration of the CagA western blot use for the figure 3. *H. pylori* strains were pre-incubated without or with 200 μ M of 1G2 for 1h. AGS cells were then co-cultured with *H. pylori* strains for 4h and IL-8 induction was measured by ELISA. The levels of CagA were analyzed by SDS-PAGE of cell lysates. The loading control has been evaluated using Ponceau coloration of the membrane.

B. Papier #2 : Conception basée sur la structure de petits inhibiteurs de molécules de l'ATPase CagA du système de sécrétion de type IV (cagT4SS) d'Helicobacter pylori.

Structure-based design of small molecule inhibitors of the cagT4SS ATPase CagA of Helicobacter pylori

¹Claire Morin[#], ¹Vijay Tailor Verma[#], ¹Tarun Arya, ¹Bastien Casu, ²Eric Jolicoeur, ²Réjean Ruel
^{2,3}Anne Marinier, ¹Jurgen Sygusch and ¹Christian Baron*

¹Department of Biochemistry and Molecular Medicine, Faculty of Medicine,
Université de Montréal, Québec, Canada

²Institut de Recherche en Immunologie et Cancérologie, Université de Montréal, Québec, Canada
and

³Department of Chemistry, Faculty of Arts and Sciences
Université de Montréal, Québec, Canada

*Corresponding author

[#]The first two authors made equal contributions to this work

<http://biorxiv.org/lookup/doi/10.1101/2023.11.06.565890>

This is the last version after peer review

i. Abstract

We here describe the structure-based design of small molecule inhibitors of the type IV secretion system of *Helicobacter pylori*. The secretion system is encoded by the *cag* pathogenicity island, and we chose Cag α , a hexameric ATPase and member of the family of VirB11-like proteins, as target for inhibitor design. We first solved the crystal structure of Cag α in a complex with the previously identified small molecule inhibitor 1G2. The molecule binds at the interface between two Cag α subunits and mutagenesis of the binding site identified Cag α residues F39 and R73 as critical for 1G2 binding. Based on the inhibitor binding site we synthesized 98 small molecule derivatives of 1G2 to improve binding of the inhibitor. We used the production of interleukin-8 of gastric cancer cells during *H. pylori* infection to screen the potency of inhibitors and we identified five molecules (1G2_1313, 1G2_1338, 1G2_2886, 1G2_2889 and 1G2_2902) that have similar or higher potency than 1G2. Differential scanning fluorimetry suggested that these five molecules bind Cag α , and enzyme assays demonstrated that some are more potent ATPase inhibitors than 1G2. Finally, scanning electron microscopy revealed that 1G2 and its derivatives inhibit the assembly of T4SS-determined extracellular pili suggesting a mechanism for their anti-virulence effect.

Keywords: *Helicobacter pylori*, *cagPAI*, Cag α , VirB11, ATPase, anti-virulence, type IV secretion system, pili, inhibitors

ii.Introduction

Helicobacter pylori (*H. pylori*) is a Gram-negative bacterium isolated from gastric samples in the 1980s by Warren and Marshall. They demonstrated that the stomach is not sterile and that *H. pylori* causes inflammatory disease while colonizing the stomach (Marshall and Warren, 1984). It was subsequently shown that chronic *H. pylori* colonization leads to gastric disease like ulcer, gastric adenocarcinoma and stomach cancer (Coussens and Werb, 2002; Amieva and Peek, 2016; Blaser, Backert and Pachathundikandi, 2019). *H. pylori* has been associated with humans for more than 1000 years and analysis of a strain from a human 5,300 years-old iceman showed a high degree of similarity with today's *H. pylori* strains (Maixner *et al.*, 2016). Up to 50 to 90% of the human population is colonized by *H. pylori* and its prevalence depend on the geographic localization of populations in the world (Breckan *et al.*, 2016; Hooi *et al.*, 2017). *H. pylori* carry a lot of difference virulence factors for the colonization of the stomach, for the establishment of a niche between epithelial cells of the stomach and others that cause inflammatory responses in human cells (Argent *et al.*, 2008; Amieva and Peek, 2016; Ansari and Yamaoka, 2020). The main virulence factors are the urease that neutralises the acidic environment, the vacuolating cytotoxin A (VacA) and the type IV secretion system (T4SS) (Argent *et al.*, 2008; Ansari and Yamaoka, 2020; Sharndama and Mba, 2022). The T4SS comprises 27 proteins coded by the cytotoxin-associated gene (*cag*) pathogenicity island (*cagPAI*). The T4SS in *H. pylori* is used for the injection of the oncoprotein CagA as well as for the transfer of peptidoglycan fragments (Backert, Tegtmeyer and Selbach, 2010; Backert, Tegtmeyer and Fischer, 2015; Cover, Lacy and Ohi, 2020; Costa *et al.*, 2021). CagA interferes with different metabolic pathways in gastric epithelial cells, leading to depolarisation of the cell, an increase of cell mobility and the loss of tight junctions (Ansari and Yamaoka, 2020; Cheok *et al.*, 2021; Freire de Melo *et al.*, 2022; Jang *et al.*, 2022). The resulting disorganization of gastric cell structure contributes to gastric disease (Kalisperati *et al.*, 2017; Yang *et al.*, 2020; Salvatori *et al.*, 2023). Not all *H. pylori* carry a *cagPAI*, but it is a major factor contributing to gastric disease and cancer (Salvatori *et al.*, 2023).

Antibiotic therapy is commonly used for the treatment of patients with gastric disease. The treatment comprises triple or quadruple therapy and often includes proton pump inhibitors and

bismuth salts (Gatta *et al.*, 2013; Ford *et al.*, 2016; Mansour-Ghanaei *et al.*, 2019; Katelaris *et al.*, 2023; Zhang *et al.*, 2023). Therapy with multiple antibiotics provokes a high selection pressure for antibiotic resistance. In addition, *H. pylori* is highly transformable, and it can acquire resistance that spreads in the environment. Over the last 10 years more than half of *H. pylori* patient isolates were found to carry at least one resistance gene against the first line antibiotics (Boyanova *et al.*, 2019; Argueta *et al.*, 2021; Contreras-Omaña, Escorcia-Saucedo and Velarde-Ruiz Velasco, 2021). In 2017 the World Health Organization published a report underlining the urgency of finding new antibiotics against *H. pylori* (Tacconelli *et al.*, 2018).

Considering the rise of antibiotic resistance, alternative therapeutic methods to fight bacterial infections have emerged that may not lead to strong selection pressure (Dieye *et al.*, 2022; Sathianarayanan *et al.*, 2022; Zhang *et al.*, 2022; Frost *et al.*, 2023). Targeting virulence factors that are not essential for bacterial survival is one of the investigated approaches (Escaich, 2008; Arya *et al.*, 2019; Buß *et al.*, 2019; Hwang *et al.*, 2021). *H. pylori* virulence factors such as the T4SS are not essential for its survival, but they are major contributors to severe gastric disease. The *cagT4SS* proteins are unique to *H. pylori* and inhibitors would therefore not target other bacteria of the microbiome. We have chosen the essential ATPase Cag α as a target (Yeo *et al.*, 2000; Haley, Blanz and Gaddy, 2014; Cover, Lacy and Ohi, 2020). Cag α is a hexameric ATPase that localizes at the inner membrane and is a homolog of VirB11 proteins that are conserved and essential for all T4SS.

Previously, we have used fragment-based screening to identify small molecules that interact with Cag α , and we identified 1G2 as a non-competitive inhibitor of its ATPase activity (Arya *et al.*, 2019). Here, we characterized the binding site by X-ray crystallography and mutagenesis identified critical amino acid residues. Based on the information of the binding site we created a family of 1G2 derivatives and some of them have interesting potential as inhibitors of T4SS activity and of extracellular assembly of Cag pili.

iii. Materials and Methods

a. Cloning and mutagenesis

Cloning of Cag α was described by Arya *et al*, 2019 (Arya *et al.*, 2019). The plasmid carrying the WT Cag α protein pHTCag α was amplified using the QuikChange II site-directed mutagenesis kit (Agilent) using 33 bp primers (Table. S1) to introduce single codon mutations to change amino acid residues at the 1G2 binding site, followed by Sanger sequencing on an ABI 3730 sequencer (Ho *et al.*, 1989; Liu and Naismith, 2008).

b. Expression and purification of Cag α

The expression and of purification Cag α wild type and mutant proteins was conducted as previously described by Arya *et al*, 2019 (Arya *et al.*, 2019). Shortly Cag α was expressed in *E. coli* BL21 (DE3) with 1 mM isopropylthio- β -galactoside (IPTG) induction. For purification, the culture pellet was suspended in binding buffer (50 mM HEPES, 500 mM NaCl, 20 mM imidazole, pH 7.5, 10% glycerol, 0.1% triton, plus two tablets of EDTA-free protease inhibitor cocktail (Roche)) and lysed using a cell disrupter (Constant Systems Inc.) at 27 kPsi, followed by centrifugation at 15,000 rpm at 4 °C to reduce cell debris. The supernatant was loaded onto a His-trap Ni-NTA column (GE Healthcare) and eluted using a linear 50 ml gradient of 40–500 mM imidazole in binding buffer. Proteins were then dialysed (25 mM sodium phosphate, 125 mM NaCl, 5 mM DTT, pH 7.4) and subjected to Size exclusion chromatography using a Superdex-200 column (GE Healthcare) with buffer 25 mM HEPES pH7.5 and 100 mM NaCl and peak fractions were analyzed by SDS-PAGE.

c. Crystallisation and structure determination

Initial crystallization conditions were established using the MCSG screen from Anatrace (USA using 6 mg/ml of Cag α and 1 mM of 1G2 (1:10 ratio). Final crystals were grown at room temperature using the hanging drop vapour diffusion method in 100 mM Bis-Tris (pH 6.5) and 2mM ammonium sulfate. Drops containing 2 μ L of protein-inhibitor-mixture (1:10 ratio) and 2 μ L

of reservoir solution were incubated for 2 weeks. Hexagonally shaped crystals appeared after 7-10 days. The crystals were cryo-protected in 100 mM Tris-HCl buffer (pH 8.5), 2 M ammonium sulfate and 25% glycerol, flash frozen in liquid nitrogen and the data were collected at microfocus beamline F1 at the Cornell High Energy Synchrotron Source (CHESS). The intensity data was processed using the HKL2000(Otwinowski and Minor, 1997) program (Table. S2). The structure was solved by molecular replacement using the coordinates of PDB ID: 1G6O as search model. Refinement and modeling were performed using REFMAC and Coot (Murshudov, Vagin and Dodson, 1997; Emsley and Cowtan, 2004). Final graphical figures and tables were generated using the Pymol-integrated Phenix software suite (Adams *et al.*, 2002). The structure was published in the PDB (PDB code: 6BGE, <https://www.rcsb.org/structure/6BGE>).

d. Docking of 1G2 and derivatives to Cag α

Autodoc Vina was used for binding energy calculations. The Cag α structure used for the binding from PDB 1G6O (RCSB PDB - 1G6O: CRYSTAL STRUCTURE OF THE *HELICOBACTER PYLORI* ATPASE, *H. PYLORI*0525, IN COMPLEX WITH ADP) was used for docking.

e. Differential scanning fluorimetry (DSF)

To assess binding of 1G2 derivatives to Cag α and its mutant proteins, DSF was used in the presence of SYPRO orange as in Arya *et al.*, 2019 (Arya *et al.*, 2019). The reaction mixture contains 5 μ M of Cag α , 10x concentration of SYPRO Orange (from 5000x stock solution (ThermoFisher)) in 50 mM HEPES (pH 7.5), 100 mM NaCl and 5% final concentration of DMSO. The fragments and nucleotides were added to final concentrations of 5 mM, and the fluorescence was monitored over 20–95 °C with a LightCycler 480 instrument (Roche).

f. Synthesis of the 1G2 derivatives

The organic reagents are prepared as Dimethylformamide (DMF) solutions: Solution 1: The heteroaryl halide building blocks solution was prepared by weighing 1.77 mmol in a 2 ml vial. DMF was added and the volume is adjusted to 400 μ l. Solution 2: The scaffold (methyl-4-

hydroxybenzoate) was weighed (1259 mg; 8.27 mmol) in a 40 ml vial, the solid was dissolved with DMF and the volume adjusted to 29.4 ml. A 0.6-2 ml microwave vial was added with 161 mg (0.493 mmol; 2.5 eq.) of Cs₂CO₃, equipped with a stirbar, charged with the heteroaryl halide solution (100 µl; 2.25 eq.) followed by scaffold solution (700 µl; limiting reagent). The suspension was transferred to a Biotage Initiator microwave reactor to run the reactions at 180 °C for 1 h. The reaction was monitored by liquid chromatography mass spectrometry (LCMS). The reaction mixtures were filtered on a filtering plate (96 deep-well plate; PE Frit 25 mm; Long drip; 2 ml) using a MeOH/DMSO (2:1) mixture. Filtration was forced using HT4X Genevac for centrifugal filtration. The filtered mixtures were added to 50 ml of AcOH (pH adjusted <5) and purified on a reverse-phase Kinetex 5 µm C18 column 21.2 x 100 mm and was eluted with MeOH - Water - 0.1% AcOH. Gradient: Isocratic 25 or 30 % for 1.5 minutes then gradient to 100% MeOH over 8.5 minutes. Tubes containing the desired compounds were identified and placed on an HT6-Genevac evaporator. After removal of the solvent, the content of the tubes was transferred to pre-tared 4 ml vials using a (1:1) DCM:MeOH mixture. The vials were placed in a HT6 Genevac evaporator and the solvents removed under reduced pressure, followed by NMR and LCMS analysis.

g. Enzyme activity assay

The ATPase activity was quantified using a malachite green binding assay (Arya *et al.*, 2019). The 100 µL reaction mixtures contained 60 nM of enzyme, 25 mM HEPES (pH 7.5), 100 mM NaCl, 200 µM MgCl₂ and 200 µM of 1G2 derivative. The reaction mixtures were incubated for 15 min at 30 °C. After incubation, ATP was added at 100 µM concentration and incubated again for 30 minutes at 30°C and then 40 µL of malachite green assay mixture was added. The formation of the blue phosphomolybdate-malachite green complex was in linear relation to the amount of released inorganic phosphate and measured at 610 nm. Color generated was estimated compared to series of standards.

h. IC₅₀ determination

IC₅₀ values were determined by incubating different concentrations of molecules (5–2,500 μM; from stocks of 100 mM) with enzyme in 25 mM HEPES (pH 7.5) and 100 mM NaCl and 200 μM of MgCl₂. Mixtures were incubated with inhibitors for 15 min, followed by addition of ATP and incubation for 30 min at 37 °C. The reactions were stopped by addition of 40 μl malachite green solution and the inorganic phosphate released was determined at 610 nm. Data were plotted as 1/rate versus inhibitor concentration for each substrate concentration and a linear fit was calculated by non-linear regression using SigmaPlot (version 11.0).

i. Bacterial strains, cell lines and culture conditions

H. pylori strain 26695 (ATCC700392) was used as a positive control, and the previously described Δ *cagV* (*H. pylori*0530) mutant recreated in our laboratory was used as negative control (Fischer *et al.*, 2002; Arya *et al.*, 2019). All the strains were cultivated on Columbia agar base (BD) containing 10% (v/v) horse serum (Wisent Inc.), 5% (v/v) laked horse Blood (Wisent Inc.) with β-cyclodextrin (2 mg/mL), vancomycin (10 mg/ml) and amphotericin B (10 mg/ml). Chloramphenicol (34 mg/ml) was added in case of the Δ *cagV* strain to select for the chloramphenicol (*cam*) gene cassette used to disrupt the gene. For liquid cultures, brain heart infusion (BHI) media (Oxoid) was supplemented with 10% fetal bovine serum (FBS) and appropriate antibiotics. Bacteria were cultivated at 37°C under microaerophilic conditions (5% oxygen, 10% CO₂).

Gastric human cells (AGS CRL-1739) cells were grown at 37°C in F12K media (Wisent Inc.) with 10% (v/v) FBS (Wisent Inc.) in a 5% CO₂-containing atmosphere. AGS cells were counted using a hemocytometer (Hausser Scientific™ Bright-Line™ Phase Hemacytometer).

j. Cell proliferation Assay

AGS cells cultivated at 5x10⁴ cells/well density were incubated overnight with 100 μM of molecules at 37°C in a 5% CO₂-containing atmosphere. The cell proliferation was evaluated using the Cell Proliferation Reagent WST-1 (CELLPRO-RO, Roche).

k. Infection of AGS by H. pylori strains and IL-8 production

H. pylori were first pre-incubated for 1h in F12K supplement with 10% FBS with or without 1G2 or its derivatives at a concentration of 200 μ M at 37°C in an incubation container under microaerophilic conditions (5% CO₂). (1) For the initial screening of the 96 1G2 derivatives, the AGS cells were cultivated in 96 well microplates with 0.3x10⁵ cells/well for 24h with a culture of H. pylori pre-incubated for 1h with the different small molecules at a multiplicity of infection (MOI) of 100 at 37°C, 5% CO₂. These experiments were performed twice in duplicates and the results of one assay are shown in Figure. S4A. (2) For the second screening of 25 1G2 derivatives the AGS cells were cultivated in 96 well microplates with 0.3x10⁵ cells/well for 24h with a culture of H. pylori pre-incubated for 1h with the different small molecules at a MOI of 100 at 37°C, 5% CO₂. These experiments were performed four times in triplicates and the results of one assay are shown in Figure. S4B. (3) For the final assays, the AGS cells were cultivated in 6-well plates with 7x10⁵ cells/well for 4h with a culture of H. pylori pre-incubated for 1h with the different small molecules at a MOI of 100 at 37°C, 5% CO₂. The supernatants from 6 independent assays were used for the determination of IL-8 levels (Fig. 3) and the T4SS pili in the same samples were counted by scanning electron microscopy (see below, Fig. 6). For all the above assays, the supernatants were sampled and centrifuged at 15,000 g to remove cells and debris; the supernatants were conserved at -20°C. The level of IL-8 in cell culture supernatants was determined using a human IL-8 ELISA kit (Invitrogen).

l. Sample preparation and western blotting

After 4h of infection, the cells were washed with phosphate-buffered saline (Wisent Inc.) and lysed in RIPA Buffer (50 mM Tris-HCl pH 8.0, 150 mM sodium chloride, 1.0% Igepal CA-630 NP-40, 0.5% sodium deoxycholate, 0.1% sodium dodecyl sulfate), complemented with a protease inhibitor cocktail for mammalian tissues (Sigma Aldrich) and a phosphatase inhibitor cocktail for tyrosine protein phosphatases, acid and alkaline phosphatases (Sigma Aldrich). The cells were harvested, incubated at 95°C for 5 min with SDS-PAGE sample buffer and centrifuged for 10 min at 10,000 rpm, followed by SDS-PAGE and western blotting. The production of proteins was assessed with

monoclonal mouse anti-*Helicobacter pylori* CagA (HyTest Ltd.) and rabbit CagA antiserum (Abcam). The actin was identified using the anti- β -Actin antibody (C4): m-IgG Fc BP-HRP (Santa Cruz, sc-528515). The secondary antibodies (rabbit and mouse) were purchased from Biorad and the HRP signal was developed using Clarity Western ECL Substrate (Biorad).

m. Scanning electron microscopy

AGS cells were cultivated on round cover glasses (Fisherbrand) at 6×10^5 cells/well density in 6-well plates. The cells were infected with *H. pylori* for 4h as explained above, washed with cold phosphate buffer (PB 0.1 M), fixed in 4% paraformaldehyde/0.1% glutaraldehyde for 30 min at 4°C, followed by another wash in PB. The samples were then incubated in osmium tetroxide 4% (0.1%) for 1 h at 4°C, followed by washing with PB. The samples were then dehydrated using a series of ethanol dilutions for 15 min each (30%, 50%, 70%, 80%, 90%, 95%, 100%, 100%), followed by drying using critical point dryer using the Leica EM CPD300. Then cells were then coated with 5 nm of carbon using the Leica EM ACE600. The sample were visualised using a Hitachi Regulus 8220 scanning electron Microscope. The length and number of T4SS pili were measured using ImageJ software (Schindelin *et al.*, 2012).

n. Statistical analysis

All the statistical analyses were performed using GraphPad Prism 9 (9.5.1). T-test and ANOVA (Kruskal-Wallis test and ordinary One-way) were used to analyse the number of pili and their size, respectively.

iv. Results

a. *X-ray analysis reveals the 1G2 binding site.*

In our previous work we identified 1G2 as a non-competitive inhibitor of Cag α and this molecule has interesting potential for development into an anti-virulence drug (Arya *et al.*, 2019). As first step towards designing more effective 1G2 derivatives, we characterized the binding site by X-ray crystallography. Cag α was co-crystallized with 1G2, and we solved the X-ray structure of the Cag α -1G2 complex in the $P6_322$ crystal space group with two molecules in the asymmetric unit (Figure. 1A) to a resolution of 2.9 Å (Table. S2). The structure was solved by molecular replacement using ADP bound Cag α (PDB code: 1G6O) as a search model. The overall structure of 1G2-bound Cag α (PDB code: 6BGE) is similar to that of the Cag α -ADP complex, but there are *differences in interactions at the protein interface, and we identified* the electron density of molecule 1G2 sandwiched between two Cag α molecules (Figure. 1A). The monomer structure of the Cag α -1G2 complex displays both N-terminal domain (NTD) and C-terminal domain (CTD) with nine α -helices labeled as $\alpha 1$ to $\alpha 9$ and 13 β -strands labeled as $\beta 1$ to $\beta 3$ (Figure. 1B). A structural overview from the top of the NTD reveals that 1G2 interacts with the NTD of both protein subunits (Figure. 1C). The 1G2 binding site is distinct from the active site to which ADP and the substrate analog ATP- γ -S bind (Yeo *et al.*, 2000; Savvides, 2003). Molecule 1G2 binds to a hydrophobic pocket created by the interaction between the NTDs of two Cag α subunits and amino acids F68 and F39 make hydrophobic contacts with the two aromatic rings of the inhibitor. R73 and D69 are the amino acids involved in forming a polar contact with 1G2. R73 interacts with the pyridine ring via a hydrogen bond and the carboxylic group of 1G2 interacts with the backbone NH group of D69 forming a potential hydrogen bond (Figure. 1D). Sequence alignments with other Cag α /VirB11 homologs show that this site is not conserved suggesting that the molecule could likely be a specific inhibitor (Figure. S1).

Structural alignment of the Cag α -1G2 complex with Cag α -ADP (PDB code: 1G6O) shows an overall similar structure (RMSD 0.6 Å), but we observe shifts of the $\beta 6$ and $\beta 7$ sheets and in the

linker region between NTD and CTD (Figure. S2). Alignment of Cag α -1G2 with Cag α apoprotein (PDB code: 1NLZ) reveals slight conformational differences in both the CTD and NTD (RMSD 0.9 Å). The α 8 and α 9 helical region of the CTD as well as the α 1 region of the NTD display changes showing that binding to molecule 1G2 impacts the conformation of the protein (Figure. S2). Overall, the results indicate that molecule 1G2 binds at the interface between Cag α proteins that multimerize via the NTD and this is consistent with the results of enzyme kinetics (non-competitive inhibition) (Arya *et al.*, 2019). Analysis of the Cag α -1G2 X-ray structure revealed subtle conformational changes in different parts of the protein including the active site as compared to the apoprotein and its complex with ADP (Figure. S2). This may explain the effect of 1G2 binding on the enzymatic activity of Cag α .

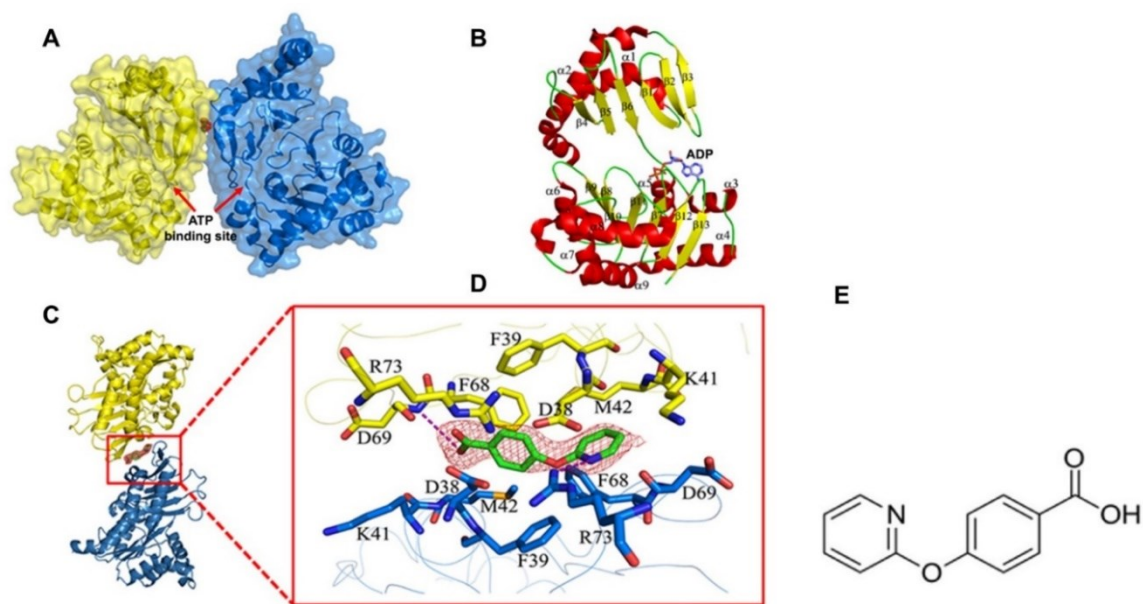


Figure 1: 1G2 Binding determined by X-ray crystallography. A) Cartoon representation of the crystal structure of Cag α crystallized as two molecules in the asymmetric unit. Red map in middle of two subunits represents molecule 1G2 and arrows indicate the ATP/ADP binding site. B) Representation of the monomeric subunit of Cag α in ribbon form: α helices, β strands and loops are represented in yellow, red and green, respectively. The nine helices are labeled as α 1 to α 9 and

the β -strands are labeled as $\beta 1$ to $\beta 13$ and the ADP binding site is indicated. C) Side view of the interaction of two subunits of protein with 1G2 in the middle represented as green stick and red map. D) Enlarged view of 1G2 binding at the interface between two protein subunits. The 2FO-FC electron density map of 1G2 was contoured at 1.5σ . E) 2D structure of 1G2.

b. Validation of the 1G2 binding site by mutagenesis of Cag α

To validate the binding site identified by X-ray crystallography (Figure. 1D) we mutagenized the *cag α* gene to change five amino acids at the binding site. We then purified the binding site mutants Cag α D38A, Cag α F39A, Cag α K41A, Cag α M42A, Cag α R73A, Cag α R73K and analysed their binding to 1G2 using differential scanning fluorimetry (DSF). The R73K mutation was introduced based on our analysis of clinical *H. pylori* strains from patient biopsies, suggesting a potential association with resistance to 1G2 (Oudouhou *et al.*, 2023). This technique determines the melting temperature of a protein in a temperature gradient in the presence of the fluorescent dye SYPRO orange. Positive shifts are generally considered as evidence for binding due to stabilization by a small molecule (Arya *et al.*, 2019). Analysis of the melting temperatures suggested that Cag α D38A and Cag α M42A bind 1G2 like the wild type protein whereas the binding of Cag α mutants F39A, K41A, R73A and R73K was reduced (Figure. 2A). These results suggest that Cag α residues F39, K41 and R73 contribute to binding of 1G2.

We next determined the ATPase activity of purified Cag α and its mutants using a malachite green assay measuring the release of inorganic phosphate from the ATP. All Cag α mutants have ATPase activities similar to the wild type protein and incubation with 1G2 at a concentration of 200 μ M reduced ATPase activity of most of them with the exception of Cag α R73A that was not inhibited (Figure. 2B). The effect of 1G2 on Cag α F39A, Cag α K41A and Cag α M42A was less pronounced than on the wild type protein. To gain more quantitative information on the effect of 1G2 on the different mutants we varied the concentration of the inhibitors and calculated IC₅₀ values as a measure of inhibitor efficacy. The IC₅₀ values for inhibition of the wild type and of Cag α D38A are in a similar range, those of Cag α K41A and Cag α M42A are significantly higher and Cag α F39A and

Cag α R73A are resistant to the inhibitor (Figure. 2C). The enzyme assay results are consistent with those obtained by DSF suggesting that Cag α residues F39 and R73 are critically important for binding of 1G2 and that K41 and M42 also contribute to the effect of the inhibitor.

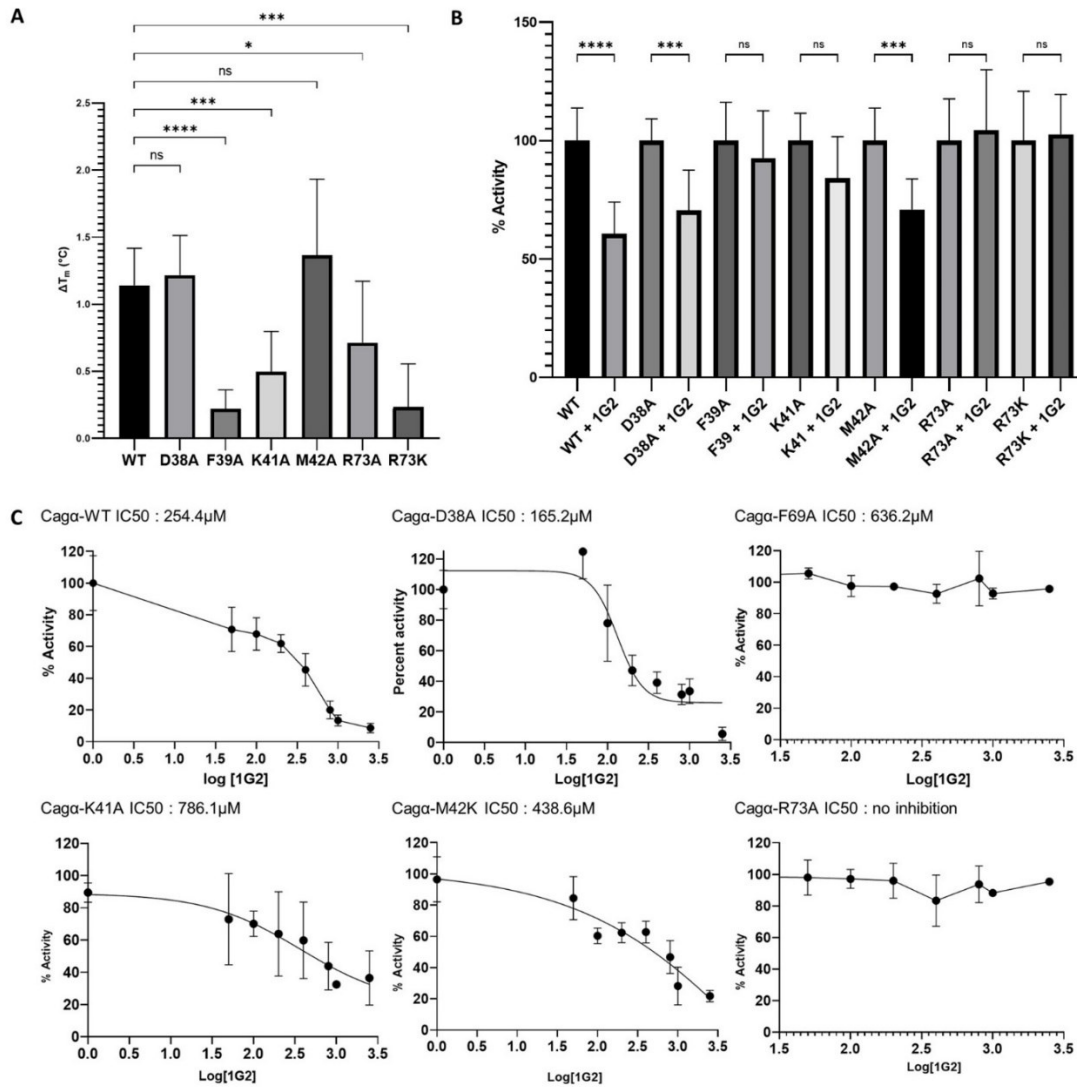


Figure 2: Characterization of active site mutants by differential scanning fluorimetry and ATPase enzyme assays. A) Changes in the melting temperature of Cag α mutant proteins were measured by DSF after incubation with molecules at 5 mM final concentration (n= 3 times triplicates). The results were analysed using One-Way ANOVA (multi-comparison from WT) ns;

non significant, * $p < 0.05$, *** $p = < 0.001$, **** $p < 0.0001$. B) Effect of 1G2 derivatives on the ATPase activity of CagA mutant proteins. CagA WT and mutant proteins were incubated with 1G2 at different concentrations and ATPase activity was measured by malachite green assay, One-way ANOVA test (non treated VS treated) ns; non significant, *** $p = < 0.001$, **** $p < 0.0001$. C) Dose-response curves of ATPase activity of mutant proteins showing IC₅₀ values in the presence of 1G2. C) Dose-response curves of ATPase activity of mutant proteins showing IC₅₀ values in the presence of 1G2 (3 times duplicates).

c. Design and selection of 1G2 derivatives molecules

Based on the results from co-crystallisation and mutagenesis of the active site we created a library of 96 1G2 derivatives by medicinal chemistry in an attempt to generate more potent inhibitors. We designed 1G2 derivatives to improve binding to amino acid residues at the inhibitor binding site and we also introduced functional groups that may modulate solubility and thereby permeation into cells (Figure. S3). The fact that a previously identified 1G2 derivative (1G2#4) (Arya *et al.*, 2019) was more efficient against CagA *in vitro* also informed this strategy since its additional methyl group may improve binding to K41. As first step to identify more potent 1G2 derivatives we screened for toxicity for human AGS (gastric adenocarcinoma) cells that are used for *H. pylori* infection experiments. Using a cell proliferation assay we identified four cytotoxic molecules, triggering more than 20% of mortality and these molecules were not further investigated. Next, we used a bacterial growth inhibition assay to test toxicity for *H. pylori* using an antibiogram-like technique with 200 μM of 1G2 and derivatives (chloramphenicol as a positive control) on filter plates and we found that none of the 92 derivatives is toxic for the bacteria (Table. S4).

To determine the effect of the 1G2 derivatives on T4SS function we quantified the production of interleukin 8 (IL-8) that is induced by the T4SS during AGS cell infection by *H. pylori*. IL-8 is an inflammatory factor induced after co-infection with *H. pylori* and it provides a quantifiable readout since it is secreted into the cell culture supernatant (Cover, Lacy and Ohi, 2020). We designed a

medium-throughput assay enabling us to measure the effects of preincubation of the molecules on IL-8 production of AGS cells in 96-well microtiter plates, followed by quantification using an ELISA assay. We conducted two rounds of screening to identify molecules that reduce IL-8 production more strongly than 1G2 in a reproducible fashion. The first round identified 25 molecules that cause similar or more pronounced reduction of IL-8 production (Figure. S4A) and a secondary screen (Figure. S4B) identified five molecules (1G2_1313, 1G2_1338, 1G2_2886, 1G2_2889 and 1G2_2902) that lead to strong reductions of IL-8 induction in a reproducible fashion (Table. 1 and Figure. S4B). The selected five molecules were further characterized using the infection model described by Arya *et al.* (Arya *et al.*, 2019) and the assays were repeated six times to gain sufficient statistical power. To assess the impact of the molecules on T4SS-dependent IL-8 induction, we subtracted the value corresponding to the control $\Delta cagV$ mutant strain, which serves as the baseline for non T4SS-dependent IL-8 induction. We observed that 1G2 reduces IL-8 production to about 20% as compared to the wild type control without inhibitor. The five selected molecules have varying effect on IL-8 production. Molecules 1G2_2886, 1G2_2889 and 1G2_2902 have comparable effects to 1G2, but 1G2_1313 and 1G2_1338 reduce IL-8 production close to the background level of the $\Delta cagV$ mutant (Figure. 3).

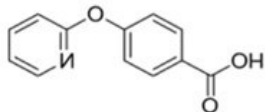
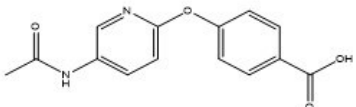
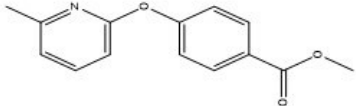
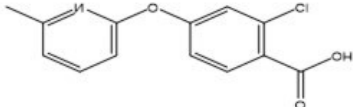
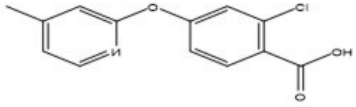
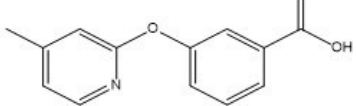
Name of compound	Structure
1G2 (4-(Pyrid-2-yloxy)benzoic acid)	
1313 4-[(5-acetamidopyridin-2-yl)oxy]benzoic acid	
1338 methyl 4-[(6-methylpyridin-2-yl)oxy]benzoate	
2886 2-chloro-4-[(6-methylpyridin-2-yl)oxy]benzoic acid	
2889 2-chloro-4-[(4-methylpyridin-2-yl)oxy]benzoic acid	
2902 3-[(4-methylpyridin-2-yl)oxy]benzoic acid	

Table 1: Structures of 1G2 derivatives identified by screening for potency in AGS cell infection assays.

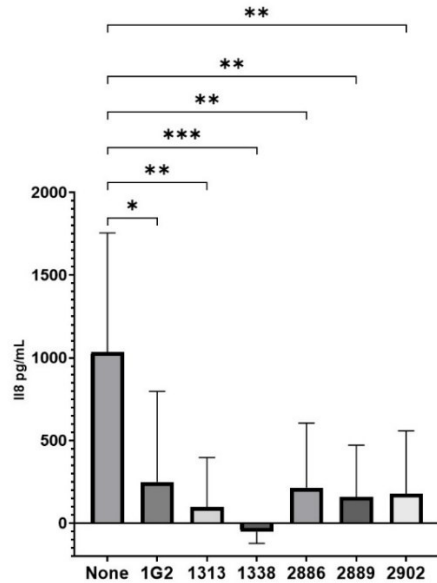


Figure 3: Quantification of the interleukin-8 production by AGS cells infected by *H. pylori* strains after treatment with the 1G2 and its derivatives. AGS cells were infected by the strain 26695 that had been preincubated with 200 μ M of 1G2 and its derivatives for 4 h and the amount of secreted IL-8 was measured by ELISA. The T4SS dependent induction of IL-8 is displayed in pg/ml (n=6 repetitions) and the value for strain Δ cagV were used as baseline. *p<0.01, ** p<0.001, ***p<0.0005, Ordinary one-way ANOVA test

d. Differential scanning fluorimetry and docking suggest that 1G2 derivatives bind Cag α .

To characterize the five selected 1G2 derivatives we first tested their binding to Cag α using the DSF approach as above. Molecules 1G2_1313, 1G2_2889 and 1G2_2902 increased the melting temperature to a lower extent than 1G2, 1G2_2886 had a similar effect as compared to 1G2 and 1G2_1338 actually decreased the melting temperature (Figure. 4). We also conducted *in silico* docking using Autodock Vina software (Trott and Olson, 2009). This approach enables a computational prediction of the binding energies and the negative value obtained for 1G2 (-6.6 Δ G/mol) is consistent with its binding to Cag α (Table. S3). The predicted binding energies for the five 1G2 derivatives (1G2_1313, 1G2_1338, 1G2_2886, 1G2_2889 and 1G2_2902) had more pronouncedly negative values (-9 to -10.2 Δ G/mol) suggesting that they may have higher affinities

for Cag α than 1G2. Whereas the DSF results are not consistent with higher affinity of the 1G2 derivatives to Cag α the docking results suggest stronger binding and we tested their effects on enzyme activity next.

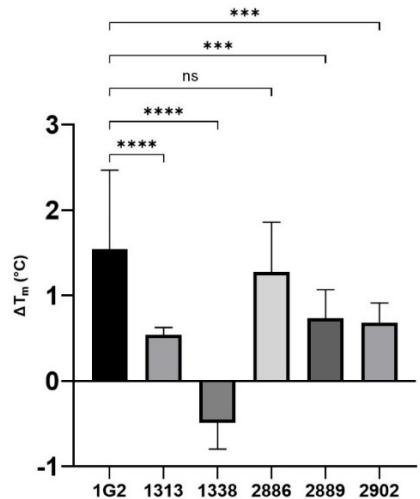


Figure 4. Melting temperature of Cag α in the presence of ligands. Melting temperatures for Cag α were determined using differential scanning fluorimetry (DSF). One-Way ANOVA (multi-comparison from 1G2), ns; non significant, *** $p < 0.001$, **** $p < 0.0001$

e. Effect of 1G2 derivatives molecules on the ATPase activity of Cag α

Using the malachite green assay as above we assessed to which degree the five 1G2 derivatives impact the enzymatic activity of Cag α . We tested the inhibitors at varying concentrations and the IC₅₀ value of molecule 1G2_1313 is similar to that of 1G2 (256 μ M) (Fig. 5). In contrast, molecules 1G2_1338 (60 μ M), 1G2_2886 (47.50 μ M), 1G2_2889 (96 μ M) and 1G2_2902 (85 μ M) have lower IC₅₀ values than 1G2. These results are consistent with the increased negative effects of these derivatives observed in the IL-8 production assay (Figure. 3) and further support the notion that these derivatives are more potent than 1G2.

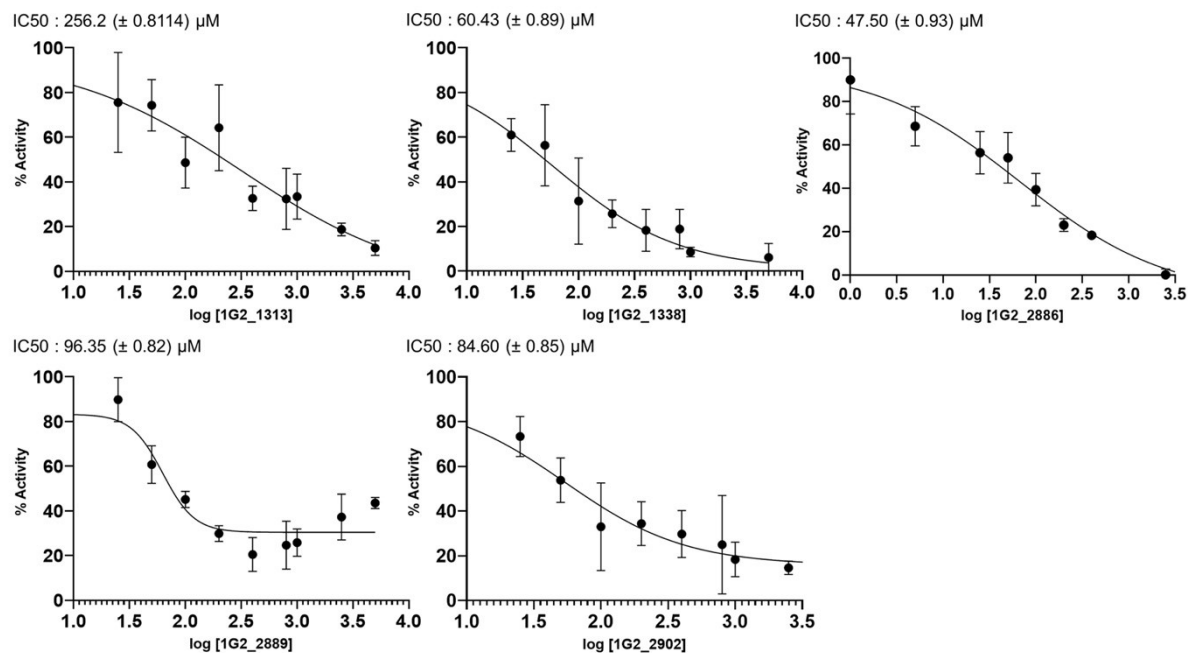
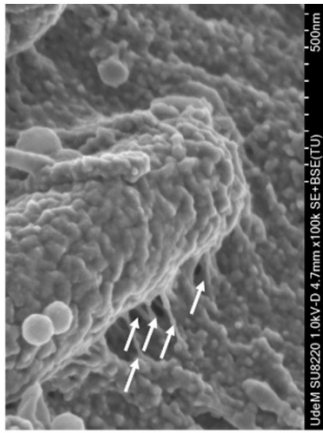


Figure 5. Enzyme assays of Cag α in the presence of molecule 1G2 and derivatives. Dose-response curves of ATPase activity showing IC₅₀ values in the presence of 1G2 and its derivatives 1G2_1313, 1G2_1338, 1G2_2886, 1G2_2889 and 1G2_2902 (concentration range: 5–2,500 μM). Experiments were conducted in triplicates.

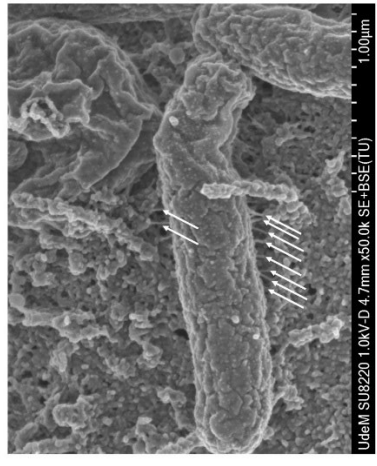
f. 1G2 and derivatives affect the assembly of T4SS pili.

Finally, we tested the effects of 1G2 and its five derivatives on the physiology of the T4SS. AGS cells were infected with *H. pylori* wild type strain 26695 that had been pre-incubated with 200 μM of the molecules, followed by infection of 4 hours and analysis of the cells. First, the presence of Cag proteins was analysed using western blotting to determine whether 1G2 and its derivatives have negative impacts on T4SS expression or stability. We do not observe any significant and reproducible effects on the amounts of the translocated virulence factor CagA or of the target Cag α suggesting that the inhibitors do not destabilize the T4SS (Figure. S5). Second, we used a recently developed quantifiable approach to analyze the T4SS-dependent assembly of extracellular pili using scanning electron microscopy (SEM) during AGS cell infection (Oudouhou *et al*, 2023)

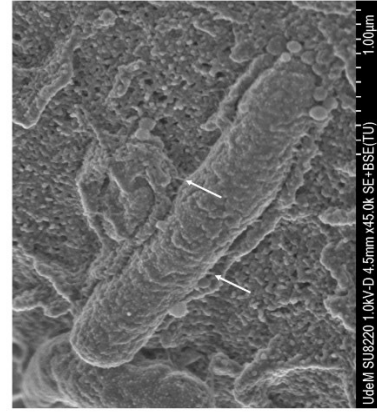
(Figure. 6A). We observe on average of 17 (± 8) T4SS pili on the wild type strain in the absence of 1G2 and very few on the T4SS-defective $\Delta cagV$ strain 1 (± 2)(Figure. 6B). In contrast, in the presence of 1G2 we observe on average 3(± 3) T4SS-pili on the wild type strain and all 1G2 derivatives have similar strong inhibitory effects on pilus assembly (Figure. 6B). These results confirm that 1G2 and its derivatives have strong negative effects on T4SS pilus assembly, and it will be interesting to gain more detailed insights into the molecular mechanism of these molecules in future.



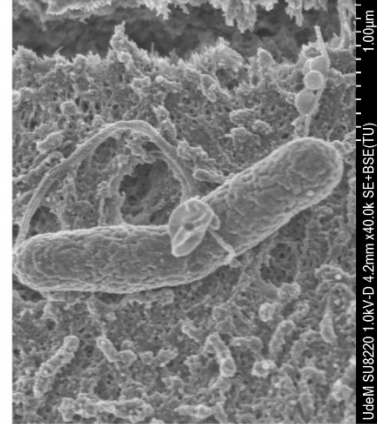
26695



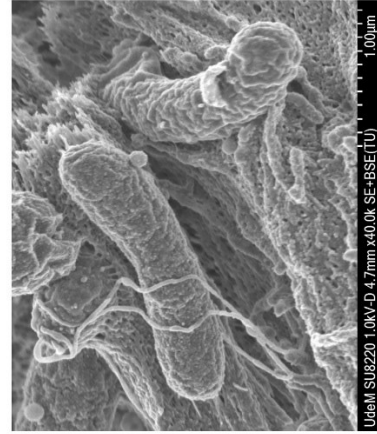
26695



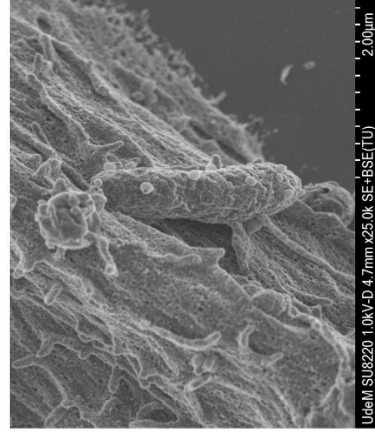
26695 + 1G2



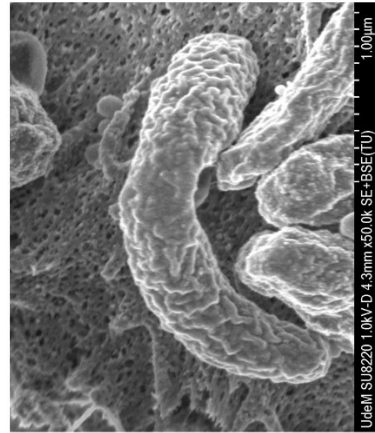
Δ cagV



26695 + 1313



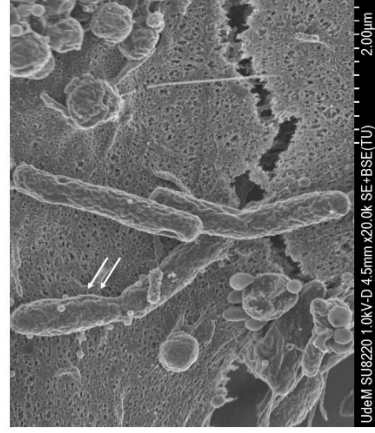
26695 + 1338



26695 + 2886



26695 + 2889



26695 + 2902

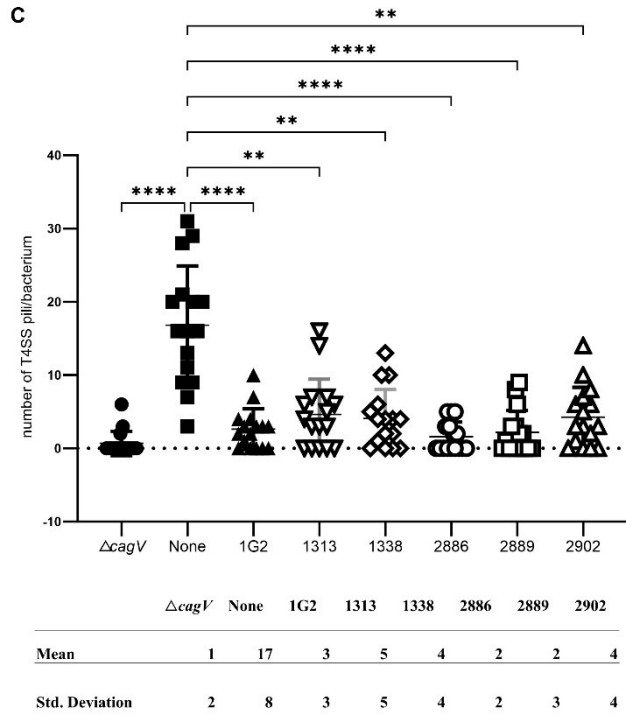


Figure 6: 1G2 and its derivatives affect the number of T4SSpili during gastric cell infection. AGS cells were preincubated with 1G2 and derivatives and infected with *H. pylori*. A) and B) The T4SSpili were observed using scanning electron microscopy; the T4SS pili are identified with white arrows. C) The T4SS pili were counted using ImageJ. The $\Delta cagV$ strain was used as negative control. (n=16 bacteria from 2 different infections). ****: $p < 0.0001$. ** $p < 0.05$, ns: non-significant, Kruskal-Wallis ANOVA (multi-comparison from non treated)

v. Discussion

The eradication therapies of *H. pylori* using antibiotics induce a high selection pressure leading to the acquisition of antibiotic resistance that can be transmitted between different strains and other members of the microbiome (Seo *et al.*, 2019; Ye *et al.*, 2020; Kakiuchi *et al.*, 2021; Wang *et al.*, 2021; Katelaris *et al.*, 2023). Targeting the nonessential virulence factors that the bacteria use to infect the host is an alternative approach to reduce the pressure of selection induced by antibiotics (Hilleringmann *et al.*, 2006; Yang *et al.*, 2021; He *et al.*, 2022; Suerbaum *et al.*, 2022; Sabino, Cotter and Mantovani, 2023). In this study we have characterized the binding site of Cag α inhibitor 1G2 using X-ray crystallography and mutagenesis suggesting a unique mechanism of inhibition via a binding site that is distinct from the ATPase active site. X-ray analysis suggested that five amino acids (D38, F39, K41, M42, R73) may form the 1G2 binding site. We mutated them in individually and DSF as well as ATPase enzyme assays showed that F39 and R73 are critically important, and that K41 and M42 also contribute to the binding of 1G2. These data suggest that we have identified the 1G2 binding site and that it functions as an inhibitor of ATPase activity by not directly interfering with substrate binding.

Based on the information gained on the inhibitor binding site we synthesized a series of 98 1G2 derivatives that may have improved binding to amino acids at the binding site and/or penetration into the cells. We tested their toxicity for mammalian cells first to focus our efforts on molecules that do not interfere with other metabolic pathways in mammalian cells (Ngo and Garneau-Tsodikova, 2018). In the spirit of our overall anti-virulence strategy, we also validated that these molecules are not toxic for *H. pylori*. We then screened the effects of 1G2 derivatives in a cell-based infection assay monitoring IL-8 production as a readout of T4SS activity to identify more potent anti-virulence molecules. Using this approach, we aimed at identifying 1G2 derivatives that have increased potency for the inhibition of Cag α and/or improved capacity to penetrate into the cells. This strategy was informed by previously identified derivative 1G2#4 that was more active as an inhibitor of Cag α ATPase activity *in vitro* than 1G2 (IC₅₀ of 82 μ M as compared to 196 μ M), but the molecule was inactive as an inhibitor of IL-8 production (Arya *et al.*, 2019), likely due to solubility issues. This molecule carries an additional methyl group that may form additional

hydrophobic interactions with the carbon chain of K41. Using screening of IL-8 production instead of inhibition of ATPase activity as a readout we avoided the identification of molecules like 1G2#4 that are more potent enzyme inhibitors, but inactive as inhibitors of the pathogen.

We then characterized the *in vitro* activity of the five molecules that have the strongest negative effects on IL-8 production as compared to 1G2 (1G2_1313, 1G2_1338, 1G2_2886, 1G2_2889 and 1G2_2902). Interestingly, when we used DSF as an estimate for binding to the target Cag α , none of the molecules led to stronger positive shifts of the melting temperature than 1G2. This suggests that the improved inhibitory activity in the IL-8 production assay is not necessarily due to stronger binding to the target. Interestingly, molecule 1G2_1338 decreased the melting temperature in the DSF assay suggesting that it may have a distinct effect on its target than 1G2. Analysis of the effects of the 1G2 derivatives on Cag α ATPase activity revealed that four of them are in fact more potent inhibitors than 1G2 (1G2_1338: 60 μ M, 1G2_2886: 47 μ M, 1G2_2889: 96 μ M, 1G2_2902: 85 μ M). These values are in the range of what we observed previously for 1G2#4, and in addition these molecules are potent inhibitors of IL-8 production reducing this readout of T4SS activity to baseline level of a Cag protein deletion mutant in the case of 1G2_1338. In addition, like 1G2, the five derivatives strongly reduce the production of extracellular T4SS pili suggesting that they share the same overall mechanism of inhibition.

The molecules identified here are the result of a first round of synthesis in the context of a structure-activity relationship (SAR) study and some are already more potent than 1G2 as enzyme inhibitors or in the IL-8 inhibition assay. The results of this work will inform future rounds of optimization by medicinal chemistry to synthesize molecules that have potential for development into drugs. In addition, since these molecules are inhibitors of the assembly of extracellular T4SS pili they could be applied for mechanistic studies of the T4SS assembly and translocation process. Small molecule inhibitors could be applied to block T4SS at different stages of the infection process enabling us to determine the time at which pilus assembly and effector translocation from *H. pylori* to mammalian cells are required.

vi. Acknowledgements

This work was supported by grants from the Cancer Research Society, the Charles Bowers Memorial Fund, the Bergeron-Jetté Foundation (CRS, #23404 and #25102) and the Natural Sciences and Engineering Research Council (NSERC, #RGPIN-2017-05123) to C.B. We are grateful to Dr. Dainelys Guadarrama Bell and other members of Dr. Antonio Nanci's laboratory at the Université de Montréal electron microscopy facility for technical support and assistance. Synchrotron X-ray data were collected at the Cornell High Energy Synchrotron Source (CHESS, MacCHESS beamline F1).

vii. Author Contributions

Claire Morin: Conceptualization, Data curation, Formal analysis, Investigation, Methodology, Writing – original draft, Writing – review & editing (*in vitro*, infection, manuscript draft and revision)

Vijay Tailor Verma: Data curation, Formal analysis, Investigation, Methodology, Writing – original draft (*in vitro*, manuscript draft)

Tarun Arya: Conceptualization, Data curation, Formal analysis, Investigation, Methodology, Validation, Writing – review & editing (crystallization, manuscript)

Bastien Casu: Conceptualization, Data curation, Formal analysis, Investigation, Methodology, Writing – review & editing (crystallization, manuscript)

Eric Jolicoeur: Investigation, Methodology, Resources, Writing – review & editing (medicinal chemistry)

Réjean Ruel: Investigation, Methodology, Resources, Validation, Writing – review & editing (medicinal chemistry)

Anne Marinier: Resources, Validation, Writing – review & editing (medicinal chemistry)

Jurgen Sygusch: Formal analysis, Investigation, Supervision, Validation (crystallization)

Christian Baron: Conceptualization, Funding acquisition, Investigation, Project administration, Supervision, Validation, Writing – review & editing

viii. References

Adams, P.D. *et al.* (2002) ‘PHENIX: building new software for automated crystallographic structure determination’, *Acta Crystallographica Section D Biological Crystallography*, 58(11), pp. 1948–1954. Available at: <https://doi.org/10.1107/S0907444902016657>.

Amieva, M. and Peek, R.M. (2016) ‘Pathobiology of *Helicobacter pylori*–Induced Gastric Cancer’, *Gastroenterology*, 150(1), pp. 64–78. Available at: <https://doi.org/10.1053/j.gastro.2015.09.004>.

Ansari, S. and Yamaoka, Y. (2020) ‘*Helicobacter pylori* Virulence Factor Cytotoxin-Associated Gene A (CagA)-Mediated Gastric Pathogenicity’, *International Journal of Molecular Sciences*, 21(19), p. 7430. Available at: <https://doi.org/10.3390/ijms21197430>.

Argent, R.H. *et al.* (2008) ‘Functional association between the *Helicobacter pylori* virulence factors VacA and CagA’, *Journal of Medical Microbiology*, 57(2), pp. 145–150. Available at : <https://doi.org/10.1099/jmm.0.47465-0>.

Argueta, E.A. *et al.* (2021) ‘Impact of antimicrobial resistance rates on eradication of *Helicobacter pylori* in a United States population’, *Gastroenterology*, p. S0016508521004017. Available at : <https://doi.org/10.1053/j.gastro.2021.02.014>.

Arya, T. *et al.* (2019) ‘Fragment-based screening identifies inhibitors of ATPase activity and of hexamer formation of Cag α from the *Helicobacter pylori* type IV secretion system’, *Scientific Reports*, 9(1), p. 6474. Available at: <https://doi.org/10.1038/s41598-019-42876-6>.

Backert, S., Tegtmeyer, N. and Fischer, W. (2015) ‘Composition, structure and function of the *Helicobacter pylori* cag pathogenicity island encoded type IV secretion system’, *Future Microbiology*, 10(6), pp. 955–965. Available at: <https://doi.org/10.2217/fmb.15.32>.

Backert, S., Tegtmeyer, N. and Selbach, M. (2010) ‘The Versatility of *Helicobacter pylori* CagA Effector Protein Functions: The Master Key Hypothesis: The Versatility of *H. pylori* CagA’, *Helicobacter*, 15(3), pp. 163–176. Available at: <https://doi.org/10.1111/j.1523-5378.2010.00759.x>.

Blaser, N., Backert, S. and Pachathundikandi, S.K. (2019) ‘Immune Cell Signaling by *Helicobacter pylori*: Impact on Gastric Pathology’, in. New York, NY: Springer US. Available at: https://doi.org/10.1007/5584_2019_360.

Boyanova, L. *et al.* (2019) ‘Multidrug resistance in *Helicobacter pylori*: current state and future directions’, *Expert Review of Clinical Pharmacology* [Preprint]. Available at: <https://doi.org/10.1080/17512433.2019.1654858>.

Breckan, R.K. *et al.* (2016) ‘The All-Age Prevalence of *Helicobacter pylori* Infection and Potential Transmission Routes. A Population-Based Study’, *Helicobacter*, 21(6), pp. 586–595. Available at: <https://doi.org/10.1111/hel.12316>.

Buß, M. *et al.* (2019) ‘Specific high affinity interaction of *Helicobacter pylori* CagL with integrin $\alpha_v\beta_6$ promotes type IV secretion of CagA into human cells’, *The FEBS Journal* [Preprint]. Available at: <https://doi.org/10.1111/febs.14962>.

Cheok, Y.Y. *et al.* (2021) ‘An Overview of *Helicobacter pylori* Survival Tactics in the Hostile Human Stomach Environment’, *Microorganisms*, 9(12), p. 2502. Available at: <https://doi.org/10.3390/microorganisms9122502>.

Contreras-Omaña, R., Escorcía-Saucedo, A.E. and Velarde-Ruiz Velasco, J.A. (2021) ‘Prevalence and impact of antimicrobial resistance in gastrointestinal infections: A review’, *Revista de Gastroenterología de México (English Edition)*, p. S2255534X21000633. Available at: <https://doi.org/10.1016/j.rgm xen.2021.06.004>.

Costa, T.R.D. *et al.* (2021) ‘Type IV secretion systems: Advances in structure, function, and activation’, *Molecular Microbiology*, 115(3), pp. 436–452. Available at: <https://doi.org/10.1111/mmi.14670>.

Coussens, L.M. and Werb, Z. (2002) ‘Inflammation and cancer’, *Nature*, 420(6917), pp. 860–867. Available at: <https://doi.org/10.1038/nature01322>.

Cover, T.L., Lacy, D.B. and Ohi, M.D. (2020) 'The *Helicobacter pylori* Cag Type IV Secretion System', *Trends in Microbiology*, 28(8), pp. 682–695. Available at : <https://doi.org/10.1016/j.tim.2020.02.004>.

Dieye, Y. *et al.* (2022) 'Recombinant *Helicobacter pylori* Vaccine Delivery Vehicle: A Promising Tool to Treat Infections and Combat Antimicrobial Resistance', *Antibiotics*, 11(12), p. 1701. Available at: <https://doi.org/10.3390/antibiotics11121701>.

Emsley, P. and Cowtan, K. (2004) 'Coot: model-building tools for molecular graphics', *Acta Crystallographica Section D Biological Crystallography*, 60(12), pp. 2126–2132. Available at: <https://doi.org/10.1107/S0907444904019158>.

Escaich, S. (2008) 'Antivirulence as a new antibacterial approach for chemotherapy', *Current Opinion in Chemical Biology*, 12(4), pp. 400–408. Available at : <https://doi.org/10.1016/j.cbpa.2008.06.022>.

Fischer, W. *et al.* (2002) 'Systematic mutagenesis of the *Helicobacter pylori* cag pathogenicity island: essential genes for CagA translocation in host cells and induction of interleukin-8: Functional dissection of the *H. pylori* type IV secretion system', *Molecular Microbiology*, 42(5), pp. 1337–1348. Available at : <https://doi.org/10.1046/j.1365-2958.2001.02714.x>.

Ford, A.C. *et al.* (2016) 'Eradication therapy for peptic ulcer disease in *Helicobacter pylori* - positive people', *Cochrane Database of Systematic Reviews* [Preprint]. Edited by Cochrane Upper GI and Pancreatic Diseases Group. Available at: <https://doi.org/10.1002/14651858.CD003840.pub5>.

Freire de Melo, F. *et al.* (2022) 'Influence of *Helicobacter pylori* oncoprotein CagA in gastric cancer: A critical-reflective analysis', *World Journal of Clinical Oncology*, 13(11), pp. 866–879. Available at : <https://doi.org/10.5306/wjco.v13.i11.866>.

Frost, I. *et al.* (2023) ‘The role of bacterial vaccines in the fight against antimicrobial resistance: an analysis of the preclinical and clinical development pipeline’, *The Lancet Microbe*, 4(2), pp. e113–e125. Available at : [https://doi.org/10.1016/S2666-5247\(22\)00303-2](https://doi.org/10.1016/S2666-5247(22)00303-2).

Gatta, L. *et al.* (2013) ‘Global eradication rates for *Helicobacter pylori* infection: systematic review and meta-analysis of sequential therapy’, *BMJ*, 347(aug07 1), pp. f4587–f4587. Available at: <https://doi.org/10.1136/bmj.f4587>.

Haley, K.P., Blanz, E.J. and Gaddy, J.A. (2014) ‘High Resolution Electron Microscopy of the *Helicobacter pylori* Cag Type IV Secretion System Pili Produced in Varying Conditions of Iron Availability’, *Journal of Visualized Experiments* [Preprint], (93). Available at: <https://doi.org/10.3791/52122>.

He, S. *et al.* (2022) ‘Targeting Cytotoxin-Associated Antigen A, a Virulent Factor of *Helicobacter pylori*-Associated Gastric Cancer: Structure-Based In Silico Screening of Natural Compounds’, *Molecules*, 27(3), p. 732. Available at : <https://doi.org/10.3390/molecules27030732>.

Hilleringmann, M. *et al.* (2006) ‘Inhibitors of *Helicobacter pylori* ATPase Cag α block CagA transport and cag virulence’, *Microbiology*, 152(10), pp. 2919–2930. Available at : <https://doi.org/10.1099/mic.0.28984-0>.

Ho, S.N. *et al.* (1989) ‘Site-directed mutagenesis by overlap extension using the polymerase chain reaction’, *Gene*, 77(1), pp. 51–59. Available at: [https://doi.org/10.1016/0378-1119\(89\)90358-2](https://doi.org/10.1016/0378-1119(89)90358-2).

Hooi, J.K.Y. *et al.* (2017) ‘Global Prevalence of *Helicobacter pylori* Infection: Systematic Review and Meta-Analysis’, *Gastroenterology*, 153(2), pp. 420–429. Available at : <https://doi.org/10.1053/j.gastro.2017.04.022>.

Hwang, H.-J. *et al.* (2021) ‘Antipathogenic Compounds That Are Effective at Very Low Concentrations and Have Both Antibiofilm and Antivirulence Effects against *Pseudomonas aeruginosa*’, *Microbiology Spectrum* [Preprint]. Edited by A.G. Oglesby. Available at: <https://doi.org/10.1128/Spectrum.00249-21>.

Jang, S. *et al.* (2022) ‘Host immune response mediates changes in *cagA* copy number and virulence potential of *Helicobacter pylori*’, *Gut Microbes*, 14(1), p. 2044721. Available at: <https://doi.org/10.1080/19490976.2022.2044721>.

Kakiuchi, T. *et al.* (2021) ‘Gut microbiota changes related to *Helicobacter pylori* eradication with vonoprazan containing triple therapy among adolescents: a prospective multicenter study’, *Scientific Reports*, 11(1), p. 755. Available at : <https://doi.org/10.1038/s41598-020-80802-3>.

Kalisperati, P. *et al.* (2017) ‘Inflammation, DNA Damage, *Helicobacter pylori* and Gastric Tumorigenesis’, *Frontiers in Genetics*, 8. Available at: <https://doi.org/10.3389/fgene.2017.00020>.

Katelaris, P. *et al.* (2023) ‘*Helicobacter pylori* World Gastroenterology Organization Global Guideline’, *Journal of Clinical Gastroenterology*, 57(2), pp. 111–126. Available at: <https://doi.org/10.1097/MCG.0000000000001719>.

Liu, H. and Naismith, J.H. (2008) ‘An efficient one-step site-directed deletion, insertion, single and multiple-site plasmid mutagenesis protocol’, *BMC biotechnology*, 8, p. 91. Available at: <https://doi.org/10.1186/1472-6750-8-91>.

Maixner, F. *et al.* (2016) ‘The 5300-year-old *Helicobacter pylori* genome of the Iceman’, *Science*, 351(6269), pp. 162–165. Available at : <https://doi.org/10.1126/science.aad2545>.

Mansour-Ghanaei, F. *et al.* (2019) ‘Efficacy and tolerability of fourteen-day sequential quadruple regimen: pantoprazole, bismuth, amoxicillin, metronidazole and or furazolidone as first-line therapy for eradication of *Helicobacter pylori*: a randomized, double-blind clinical trial’, *EXCLI Journal*; 18: Doc644; ISSN 1611-2156 [Preprint]. Available at: <https://doi.org/10.17179/excli2019-1613>.

Marshall, B. and Warren, J.R. (1984) ‘UNIDENTIFIED CURVED BACILLI IN THE STOMACH OF PATIENTS WITH GASTRITIS AND PEPTIC ULCERATION’, *The Lancet*, 323(8390), pp. 1311–1315. Available at: [https://doi.org/10.1016/S0140-6736\(84\)91816-6](https://doi.org/10.1016/S0140-6736(84)91816-6).

Murshudov, G.N., Vagin, A.A. and Dodson, E.J. (1997) 'Refinement of Macromolecular Structures by the Maximum-Likelihood Method', *Acta Crystallographica Section D Biological Crystallography*, 53(3), pp. 240–255. Available at: <https://doi.org/10.1107/S0907444996012255>.

Ngo, H.X. and Garneau-Tsodikova, S. (2018) 'What are the drugs of the future?', *MedChemComm*, 9(5), pp. 757–758. Available at: <https://doi.org/10.1039/C8MD90019A>.

Otwinowski, Z. and Minor, W. (1997) '[20] Processing of X-ray diffraction data collected in oscillation mode', in *Methods in Enzymology*. Elsevier, pp. 307–326. Available at: [https://doi.org/10.1016/S0076-6879\(97\)76066-X](https://doi.org/10.1016/S0076-6879(97)76066-X).

Oudouhou, F. *et al.* (2023) *Inhibition of the type IV secretion system from antibiotic-resistant Helicobacter pylori clinical isolates supports the potential of CagA as an anti-virulence target*. preprint. Microbiology. Available at: <https://doi.org/10.1101/2023.09.01.555934>.

Sabino, Y.N.V., Cotter, P.D. and Mantovani, H.C. (2023) 'Anti-virulence compounds against Staphylococcus aureus associated with bovine mastitis: A new therapeutic option?', *Microbiological Research*, 271, p. 127345. Available at : <https://doi.org/10.1016/j.micres.2023.127345>.

Salvatori, S. *et al.* (2023) '*Helicobacter pylori* and Gastric Cancer: Pathogenetic Mechanisms', *International Journal of Molecular Sciences*, 24(3), p. 2895. Available at : <https://doi.org/10.3390/ijms24032895>.

Sathianarayanan, S. *et al.* (2022) 'A new approach against *Helicobacter pylori* using plants and its constituents: A review study', *Microbial Pathogenesis*, 168, p. 105594. Available at: <https://doi.org/10.1016/j.micpath.2022.105594>.

Savvides, S.N. (2003) 'VirB11 ATPases are dynamic hexameric assemblies: new insights into bacterial type IV secretion', *The EMBO Journal*, 22(9), pp. 1969–1980. Available at : <https://doi.org/10.1093/emboj/cdg223>.

Schindelin, J. *et al.* (2012) ‘Fiji: an open-source platform for biological-image analysis’, *Nature Methods*, 9(7), pp. 676–682. Available at: <https://doi.org/10.1038/nmeth.2019>.

Seo, J.W. *et al.* (2019) ‘The analysis of virulence factors and antibiotic resistance between *Helicobacter pylori* strains isolated from gastric antrum and body’, *BMC Gastroenterology*, 19(1). Available at: <https://doi.org/10.1186/s12876-019-1062-5>.

Sharndama, H.C. and Mba, I.E. (2022) ‘*Helicobacter pylori*: an up-to-date overview on the virulence and pathogenesis mechanisms’, *Brazilian Journal of Microbiology*, 53(1), pp. 33–50. Available at : <https://doi.org/10.1007/s42770-021-00675-0>.

Suerbaum, S. *et al.* (2022) ‘Identification of Antimotilins, Novel Inhibitors of *Helicobacter pylori* Flagellar Motility That Inhibit Stomach Colonization in a Mouse Model’, *mBio*. Edited by R. Rappuoli, 13(2), pp. e03755-21. Available at: <https://doi.org/10.1128/mbio.03755-21>.

Tacconelli, E. *et al.* (2018) ‘Discovery, research, and development of new antibiotics: the WHO priority list of antibiotic-resistant bacteria and tuberculosis’, *The Lancet Infectious Diseases*, 18(3), pp. 318–327. Available at: [https://doi.org/10.1016/S1473-3099\(17\)30753-3](https://doi.org/10.1016/S1473-3099(17)30753-3).

Trott, O. and Olson, A.J. (2009) ‘AutoDock Vina: Improving the speed and accuracy of docking with a new scoring function, efficient optimization, and multithreading’, *Journal of Computational Chemistry*, p. NA-NA. Available at: <https://doi.org/10.1002/jcc.21334>.

Wang, L. *et al.* (2021) ‘Dynamic changes in antibiotic resistance genes and gut microbiota after *Helicobacter pylori* eradication therapies’, *Helicobacter* [Preprint]. Available at : <https://doi.org/10.1111/hel.12871>.

Yang, D. *et al.* (2021) ‘Paeonol Attenuates Quorum-Sensing Regulated Virulence and Biofilm Formation in *Pseudomonas aeruginosa*’, *Frontiers in Microbiology*, 12, p. 692474. Available at : <https://doi.org/10.3389/fmicb.2021.692474>.

Yang, L. *et al.* (2020) ‘Gastric cancer: Epidemiology, risk factors and prevention strategies’, *Chinese Journal of Cancer Research*, 32(6), pp. 695–704. Available at : <https://doi.org/10.21147/j.issn.1000-9604.2020.06.03>.

Ye, Q. *et al.* (2020) ‘Changes in the human gut microbiota composition caused by *Helicobacter pylori* eradication therapy: A systematic review and meta-analysis’, *Helicobacter*, p. e12713. Available at : <https://doi.org/10.1111/hel.12713>.

Yeo, H.-J. *et al.* (2000) ‘Crystal Structure of the Hexameric Traffic ATPase of the *Helicobacter pylori* Type IV Secretion System’, *Molecular Cell*, 6(6), pp. 1461–1472. Available at : [https://doi.org/10.1016/S1097-2765\(00\)00142-8](https://doi.org/10.1016/S1097-2765(00)00142-8).

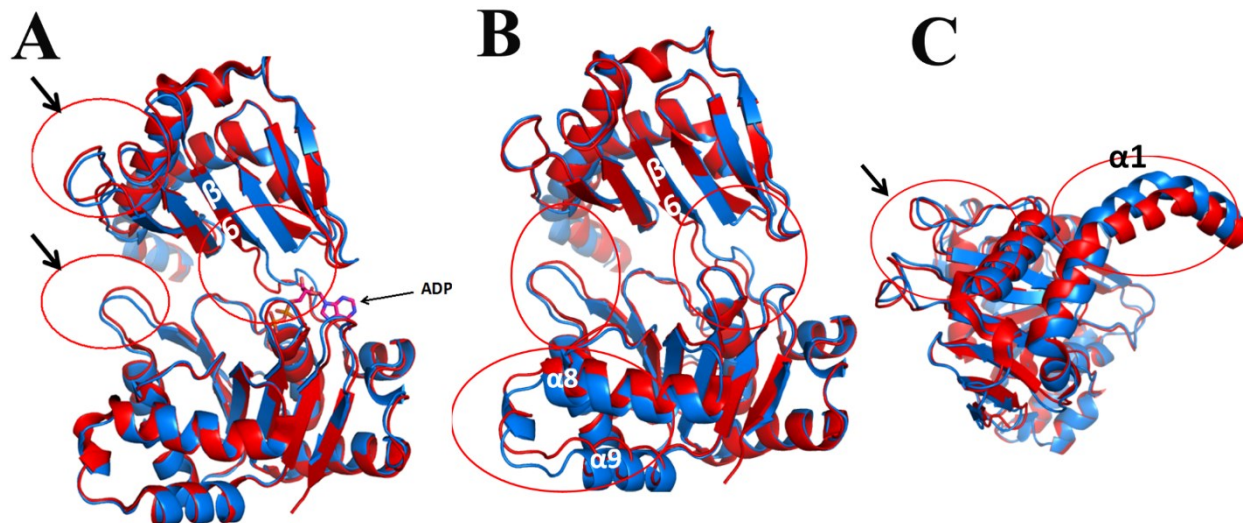
Zhang, Y. *et al.* (2022) ‘Perspectives from recent advances of *Helicobacter pylori* vaccines research’, *Helicobacter*, 27(6). Available at : <https://doi.org/10.1111/hel.12926>.

Zhang, Y. *et al.* (2023) ‘New regimens as first-line eradication therapy for *Helicobacter pylori* infection in patients allergic to penicillin: A randomized controlled trial’, *Helicobacter* [Preprint]. Available at: <https://doi.org/10.1111/hel.12956>.

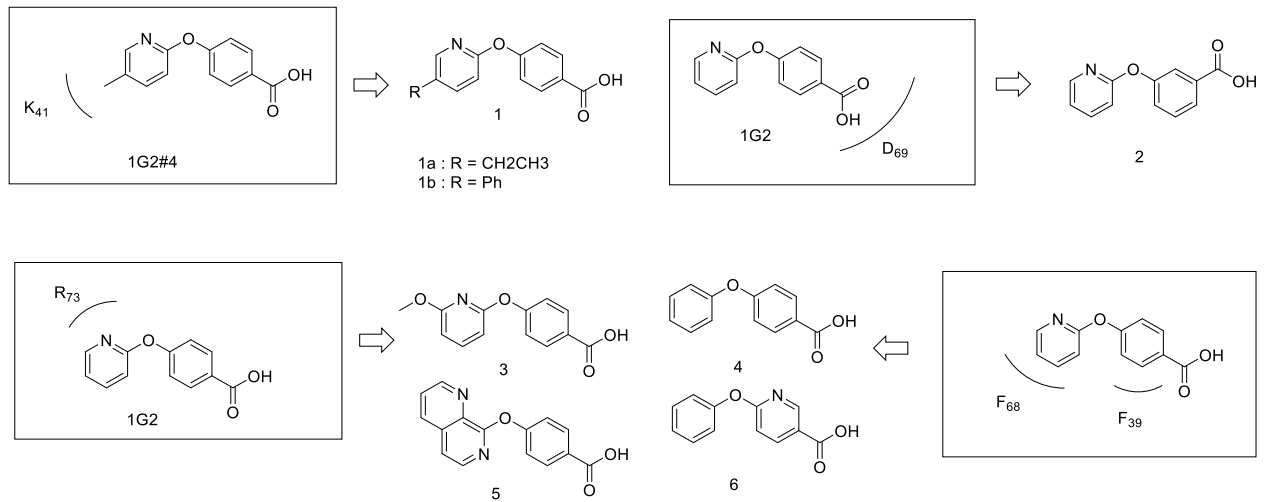
ix. Supplementary information

H.pylori_Cag alpha	MTEDRLSAEDKKFLE--VERALKEAALNPLRHATEELFGDFLKMENITEICYNGNKVVVWL	59
A.tumefaciens_VirB11	-----ME--VDPQLRILLLKPILEWLDPRTEEVAINRRPGEAFVR	37
B.suis_VirB11	-----MMSNRSDFIIVPEAAVK--RAASVNFHLEPLRPWLDDPQITEVCVNRPEGEVFC	52
pKM101_traG	-----MTDAAFYQLGGLRLEYLEDPTVFEIRINCFQEIVCD	35
R388_TrwD	-----MSTVSKASPLSSGNRVG--KDQAVAQLLRPLRFLDAPEVTELSICRPGEVWTK	52
	: * . * :	
H.pylori_Cag alpha	KNNGEWQPFQVDRKAFSLSRMLMHFARCCASFKKKTIDNYENPILSSNLANGERVQIVLS	119
A.tumefaciens_VirB11	Q-AGAFLEKFLPV-S--YDDLEDIALAGALRKQDV-GPRNPICATELDPGERLQICLP	91
B.suis_VirB11	R-ASAWEYVAVPNLD--YEHLISLGTATARFVDQDI-SDSRPVLSAILPMGERIQIVRP	107
pKM101_traG	T-FSGRRVQNAAIT--ADFIRNLAKSLVSS--NK-LTMQAINDVILPGGIRGVICLP	87
R388_TrwD	T-FEGWQVHEVPFELT--EPFLQALITAIIVY--NG-VAPKSVNVVVLPGGQRGTIAQA	104
	: : : * * * *	
H.pylori_Cag alpha	PVTVNDETISISIRIIPSKTIVPHSFFEEQGFYNLLD-----	155
A.tumefaciens_VirB11	PT-VPSGTVSLTIRRPSSRVSSSLKEVSSRYDAPRWVQWKERK-----	135
B.suis_VirB11	PA-CEHGTISVTRKPSFTRRTLEDYQQGGFFKHVRPMSK-----	148
pKM101_traG	PA-VIDGTTAVAFKDLAADKKNLEQLTSEGIFSDCRKITGSKQSLTDDDFL-----	138
R388_TrwD	PA-VIDGTLFSLFKHSLVVKITLEELDAEGAFDTFTDVSFNKPSAEENHYLTVQDFTRL	163
	* . * : : *	
H.pylori_Cag alpha	-NKEQA-----ISAIKDGIAGKNVIVCGGTGSGKTTIKSIMEFIPKEERII	204
A.tumefaciens_VirB11	DQHDEAILRYDNGDLEAFHACVVGRLTMLLCPGTGSGKTTMSKTLINAIIPQERLI	195
B.suis_VirB11	TPFEQELLALKEAGDYMSFLRRAVQLERIVVAGETGSGKTTLMKALMQEIPFDQLI	208
pKM101_traG	-----KELHSSEKWPFLQTAVEKRTIVICGETGSGKTVLTRALLKSLHKDERVIL	191
R388_TrwD	EPFEVELLKLKRDGTIREFLEKCVLYKRNIIAGKTGSGKTTFARSLIEKVPPEERII	223
	: : : : * * * * * : : : : * * * * :	
H.pylori_Cag alpha	EDTEELVFKHHKNYTLQFFGGN-----ITSADCLKSCLMRPDRILGELRSSEAYD	256
A.tumefaciens_VirB11	EDTLELVIPIH-ENHVRLLYSKNGA--GLGAVTAHELLQASLRMRPDRILLGEIRDDA	252
B.suis_VirB11	EDVPELFLPDHPNHVHLFYPSEAKEEENAPVTAATLLRSLCRMKPTRILLAEIRGGEAYD	268
pKM101_traG	EDVHEVTVDHVVEAVYMMYGDAGK--IGFVSATDALRACMRLTPGRIIMTELRDDAAWD	248
R388_TrwD	EDVHELFLPNHPNRVHMLYGYG---AGRVSADCLAACMRQSPDRIFLAELRGNEAWE	278
	** . * : : : : : : : * : : * * * * : * : * . * :	
H.pylori_Cag alpha	FYNVLCSGHGKTLTTLHAGSSEEAIFIRLANMSSNSAARNIKFESLIEGFKDLIDMIVHI	316
A.tumefaciens_VirB11	YLSEVVSGHPGSISTIHGANPVQGFKKLFLSVKSSAQGASLEDRTLIDMLATAVDVIVF	312
B.suis_VirB11	FINVAASGHGGSITSCHAGSCELTFFERLALMVLQNRQGRQLPYEIRRLLYLVVDVVHV	328
pKM101_traG	YLKALNTGHGPGVMSTHANSARDAFNRIGLLIKATPIGRMLDMSDIRMLYSTIDVVVHM	308
R388_TrwD	YLNSLNTGHGGSITTHANNALQTFFERCATLIIKSDVGRQLEMEMIKLVLYTTIDVVLFF	338
	: . : * * * : : * . * : : : : : : : : : * : : : :	
H.pylori_Cag alpha	NHH----KQCEDEFYIKHR-----	330
A.tumefaciens_VirB11	RA---HGDIEVGEIWLAAADARRRGETIGDLLNQ	344
B.suis_VirB11	HNGVHDGTGFHISEVWYDPNTRKALS-LQHSEKT-	361
pKM101_traG	E-----KRIKIEIYDFPEYKMQCV-NGSL----	331
R388_TrwD	K-----DKLVEVYFDPIFSKSKM-A-----	358
	. * . :	

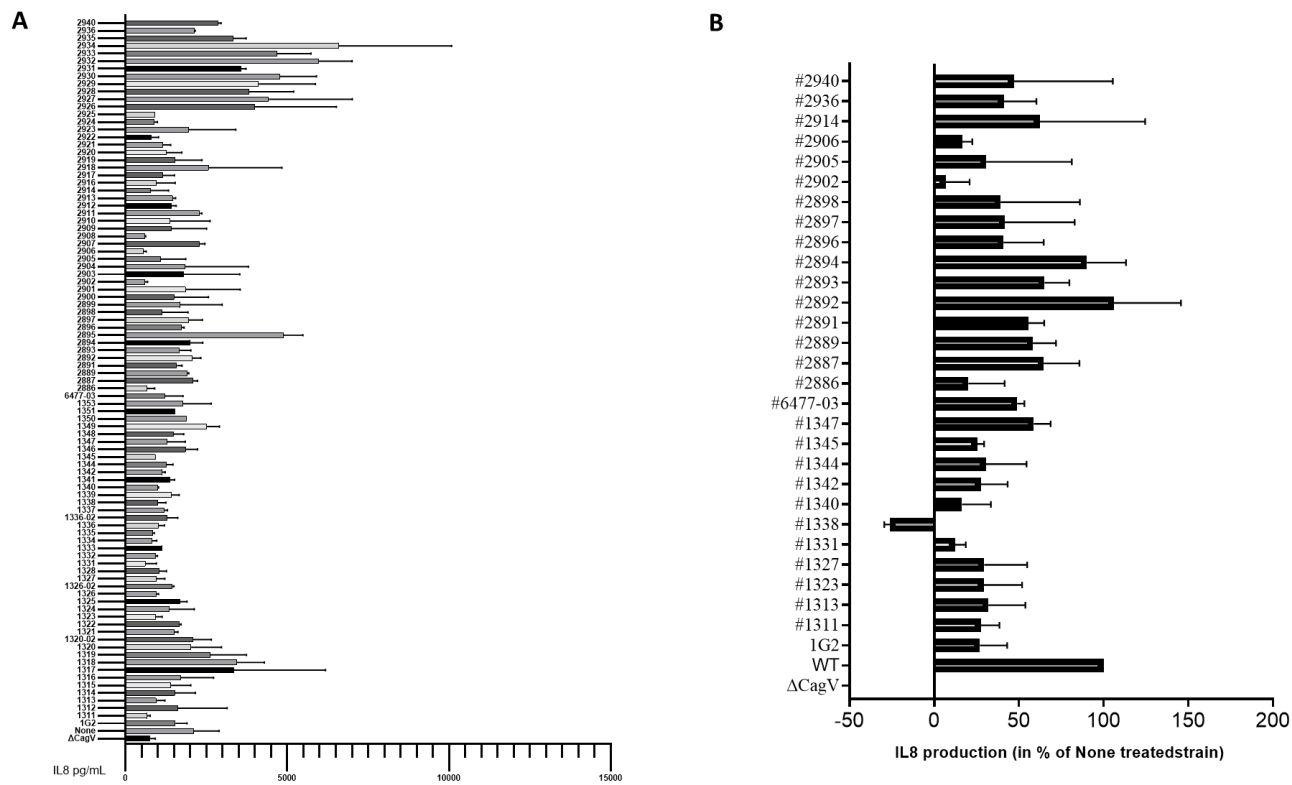
supplementary Figure 1. Multiple sequence alignment of CagA/VirB11 homologs. Selected CagA/VirB11 homologs from the T4SS of *Agrobacterium tumefaciens* C58, *Brucella suis* 1330, plasmids pKM101 and R388 were aligned using the clustal omega online tool (<https://www.ebi.ac.uk/Tools/msa/clustalo/>). The amino acids corresponding to the 1G2 binding site on CagA are indicated in red and the ATPase active site is labelled green with a box.



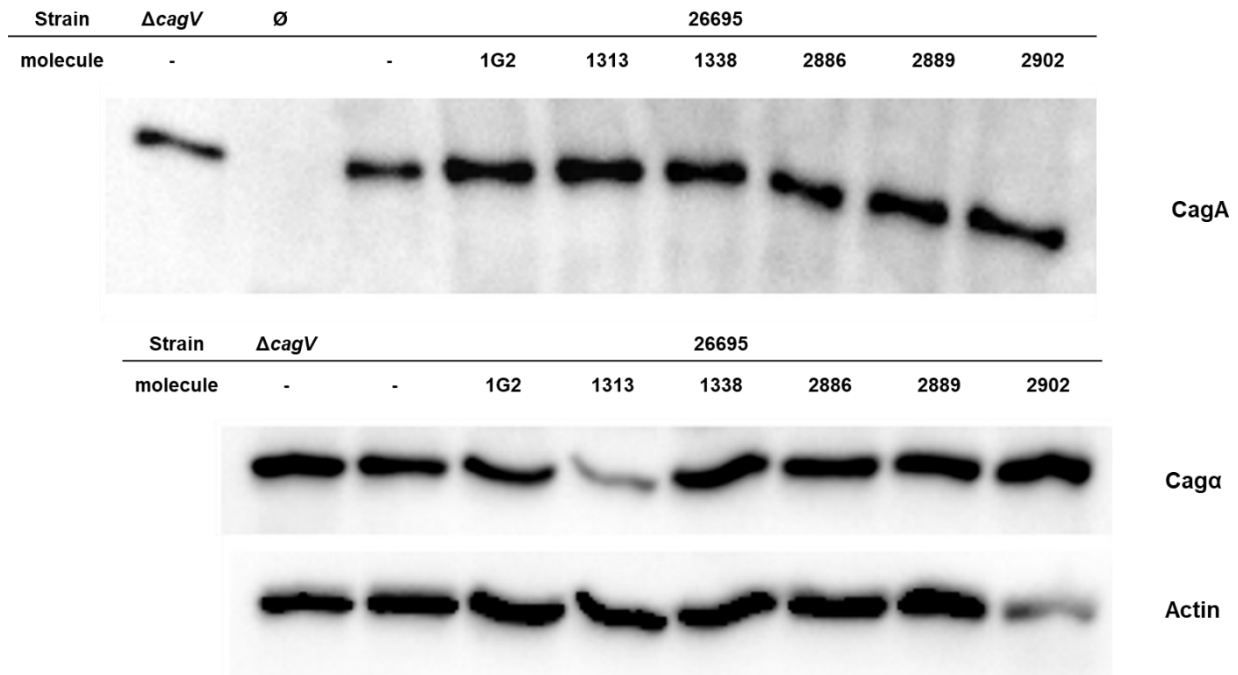
supplementary Figure 2. Crystal structures of the Cag α -1G2 complex compared to previously determined structures of Cag α . A) Cag α -1G2 complex (blue) and Cag α -ADP complex (red), PDB ID : 1G6O; B) Cag α -1G2 complex (blue) and Cag α apoprotein structure (red), PDB ID : 1NLZ; C) view from the of top of structure, Caga-1G2 complex (blue) and Cag α apoprotein (red). Arrows and red circles indicate structural changes in different parts of the protein.



supplementary Figure 3: Design of 1G2 analogs. Overview of the synthetic analogs designed to probe the putative interactions between the 1G2 derivatives and the various amino acids at the binding site.



supplementary Figure 4: Results of the screens of 1G2 derivatives. AGS cells were infected for 24h with *H. pylori* pre-incubated with 200 μ M of molecules and the amounts of secreted IL-8 were measured by ELISA A) the first screening was done twice with duplicates, only a single set of results is presented due to significant standard deviation observed in certain molecules, resulting in an unreadable graph, pg/mL B) The results of the IL-8 quantification were analyzed by pairs comparing the non-treated result (100% induction) with the treated results (triplicates). The Δ cagV strain was used as negative control and analyzed using the strain 26695.



supplementary Figure 5: Expression of Cag protein during AGS cells infection with or without treatment with 1G2 and its derivatives. Cell lysates of *H. pylori* strains were separated by SDS-PAGE, followed by western blotting with specific antisera. CagA and Cag α proteins were detected using specific antibodies and actin was used as a loading control. Representative results from four repetitions are shown.

supplementary Table 1: Primers for the creation of 1G2 binding site mutants

PRIMER'S NAME	CODON	AA	PRIMER 5' to 3'
calpha_D38A_F	GAT-	D38A	GAAGAACTTTTTGGTGCCTTTTTAAAAATGGAA
calpha_D38A_R	>GCG		TTCCATTTTTAAAAACGCACCAAAAAGTTCCTC
calpha_F39A_F	TTT-	F39A	GAACTTTTTTGGTGATGCGTTAAAAATGGAAAAT
calpha_F39A_R	>GCG		ATTTCCATTTTTAACGCATCACCAAAAAGTTC
calpha_K41A_F	AAA-	K41A	TTTGGTGATTTTTTAGCGATGGAAAATATCACT
calpha_K41A_R	>GCG		AGTGATATTTCCATCGCTAAAAAATCACCAAA
calpha_M42A_F	ATG-	M42A	GGTGATTTTTTAAAAGCGGAAAATATCACTGAG
calpha_M42A_R	>GCG		CTCAGTGATATTTCCATTTTTAAAAAATCACC
calpha_F68A_F	TTT-	F68A	GGCGAATGGCAACCAGCGGATGTGAGAGACAGG
calpha_F68A_R	>GCG		CCTGTCTCTCACATCCGCTGGTTGCCATTCGCC
calpha_R73A_F	AGG-	R73A	CAGGCTAAAGGCTTTCGCGTCTCTCACATCAAA
calpha_R73A_R	>GCG		TTTGATGTGAGAGACGCGAAAGCCTTTAGCCTG
calpha_R73K_F	AGG-	R-73K	CAGGCTAAAGGCTTTTTTGTCTCTCACATCAAA
calpha_R73K_R	>AAA		TTTGATGTGAGAGACAAAAAAGCCTTTAGCCTG

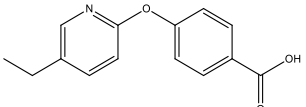
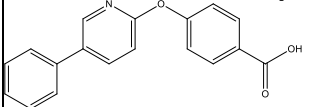
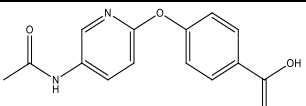
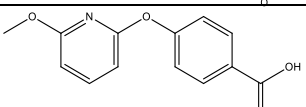
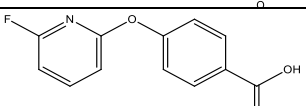
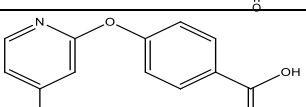
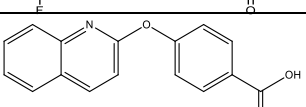
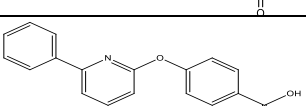
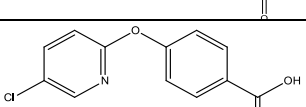
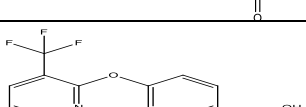
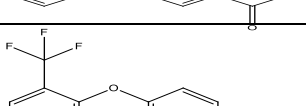
supplementary Table 2: X-ray data collection and refinement statistics.

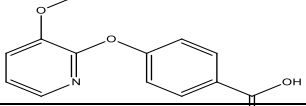
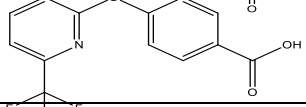
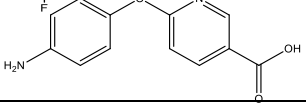
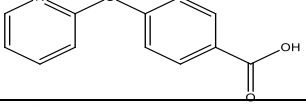
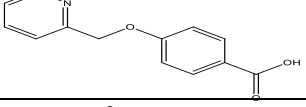
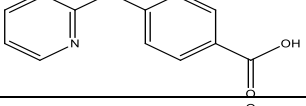
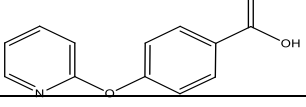
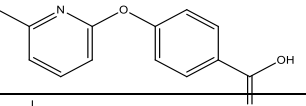
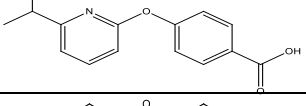
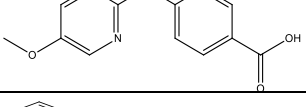
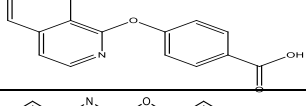
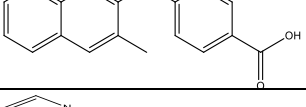
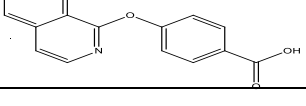
	Cagα-1G2
Resolution range	38.5 - 2.9 (3.00 - 2.90)
Space group	<i>P</i> 6 ₃ 22
Unit cell	112.075 112.075 231.006 90 90 120
Total reflections	165306
Unique reflections	18083 (1737)
Multiplicity	5.2
Completeness (%)	92.4 (90.74)
Mean I/sigma(I)	7.4(2.4)
Wilson B-factor	45.43
R-merge	0.12
R-pim	0.08
Reflections used in refinement	18049 (1734)
Reflections used for R-free	976 (92)
<i>R</i>_{work} / <i>R</i>_{free}	0.230 (0.313) / 0.278 (0.423)
Protein residues	646
RMS (bonds)	0.012
RMS (angles)	1.59
Ramachandran favored (%)	95.1
Ramachandran allowed (%)	4.59
Ramachandran outliers (%)	0.31
Clashscore	3.87
Average B-factor	46.27
Coordinate error	0.203
PDB	6BGE

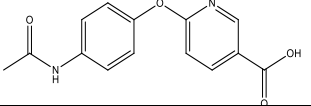
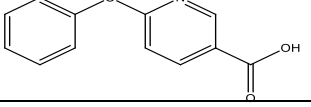
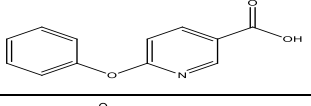
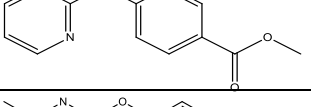
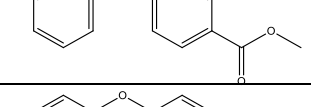
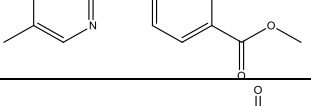
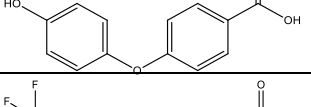
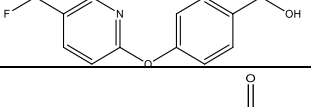
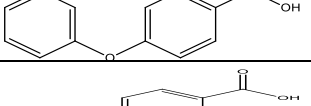
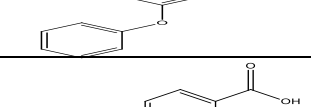
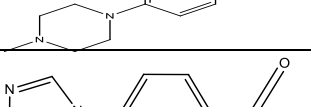
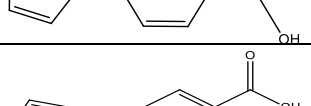
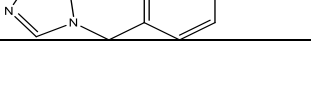
supplementary Table 3: Docking of derivatives of molecule 1G2 with target Cag α . Binding energy is shown as kcal/mol as calculated by Autodock Vina software.

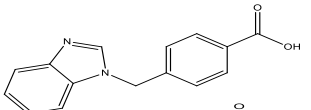
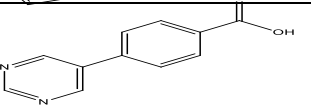
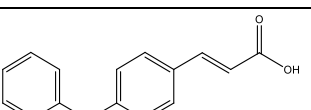
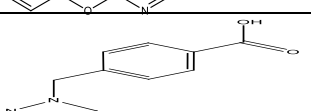
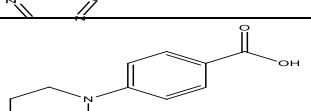
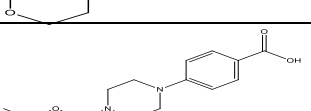
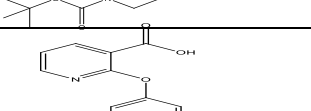
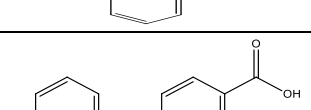
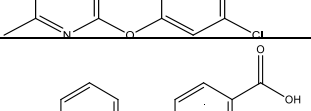
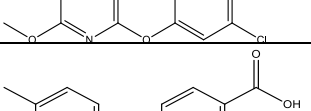
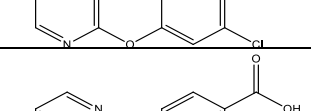
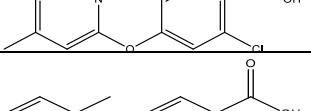
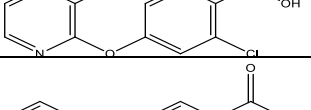
Molecule	Binding energy ($\Delta G/mol$)
1G2	-6.6
1G2_1313	-10.2
1G2_1338	-9
1G2_2886	-9.4
1G2_2889	-9.4
1G2_2902	-9.6

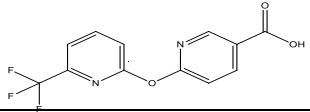
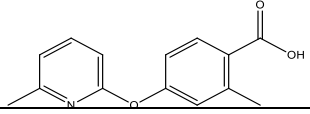
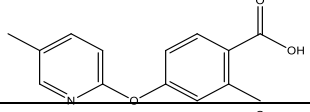
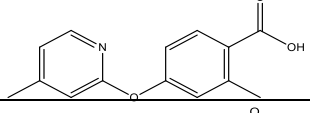
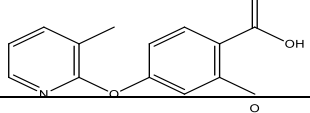
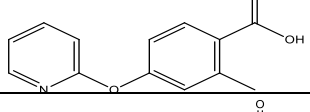
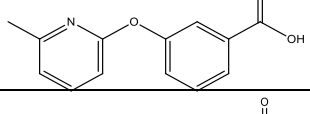
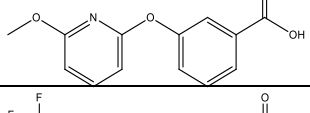
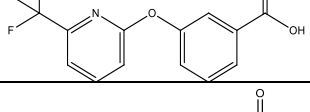
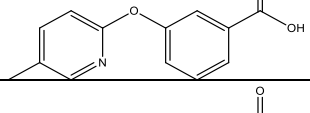
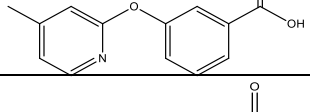
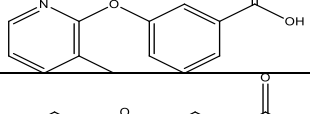
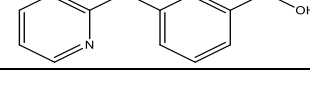
supplementary Table 4: List of 1G2 derivatives created by medicinal chemistry. Structures, composition, names assigned after synthesis, numbers, AGS cell cytotoxicity and inhibition of *H. pylori* 26696 growth.

Structure	Composition	UM#	Name	Cells cytotoxicity	26695 growth inhibition
	C14H13NO3	UM0141311-01	#1311	None	None
	C18H13NO3	UM0141312-01	#1312	None	None
	C14H12N2O4	UM0141313-01	#1313	None	None
	C13H11NO4	UM0141314-01	#1314	None	None
	C12H8FNO3	UM0141315-01	#1315	None	None
	C12H8FNO3	UM0141316-01	#1316	None	None
	C16H11NO3	UM0141317-01	#1317	None	None
	C18H13NO3	UM0141318-01	#1318	None	None
	C12H8ClNO3	UM0141319-01	#1319	None	None
	C13H8F3NO3	UM0141320-01	#1320	None	None
	C13H8F3NO3	UM0141320-02	#1320-02	None	None

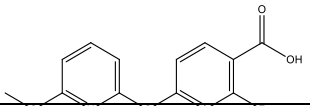
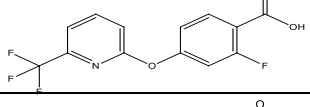
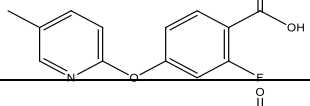
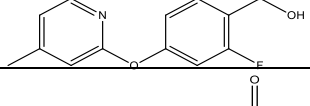
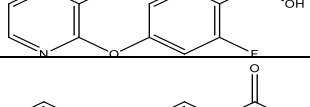
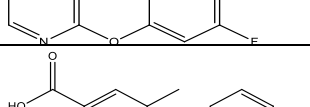
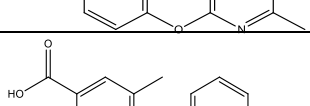
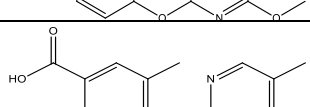
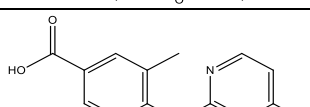
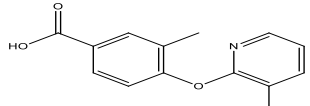
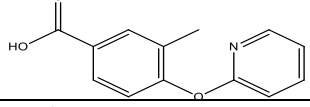
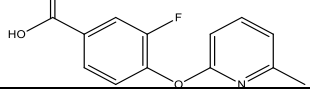

	C13H11NO4	UM0141321-01	#1321	None	None
	C13H8F3NO3	UM0141322-01	#1322	None	None
	C12H10N2O3	UM0141323-01	#1323	None	None
	C12H9NO2S	UM0141324-01	#1324	None	None
	C13H11NO3	UM0141325-01	#1325	None	None
	C12H9NO3	UM0141326-01	#1326	None	None
	C12H9NO3	UM0141326-02	#1326-02	None	None
	C13H11NO3	UM0141327-01	#1327	None	None
	C15H15NO3	UM0141328-01	#1328	None	None
	C13H11NO4	UM0141331-01	#1331	None	None
	C16H11NO3	UM0141332-01	#1332	None	None
	C17H13NO3	UM0141333-01	#1333	None	None
	C15H10N2O3	UM0141334-01	#1334	None	None

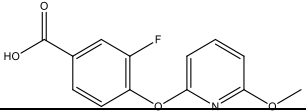
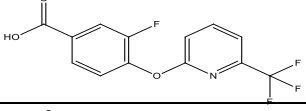
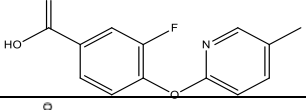
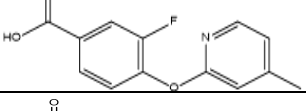
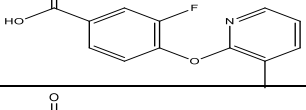
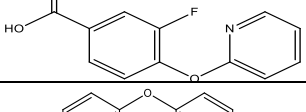
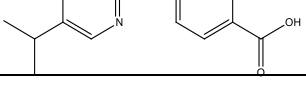
	C14H12N2O4	UM0141335-01	#1335	None	None
	C12H9NO3	UM0141336-01	#1336	None	None
	C12H9NO3	UM0141336-02	#1336-02	None	None
	C13H11NO3	UM0141337-01	#1337	None	None
	C14H13NO3	UM0141338-01	#1338	None	None
	C14H13NO3	UM0141339-01	#1339	None	None
	C13H10O4	UM0141340-01	#1340	None	None
	C13H8F3NO3	UM0141341-01	#1341	None	None
	C13H10O3	UM0141342-01	#1342	None	None
	C13H10O3	UM0141343-01	#1343	yes	None
	C12H16N2O2	UM0141344-01	#1344	None	None
	C10H8N2O2	UM0141345-01	#1345	None	None
	C11H10N2O2	UM0141346-01	#1346	None	None

	C15H12N2O2	UM0141347-01	#1347	None	None
	C11H8N2O2	UM0141348-01	#1348	None	None
	C14H11NO3	UM0141349-01	#1349	None	None
	C10H9N3O2	UM0141350-01	#1350	None	None
	C11H13NO3	UM0141351-01	#1351	None	None
	C16H22N2O4	UM0141353-01	#1353	None	None
	C12H9NO3	UM0016477-03	#6477-03	None	None
	C13H10ClNO3	UM0142886-01	#2886	None	None
	C13H10ClNO4	UM0142887-01	#2887	None	None
	C13H10ClNO3	UM0142888-01	#2888	yes	None
	C13H10ClNO3	UM0142889-01	#2889	none	None
	C13H10ClNO3	UM0142890-01	#2890	Yes	None
	C12H8ClNO3	UM0142891-01	#2891	none	None

	C12H7F3N2O3	UM0142892-01	#2892	none	None
	C14H13NO3	UM0142893-01	#2893	none	None
	C14H13NO3	UM0142894-01	#2894	none	None
	C14H13NO3	UM0142895-01	#2895	none	None
	C14H13NO3	UM0142896-01	#2896	none	None
	C13H11NO3	UM0142897-01	#2897	none	None
	C13H11NO3	UM0142898-01	#2898	none	None
	C13H11NO4	UM0142899-01	#2899	none	None
	C13H8F3NO3	UM0142900-01	#2900	none	None
	C13H11NO3	UM0142901-01	#2901	none	None
	C13H11NO3	UM0142902-01	#2902	none	None
	C13H11NO3	UM0142903-01	#2903	none	None
	C12H9NO3	UM0142904-01	#2904	none	None

	C14H13NO4	UM0142905-01	#2905	none	None
	C14H13NO5	UM0142906-01	#2906	none	None
	C14H13NO3	UM0142907-01	#2907	none	None
	C14H13NO4	UM0142908-01	#2908	none	None
	C14H10F3NO3	UM0142909-01	#2909	none	None
	C14H13NO3	UM0142910-01	#2910	none	None
	C14H13NO3	UM0142911-01	#2911	none	None
	C14H13NO3	UM0142912-01	#2912	none	None
	C13H11NO3	UM0142913-01	#2913	none	None
	C17H13NO3	UM0142914-01	#2914	none	None
	C17H10F3NO3	UM0142915-01	#2915	yes	None
	C17H13NO3	UM0142916-01	#2916	None	None
	C13H10FNO3	UM0142917-01	#2917	None	None

	C13H10FNO4	UM0142918-01	#2918	None	None
	C13H7F4NO3	UM0142919-01	#2919	None	None
	C13H10FNO3	UM0142920-01	#2920	None	None
	C13H10FNO3	UM0142921-01	#2921	None	None
	C13H10FNO3	UM0142922-01	#2922	None	None
	C12H8FNO3	UM0142923-01	#2923	None	None
	C14H13NO3	UM0142924-01	#2924	None	None
	C14H13NO4	UM0142925-01	#2925	None	None
	C14H13NO3	UM0142926-01	#2926	None	None
	C14H13NO3	UM0142927-01	#2927	None	None
	C14H13NO3	UM0142928-01	#2928	None	None
	C13H11NO3	UM0142929-01	#2929	None	None
	C13H10FNO3	UM0142930-01	#2930	None	None

	C13H10FNO4	UM0142931-01	#2931	None	None
	C13H7F4NO3	UM0142932-01	#2932	None	None
	C13H10FNO3	UM0142933-01	#2933	None	None
	C13H10FNO3	UM0142934-01	#2934	None	None
	C13H10FNO3	UM0142935-01	#2935	None	None
	C12H8FNO3	UM0142936-01	#2936	None	None
	C15H15NO3	UM0142940-01	#2940	None	None

IV. Conclusion et discussion

Le monde fait face à une pandémie silencieuse qui est la résistance aux antibiotiques. Afin de contrecarrer ces résistances, il est urgent de trouver de nouvelles approches thérapeutiques. Depuis 30 ans, aucun nouvel antibiotique n'a été mis sur le marché, mais la prolifération des résistances aux antibiotiques accélère (163,182,183). L'utilisation inappropriée des antibiotiques, le surdosage ou sous-dosage et le manque d'innovation ont entraîné au cours des dernières décennies un véritable problème dans les milieux hospitaliers (163,184,185). Les prédictions de l'organisation mondiale de la santé par rapport au défi du traitement d'infections bactériales dans les 10 prochaines années sont alarmantes. C'est pourquoi il faut trouver de nouveaux antibiotiques et aussi des alternatives thérapeutiques (186). Des vaccins, la thérapie aux bactériophages ou encore les remèdes ancestraux sont étudiés depuis plusieurs années, mais ce genre de thérapies fait face à de nombreuses limitations (138). La montée de la bio-informatique, de l'arrimage moléculaire et de la biologie structurale permettent l'invention de nouvelles formes de thérapie. Au lieu de cibler les fonctions essentielles pour la bactérie, on peut également cibler les outils que la bactérie utilise pour infecter l'hôte. L'utilisation de petites molécules inhibitrices de facteurs de virulence pourrait être une nouvelle forme de thérapie (152,156,187).

Dans cet esprit, nous avons élaboré un projet comprenant le design d'une nouvelle famille de molécules anti-facteurs de virulence. Nous avons ciblé *H. pylori*, une bactérie responsable de maladies gastriques sévères qui est la bactérie pathogène la plus répandue chez l'humain (63,188,189). Cette bactérie possède de nombreux facteurs de virulence, dont certains reconnus comme étant responsables des maladies gastriques sévères telles que les ulcères de l'estomac ou le cancer de l'estomac. Il a été reconnu que l'un de ces facteurs de virulence, le SST4, est impliqué dans l'apparition de maladies gastriques en permettant l'injection de CagA, la première protéine bactériale oncogène identifiée (20). Malgré sa similarité aux SST4 d'autres espèces, il est intéressant de noter que le SST4 de *H. pylori* reste unique comprenant de nombreuses protéines essentielles pas présentes dans d'autres SST4. Une protéine très bien caractérisée est Cag α , il s'agit d'une ATPase identifiée dans les années 2000 qui est un homologue de VirB11. Cette protéine est un hexamère et se situe au niveau de la membrane interne de la bactérie. Cette protéine a déjà été

l'objet d'études pour le design de molécules inhibitrices, cependant ces recherches ne semblent plus en cours (169). Cependant, Cag α serait une cible privilégiée pour le design de molécules inhibitrices car elle reste spécifique à *H. pylori*.

Dans nos travaux, nous avons démontré que l'utilisation de petites molécules pour inhiber la fonction d'un facteur de virulence est possible. Après l'identification de 1G2 par Arya *et al*, comme potentielle molécule inhibitrice de Cag α , nous avons caractérisé son mécanisme d'inhibition en combinant l'observation *in vitro* de son effet sur Cag α purifiée ainsi que sur un modèle d'infection de cellules gastriques humaines.

Premièrement, 1G2 a été testée sur des souches cliniques issues de biopsies gastriques. Il y a une grande variabilité génétique entre souches de *H. pylori* et elles ne possèdent pas toutes un SST4 complet et fonctionnel. Donc l'étude de 1G2 et de ses dérivées sur des souches identifiées en clinique pourrait démontrer leur potentielle utilisation pour le traitement de patients. Nous avons testé 1G2 sur des souches résistantes à au moins un antibiotique de première ligne. Nous avons aussi déterminé par PCR la présence du *cagPAI*. En utilisant les techniques de microscopie électronique et la quantification d'IL-8, un marqueur d'inflammation, nous avons identifié une souche #3793 qui montrait la même réponse à 1G2 que la souche de laboratoire 26695. En effet, nous avons observé que l'induction d'IL-8 était significativement réduite comparée aux résultats sans traitement et le SST4 n'était pas visible en microscopie. De façon intéressante, deux des souches identifiées comme possédant le *cagPAI*, ne répondaient pas au traitement avec 1G2 comme la souche 26696. Aucun effet sur l'induction des IL-8 n'a été observé. L'analyse des images de microscopie électronique à balayage (SEM), montrait que les souches ne présentaient pas de SST4. Ceci a mené à l'hypothèse que ces souches, malgré la présence du *cagPAI*, ne possédaient pas un SST4 avec un pilus extracellulaire. Une autre souche qui a attiré notre attention induisait les IL-8 même en présence de 1G2. Après le séquençage du gène de Cag α , nous avons observé que cette souche porte une mutation au niveau du site de liaison de 1G2, avec R73 remplacée par une K. Cette mutation pourrait expliquer le fait que 1G2 ne soit pas actif sur cette souche.

Ensuite, nous avons utilisé différentes techniques *in vitro* afin de caractériser le mécanisme d'inhibition de 1G2. Utilisant le *differential scanning fluorimetry* (DSF) en complément de

l'évaluation de l'activité ATPase de Cag α , nous avons identifié les résidus du site de liaison de 1G2 les plus importants pour l'effet de la molécule. Les modifications des résidus F39, K41, et R73 ont mené à une perte de liaison de 1G2 en DSF. L'activité ATPase de Cag α de ces mutants n'est pas affectée par 1G2 ce qui est consistant avec son interaction non compétitive avec Cag α .

Basée sur ces observations et l'étude de molécules similaires à 1G2 faite par Arya *et al*, la création d'une librairie de molécules dérivées de 1G2 a été effectuée par chimie médicinale. Le but de ces travaux était de créer des molécules ayant une meilleure efficacité sur Cag α et *H. pylori*. La sélection des molécules a été réalisée en utilisant le modèle d'infection cellulaire décrit par Arya *et al* (176). Des cellules gastriques humaines ont été infectées par une souche de laboratoire de phénotype sauvage de *H. pylori*, pré-incubée avec une des molécules de la librairie. L'induction des IL-8 a ensuite été quantifiée en utilisant un kit ELISA. Parmi les 96 molécules créées, cinq (1313, 1338, 2886, 2889 et 2902) présentaient un bon potentiel inhibiteur. En effet, dans le modèle d'infection, ces cinq molécules réduisaient l'induction des IL-8 plus fortement que 1G2. L'analyse des images de microscopie électronique à balayage de l'infection a montré que la préincubation de *H. pylori* avec les molécules induit une perte de l'assemblage du pilus extérieur du SST4. De plus, l'étude *in vitro* a montré une interaction forte entre les molécules et la cible.

Basée sur ces observations, nous proposons que les molécules 1G2 en interagissant avec Cag α inhibent l'assemblage du cagSST4. En effet les molécules se fixent entre deux monomères de Cag α , induisant un changement de la conformation hexamérique et la formation de quadrimères et trimères de Cag α (176). Nous proposons que la perte de la conformation naturelle de Cag α serait à l'origine de l'inhibition de l'assemblage du cagSST4 et du pilus extérieur. Par conséquent, la virulence est grandement diminuée car CagA ne peut pas être injecté dans les cellules épithéliales et donc ne peut pas interférer avec les voies métaboliques des cellules de l'hôte (52,190). L'interaction des molécules inhibitrices avec Cag α entraîne une cascade de réactions qui résulte de l'inhibition du système entier du SST4, empêchant l'injection de CagA.

Afin de poursuivre cette étude, il serait intéressant d'utiliser des méthodes d'identification de structures à haute définition comme la Cryo-EM (*cryo electron microscopy*), qui permet la visualisation des interactions molécules - protéines (191,192). De plus, nous connaissons

maintenant le site de liaison de 1G2 et nous avons créé une librairie de molécules dérivées en utilisant la chimie médicinale, mais cette technique prend du temps et la synthèse des molécules n'est pas toujours possible. Il serait intéressant d'utiliser des méthodes comme l'arrimage moléculaire ou d'intelligence artificielle afin de créer des molécules à forte affinité avec la cible (187).

Toutes nos observations montrent un effet de 1G2 et ses dérivés sur l'ensemble the SST4. Afin d'approfondir notre compréhension du mécanisme, il faudra tout d'abord effectuer une évaluation de la translocation de CagA qui est phosphorylée après sa translocation dans les cellules gastriques (55,190,193,194). Afin d'obtenir des résultats optimaux, une immunoprécipitation est la plus efficace (195–197). De plus en utilisant la microscopie immuno-électronique, on pourrait localiser CagA ainsi que les points d'interaction entre le SST4 et les cellules gastrique (198–200). En complément, il serait intéressant d'utiliser la microscopie électronique en volume qui permet par tranche des échantillons d'obtenir un modèle 3D d'un échantillon (201).

Enfin, les molécules dérivées de 1G2 devraient être testés sur les souches cliniques disponibles dans notre base de données et plus particulièrement la molécule 1338 sur la souches clinique #3822 afin de vérifier si la mutation observée est responsable de la résistance contre 1G2.

Une suite potentielle à l'étude de nos molécules serait d'analyser les effets chez un modèle animal comme la gerbille utilisée en tant que modèle pour l'infection par *H. pylori* (202,203). Il serait également intéressant de regarder les effets des molécules sur différents stades d'infection chez l'animal, de déterminer le meilleur moment pour utiliser ces molécules et ses effets sur le microbiome en comparaison avec une thérapie d'éradication avec antibiotiques. De plus, le modèle animal permettrait de voir les potentielles synergies entre molécules inhibitrices de Cag α et/ou avec les traitements antibiotiques déjà mis en place.

En conclusion, nous avons démontré qu'il est possible d'inhiber spécifiquement un facteur de virulence chez *H. pylori* avec une petite molécule organique. À partir de cette molécule, nous avons créé une librairie de molécules dérivées également efficaces. Nos observations ouvrent la voie à

d'autres études sur les molécules anti-facteur de virulence et le potentiel de celles-ci pour une utilisation thérapeutique contre les infections bactériennes.

V. Références

1. Marshall B, Warren JR. UNIDENTIFIED CURVED BACILLI IN THE STOMACH OF PATIENTS WITH GASTRITIS AND PEPTIC ULCERATION. *The Lancet*. juin 1984;323(8390):1311-5.
2. Amieva M, Peek RM. Pathobiology of *Helicobacter pylori*-Induced Gastric Cancer. *Gastroenterology*. janv 2016;150(1):64-78.
3. Oertli M, Noben M, Engler DB, Semper RP, Reuter S, Maxeiner J, et al. *Helicobacter pylori* - glutamyl transpeptidase and vacuolating cytotoxin promote gastric persistence and immune tolerance. *Proc Natl Acad Sci*. 19 févr 2013;110(8):3047-52.
4. Rad R, Brenner L, Bauer S, Schwendy S, Layland L, da Costa CP, et al. CD25+/Foxp3+ T Cells Regulate Gastric Inflammation and *Helicobacter pylori* Colonization In Vivo. *Gastroenterology*. août 2006;131(2):525-37.
5. Kalisperati P, Spanou E, Pateras IS, Korkolopoulou P, Varvarigou A, Karavokyros I, et al. Inflammation, DNA Damage, *Helicobacter pylori* and Gastric Tumorigenesis. *Front Genet* [Internet]. 27 févr 2017 [cité 24 févr 2023];8. Disponible sur: <http://journal.frontiersin.org/article/10.3389/fgene.2017.00020/full>
6. Robinson K, White J, Winter J. Differential inflammatory response to *Helicobacter pylori* infection: etiology and clinical outcomes. *J Inflamm Res*. août 2015;137.
7. Salvatori S, Marafini I, Laudisi F, Monteleone G, Stolfi C. *Helicobacter pylori* and Gastric Cancer: Pathogenetic Mechanisms. *Int J Mol Sci*. 2 févr 2023;24(3):2895.
8. Cullen TW, Giles DK, Wolf LN, Ecobichon C, Boneca IG, Trent MS. *Helicobacter pylori* versus the host: remodeling of the bacterial outer membrane is required for survival in the gastric mucosa. *PLoS Pathog*. déc 2011;7(12):e1002454.
9. Lina TT. Immune evasion strategies used by *Helicobacter pylori*. *World J Gastroenterol*. 2014;20(36):12753.
10. Coussens LM, Werb Z. Inflammation and cancer. *Nature*. déc 2002;420(6917):860-7.
11. Elbehiry A, Marzouk E, Aldubaib M, Abalkhail A, Anagreyyah S, Anajirih N, et al. *Helicobacter pylori* Infection: Current Status and Future Prospects on Diagnostic, Therapeutic and Control Challenges. *Antibiotics*. 17 janv 2023;12(2):191.
12. Malfertheiner P, Chan FK, McColl KE. Peptic ulcer disease. *The Lancet*. oct 2009;374(9699):1449-61.

13. Zamani M, Ebrahimitabar F, Zamani V, Miller WH, Alizadeh-Navaei R, Shokri-Shirvani J, et al. Systematic review with meta-analysis: the worldwide prevalence of *Helicobacter pylori* infection. *Aliment Pharmacol Ther.* 2018;47(7):868-76.
14. Huang RJ, Laszkowska M, In H, Hwang JH, Epplein M. Controlling Gastric Cancer in a World of Heterogeneous Risk. *Gastroenterology.* avr 2023;164(5):736-51.
15. Sung H, Ferlay J, Siegel RL, Laversanne M, Soerjomataram I, Jemal A, et al. Global Cancer Statistics 2020: GLOBOCAN Estimates of Incidence and Mortality Worldwide for 36 Cancers in 185 Countries. *CA Cancer J Clin.* mai 2021;71(3):209-49.
16. Yang L, Ying X, Liu S, Lyu G, Xu Z, Zhang X, et al. Gastric cancer: Epidemiology, risk factors and prevention strategies. *Chin J Cancer Res.* 2020;32(6):695-704.
17. Butcher LD, den Hartog G, Ernst PB, Crowe SE. Oxidative Stress Resulting From *Helicobacter pylori* Infection Contributes to Gastric Carcinogenesis. *Cell Mol Gastroenterol Hepatol.* mai 2017;3(3):316-22.
18. Handa O, Naito Y, Yoshikawa T. *Helicobacter pylori*: a ROS-inducing bacterial species in the stomach. *Inflamm Res.* déc 2010;59(12):997-1003.
19. Ansari S, Yamaoka Y. *Helicobacter pylori* Virulence Factor Cytotoxin-Associated Gene A (CagA)-Mediated Gastric Pathogenicity. *Int J Mol Sci.* 8 oct 2020;21(19):7430.
20. Freire de Melo F, Marques HS, Rocha Pinheiro SL, Lemos FFB, Silva Luz M, Nayara Teixeira K, et al. Influence of *Helicobacter pylori* oncoprotein CagA in gastric cancer: A critical-reflective analysis. *World J Clin Oncol.* 24 nov 2022;13(11):866-79.
21. Department of Medical Microbiology, Istanbul University Cerrahpasa Faculty of Medicine, Istanbul, Turkey, Ozbey D, Demiryas S, Department of General Surgery, Istanbul University Cerrahpasa Faculty of Medicine, Istanbul, Turkey, Akkus S, Department of Medical Microbiology, Istanbul University Cerrahpasa Faculty of Medicine, Istanbul, Turkey, et al. The Relationship between Gastroduodenal Pathologies and *Helicobacter pylori* cagL (Cytotoxin-Associated Gene L) Polymorphism. *Turk J Gastroenterol* [Internet]. 15 févr 2023 [cité 24 févr 2023]; Disponible sur: <https://turkjgastroenterol.org/en/the-relationship-between-gastroduodenal-pathologies-and-helicobacter-pylori-cagl-cytotoxin-associated-gene-l-polymorphism-137018>
22. Suerbaum S, Michetti P. *Helicobacter pylori* Infection. *N Engl J Med.* 10 oct 2002;347(15):1175-86.
23. Celli JP, Turner BS, Afdhal NH, Keates S, Ghiran I, Kelly CP, et al. *Helicobacter pylori* moves through mucus by reducing mucin viscoelasticity. *Proc Natl Acad Sci.* 25 août 2009;106(34):14321-6.

24. Scott DR, Marcus EA, Weeks DL, Sachs G. Mechanisms of acid resistance due to the urease system of *Helicobacter pylori*. *Gastroenterology*. juill 2002;123(1):187-95.
25. Schreiber S, Konradt M, Groll C, Scheid P, Hanauer G, Werling HO, et al. The spatial orientation of *Helicobacter pylori* in the gastric mucus. *Proc Natl Acad Sci*. 6 avr 2004;101(14):5024-9.
26. Robinson K, Letley DP, Kaneko K. The Human Stomach in Health and Disease: Infection Strategies by *Helicobacter pylori*. In: Tegtmeyer N, Backert S, éditeurs. *Molecular Pathogenesis and Signal Transduction by Helicobacter pylori* [Internet]. Cham: Springer International Publishing; 2017 [cité 10 avr 2023]. p. 1-26. (Current Topics in Microbiology and Immunology; vol. 400). Disponible sur: http://link.springer.com/10.1007/978-3-319-50520-6_1
27. Benoit S, Maier RJ. Dependence of *Helicobacter pylori* Urease Activity on the Nickel-Sequestering Ability of the UreE Accessory Protein. *J Bacteriol*. 15 août 2003;185(16):4787-95.
28. Sgouras D, Tegtmeyer N, Wessler S. Activity and Functional Importance of *Helicobacter pylori* Virulence Factors. In: Kamiya S, Backert S, éditeurs. *Helicobacter pylori in Human Diseases* [Internet]. Cham: Springer International Publishing; 2019 [cité 10 avr 2023]. p. 35-56. (Advances in Experimental Medicine and Biology; vol. 1149). Disponible sur: http://link.springer.com/10.1007/5584_2019_358
29. Cheok YY, Lee CYQ, Cheong HC, Vadivelu J, Looi CY, Abdullah S, et al. An Overview of *Helicobacter pylori* Survival Tactics in the Hostile Human Stomach Environment. *Microorganisms*. 3 déc 2021;9(12):2502.
30. Bury-Mone S, Skouloubris S, Labigne A, De Reuse H. The *Helicobacter pylori* UreI protein: role in adaptation to acidity and identification of residues essential for its activity and for acid activation. *Mol Microbiol*. nov 2001;42(4):1021-34.
31. Xia X. Multiple regulatory mechanisms for pH homeostasis in the gastric pathogen, *Helicobacter pylori*. In: *Advances in Genetics* [Internet]. Elsevier; 2022 [cité 10 avr 2023]. p. 39-69. Disponible sur: <https://linkinghub.elsevier.com/retrieve/pii/S0065266022000025>
32. Stingl K. Staying alive overdosed: How does control urease activity? *Int J Med Microbiol*. 1 sept 2005;295(5):307-15.
33. Ansari S, Yamaoka Y. *Helicobacter pylori* Virulence Factors Exploiting Gastric Colonization and its Pathogenicity. *Toxins*. 19 nov 2019;11(11):677.

34. Argent RH, Thomas RJ, Letley DP, Rittig MG, Hardie KR, Atherton JC. Functional association between the *Helicobacter pylori* virulence factors VacA and CagA. *J Med Microbiol.* 1 févr 2008;57(2):145-50.
35. Atherton JC, Cao P, Peek RM, Tummuru MKR, Blaser MJ, Cover TL. Mosaicism in Vacuolating Cytotoxin Alleles of *Helicobacter pylori*: ASSOCIATION OF SPECIFIC *vacA* TYPES WITH CYTOTOXIN PRODUCTION AND PEPTIC ULCERATION. *J Biol Chem.* 28 juill 1995;270(30):17771-7.
36. Ansari S, Yamaoka Y. Role of vacuolating cytotoxin A in *Helicobacter pylori* infection and its impact on gastric pathogenesis. *Expert Rev Anti Infect Ther* [Internet]. 14 juin 2020 [cité 18 juin 2020]; Disponible sur: <https://www.tandfonline.com/doi/full/10.1080/14787210.2020.1782739>
37. Kao CY, Sheu BS, Wu JJ. *Helicobacter pylori* infection: An overview of bacterial virulence factors and pathogenesis. *Biomed J.* févr 2016;39(1):14-23.
38. Li H, Liao T, Debowski AW, Tang H, Nilsson HO, Stubbs KA, et al. Lipopolysaccharide Structure and Biosynthesis in *Helicobacter pylori*. *Helicobacter.* déc 2016;21(6):445-61.
39. Slomiany BL, Slomiany A. Role of LPS-elicited signaling in triggering gastric mucosal inflammatory responses to *H. pylori*: modulatory effect of ghrelin. *Inflammopharmacology.* août 2017;25(4):415-29.
40. Almorish MA, Al-Absi B, Elkhalifa AME, Elamin E, Elderdery AY, Alhamidi AH. ABO, Lewis blood group systems and secretory status with *H.pylori* infection in yemeni dyspeptic patients: a cross- sectional study. *BMC Infect Dis.* 8 août 2023;23(1):520.
41. Wang G, Ge Z, Rasko DA, Taylor DE. Lewis antigens in *Helicobacter pylori*: biosynthesis and phase variation. *Mol Microbiol.* juin 2000;36(6):1187-96.
42. Monteiro MA, Chan KH, Rasko DA, Taylor DE, Zheng PY, Appelmelk BJ, et al. Simultaneous expression of type 1 and type 2 Lewis blood group antigens by *Helicobacter pylori* lipopolysaccharides. Molecular mimicry between *h. pylori* lipopolysaccharides and human gastric epithelial cell surface glycoforms. *J Biol Chem.* 8 mai 1998;273(19):11533-43.
43. Silva LM, Correia VG, Moreira ASP, Domingues MRM, Ferreira RM, Figueiredo C, et al. *Helicobacter pylori* lipopolysaccharide structural domains and their recognition by immune proteins revealed with carbohydrate microarrays. *Carbohydr Polym.* 1 févr 2021;253:117350.
44. Christie PJ, Gomez Valero L, Buchrieser C. Biological Diversity and Evolution of Type IV Secretion Systems. In: Backert S, Grohmann E, éditeurs. *Type IV Secretion in Gram-Negative and Gram-Positive Bacteria* [Internet]. Cham: Springer International Publishing; 2017 [cité 13

avr 2023]. p. 1-30. (Current Topics in Microbiology and Immunology; vol. 413). Disponible sur: http://link.springer.com/10.1007/978-3-319-75241-9_1

45. Binns AN, Thomashow MF. Cell Biology of Agrobacterium Infection and Transformation of Plants. *Annu Rev Microbiol.* oct 1988;42(1):575-606.
46. Sheedlo MJ, Ohi MD, Lacy DB, Cover TL. Molecular architecture of bacterial type IV secretion systems. *Dehio C, éditeur. PLOS Pathog.* 11 août 2022;18(8):e1010720.
47. Tegtmeyer N, Wessler S, Necchi V, Rohde M, Harrer A, Rau TT, et al. *Helicobacter pylori* Employs a Unique Basolateral Type IV Secretion Mechanism for CagA Delivery. *Cell Host Microbe.* oct 2017;22(4):552-560.e5.
48. Cover TL, Lacy DB, Ohi MD. The *Helicobacter pylori* Cag Type IV Secretion System. *Trends Microbiol* [Internet]. mars 2020 [cité 18 juin 2020]; Disponible sur: <https://linkinghub.elsevier.com/retrieve/pii/S0966842X20300408>
49. Chen D, Li C, Zhao Y, Zhou J, Wang Q, Xie Y. Bioinformatics analysis for the identification of differentially expressed genes and related signaling pathways in *H. pylori*- CagA transfected gastric cancer cells. *PeerJ.* 15 avr 2021;9:e11203.
50. Doohan D, Miftahussurur M, Matsuo Y, Kido Y, Akada J, Matsuhisa T, et al. Characterization of a novel *Helicobacter pylori* East Asian-type CagA ELISA for detecting patients infected with various cagA genotypes. *Med Microbiol Immunol (Berl)* [Internet]. 23 sept 2019 [cité 28 oct 2019]; Disponible sur: <http://link.springer.com/10.1007/s00430-019-00634-5>
51. Li N, Feng Y, Hu Y, He C, Xie C, Ouyang Y, et al. *Helicobacter pylori* CagA promotes epithelial mesenchymal transition in gastric carcinogenesis via triggering oncogenic YAP pathway. *J Exp Clin Cancer Res* [Internet]. déc 2018 [cité 26 nov 2018];37(1). Disponible sur: <https://jeccr.biomedcentral.com/articles/10.1186/s13046-018-0962-5>
52. Hatakeyama M. *Helicobacter pylori* CagA and Gastric Cancer: A Paradigm for Hit-and-Run Carcinogenesis. *Cell Host Microbe.* mars 2014;15(3):306-16.
53. Jiménez-Soto LF, Haas R. The CagA toxin of *Helicobacter pylori*: abundant production but relatively low amount translocated. *Sci Rep.* sept 2016;6(1):23227.
54. Dangtakot R, Intuyod K, Chamgramol Y, Pairojkul C, Pinlaor S, Jantawong C, et al. CagA + *Helicobacter pylori* infection and N -nitrosodimethylamine administration induce cholangiocarcinoma development in hamsters. *Helicobacter* [Internet]. 24 mai 2021 [cité 23 juin 2021]; Disponible sur: <https://onlinelibrary.wiley.com/doi/10.1111/hel.12817>

55. Tohidpour A, Gorrell RJ, Roujeinikova A, Kwok T. The Middle Fragment of *Helicobacter pylori* CagA Induces Actin Rearrangement and Triggers Its Own Uptake into Gastric Epithelial Cells. *Toxins*. 28 juill 2017;9(8):237.
56. Chang CC, Kuo WS, Chen YC, Perng CL, Lin HJ, Ou YH. Fragmentation of CagA Reduces Hummingbird Phenotype Induction by *Helicobacter pylori*. *PloS One*. 2016;11(3):e0150061.
57. Krause S, Bárcena M, Pansegrau W, Lurz R, Carazo JM, Lanka E. Sequence-related protein export NTPases encoded by the conjugative transfer region of RP4 and by the *cag* pathogenicity island of *Helicobacter pylori* share similar hexameric ring structures. *Proc Natl Acad Sci*. 28 mars 2000;97(7):3067-72.
58. Savvides SN. VirB11 ATPases are dynamic hexameric assemblies: new insights into bacterial type IV secretion. *EMBO J*. 1 mai 2003;22(9):1969-80.
59. Yeo HJ, Savvides SN, Herr AB, Lanka E, Waksman G. Crystal Structure of the Hexameric Traffic ATPase of the *Helicobacter pylori* Type IV Secretion System. *Mol Cell*. déc 2000;6(6):1461-72.
60. Hare S, Fischer W, Williams R, Terradot L, Bayliss R, Haas R, et al. Identification, structure and mode of action of a new regulator of the *Helicobacter pylori* HP0525 ATPase. *EMBO J*. 28 nov 2007;26(23):4926-34.
61. Duan M, Li Y, Liu J, Zhang W, Dong Y, Han Z, et al. Transmission routes and patterns of *helicobacter pylori*. *Helicobacter* [Internet]. févr 2023 [cité 14 févr 2023];28(1). Disponible sur: <https://onlinelibrary.wiley.com/doi/10.1111/hel.12945>
62. Harris RB, Oren E, Bui D, Brown HE. Serologic Evidence for Fecal–Oral Transmission of *Helicobacter pylori*. *Am J Trop Med Hyg*. 6 janv 2016;94(1):82-8.
63. Hooi JKY, Lai WY, Ng WK, Suen MMY, Underwood FE, Tanyingoh D, et al. Global Prevalence of *Helicobacter pylori* Infection: Systematic Review and Meta-Analysis. *Gastroenterology*. août 2017;153(2):420-9.
64. Covacci A, Telford JL, Giudice GD, Parsonnet J, Rappuoli R. *Helicobacter pylori* Virulence and Genetic Geography. *Science*. 21 mai 1999;284(5418):1328-33.
65. Ren S, Cai P, Liu Y, Wang T, Zhang Y, Li Q, et al. Prevalence of *HELICOBACTER PYLORI* infection in China: A systematic review and meta-analysis. *J Gastroenterol Hepatol*. mars 2022;37(3):464-70.
66. Maixner F, Krause-Kyora B, Turaev D, Herbig A, Hoopmann MR, Hallows JL, et al. The 5300-year-old *Helicobacter pylori* genome of the Iceman. *Science*. 8 janv 2016;351(6269):162-5.

67. Shah SC, McKinley M, Gupta S, Peek RM, Martinez ME, Gomez SL. Population-Based Analysis of Differences in Gastric Cancer Incidence Among Races and Ethnicities in Individuals Age 50 Years and Older. *Gastroenterology*. nov 2020;159(5):1705-1714.e2.
68. Jackson LK, Potter B, Schneider S, Fitzgibbon M, Blair K, Farah H, et al. *Helicobacter pylori* diversification during chronic infection within a single host generates sub-populations with distinct phenotypes. *Blanke SR, éditeur. PLOS Pathog*. 28 déc 2020;16(12):e1008686.
69. Rodriguez AM, Urrea DA, Prada CF. *Helicobacter pylori* virulence factors: relationship between genetic variability and phylogeographic origin. *PeerJ*. 26 nov 2021;9:e12272.
70. Moodley Y, Brunelli A, Ghirotto S, Klyubin A, Maady AS, Tyne W, et al. *Helicobacter pylori* 's historical journey through Siberia and the Americas. *Proc Natl Acad Sci*. 22 juin 2021;118(25):e2015523118.
71. Mannion A, Dzink-Fox J, Shen Z, Piazuolo MB, Wilson Keith T, Correa P, et al. *Helicobacter pylori* antimicrobial resistance and gene variants in high and low gastric cancer risk populations. *J Clin Microbiol*. 10 mars 2021;JCM.03203-20, jcm;JCM.03203-20v1.
72. Reshetnyak VI, Burmistrov AI, Maev IV. *Helicobacter pylori* : Commensal, symbiont or pathogen? *World J Gastroenterol*. 21 févr 2021;27(7):545-60.
73. Noelia FY, Rusman F, Diosque P, Tomasini N. Genome data vs MLST for exploring intraspecific evolutionary history in bacteria: Much is not always better. *Infect Genet Evol*. juill 2021;104990.
74. Martin-Nuñez GM, Cornejo-Pareja I, Clemente-Postigo M, Tinahones FJ. Gut Microbiota: The Missing Link Between *Helicobacter pylori* Infection and Metabolic Disorders? *Front Endocrinol*. 17 juin 2021;12:639856.
75. Sorini C, Tripathi KP, Wu S, Higdon SM, Wang J, Cheng L, et al. Metagenomic and single-cell RNA-Seq survey of the *Helicobacter pylori*-infected stomach in asymptomatic individuals. *JCI Insight*. 22 févr 2023;8(4):e161042.
76. Wang Z, Shao SL, Xu XH, Zhao X, Wang MY, Chen A, et al. *Helicobacter pylori* and gastric microbiota homeostasis: progress and prospects. *Future Microbiol*. 23 janv 2023;fmb-2022-0102.
77. Guo Y, Cao XS, Zhou MG, Yu B. Gastric microbiota in gastric cancer: Different roles of *Helicobacter pylori* and other microbes. *Front Cell Infect Microbiol*. 10 janv 2023;12:1105811.
78. Francisco AJ. *Helicobacter Pylori* Infection Induces Intestinal Dysbiosis That Could Be Related to the Onset of Atherosclerosis. *Bayliak M, éditeur. BioMed Res Int*. 22 oct 2022;2022:1-16.

79. Nikitina D, Lehr K, Vilchez-Vargas R, Jonaitis LV, Urba M, Kupcinskas J, et al. Comparison of genomic and transcriptional microbiome analysis in gastric cancer patients and healthy individuals. *World J Gastroenterol*. 21 févr 2023;29(7):1202-18.
80. Bik EM, Eckburg PB, Gill SR, Nelson KE, Purdom EA, Francois F, et al. Molecular analysis of the bacterial microbiota in the human stomach. *Proc Natl Acad Sci*. 17 janv 2006;103(3):732-7.
81. Chattopadhyay I, Gundamaraju R, Rajeev A. Diversification and deleterious role of microbiome in gastric cancer. *Cancer Rep Hoboken NJ*. nov 2023;6(11):e1878.
82. PubChem. Tetracycline [Internet]. [cité 11 avr 2023]. Disponible sur: <https://pubchem.ncbi.nlm.nih.gov/compound/54675776>
83. PubChem. Metronidazole [Internet]. [cité 5 avr 2023]. Disponible sur: <https://pubchem.ncbi.nlm.nih.gov/compound/4173>
84. PubChem. Clarithromycin [Internet]. [cité 11 avr 2023]. Disponible sur: <https://pubchem.ncbi.nlm.nih.gov/compound/84029>
85. PubChem. Amoxicillin [Internet]. [cité 11 avr 2023]. Disponible sur: <https://pubchem.ncbi.nlm.nih.gov/compound/33613>
86. Sherman P, Hassall E, Hunt R, Fallone C, Veldhuyzen van Zanten S, Thomson A, et al. Canadian *Helicobacter* Study Group Consensus Conference on the Approach to *Helicobacter Pylori* Infection in Children and Adolescents. *Can J Gastroenterol*. 1999;13(7):553-9.
87. Katelaris P, Hunt R, Bazzoli F, Cohen H, Fock KM, Gemilyan M, et al. *Helicobacter pylori* World Gastroenterology Organization Global Guideline. *J Clin Gastroenterol*. févr 2023;57(2):111-26.
88. Aumpan N, Mahachai V, Vilaichone R. Management of *Helicobacter pylori* infection. *JGH Open*. janv 2023;7(1):3-15.
89. Qian HS, Li WJ, Dang YN, Li LR, Xu XB, Yuan L, et al. Ten-Day Vonoprazan-Amoxicillin Dual Therapy as a First-Line Treatment of *Helicobacter pylori* Infection Compared With Bismuth-Containing Quadruple Therapy. *Am J Gastroenterol* [Internet]. 2 déc 2022 [cité 14 févr 2023]; Publish Ahead of Print. Disponible sur: <https://journals.lww.com/10.14309/ajg.0000000000002086>
90. Dore MP, Lu H, Graham DY. Role of bismuth in improving *Helicobacter pylori* eradication with triple therapy. *Gut*. mai 2016;65(5):870-8.

91. Versalovic J. Point mutations in the 23S rRNA gene of *Helicobacter pylori* associated with different levels of clarithromycin resistance. *J Antimicrob Chemother.* 1 août 1997;40(2):283-6.
92. Smiley R, Bailey J, Sethuraman M, Posecion N, Showkat Ali M. Comparative proteomics analysis of sarcosine insoluble outer membrane proteins from clarithromycin resistant and sensitive strains of *Helicobacter pylori*. *J Microbiol.* oct 2013;51(5):612-8.
93. Hirata K, Suzuki H, Nishizawa T, Tsugawa H, Muraoka H, Saito Y, et al. Contribution of efflux pumps to clarithromycin resistance in *Helicobacter pylori*: Efflux pumps and CLR resistance in *H. pylori*. *J Gastroenterol Hepatol.* mai 2010;25:S75-9.
94. Fontana C, Favaro M, Minelli S, Criscuolo AA, Pietroiusti A, Galante A, et al. New Site of Modification of 23S rRNA Associated with Clarithromycin Resistance of *Helicobacter pylori* Clinical Isolates. *Antimicrob Agents Chemother.* déc 2002;46(12):3765-9.
95. Gerrits MM, van Vliet AH, Kuipers EJ, Kusters JG. *Helicobacter pylori* and antimicrobial resistance: molecular mechanisms and clinical implications. *Lancet Infect Dis.* nov 2006;6(11):699-709.
96. Poole K. Resistance to β -lactam antibiotics. *Cell Mol Life Sci* [Internet]. août 2004 [cité 4 mai 2023];61(17). Disponible sur: <http://link.springer.com/10.1007/s00018-004-4060-9>
97. Van Zwet A, Vandenbrouke-Grauls C, Thijs J, Van Der Wouden E, Gerrits M, Kusters J. Stable amoxicillin resistance in *Helicobacter pylori*. *The Lancet.* nov 1998;352(9140):1595.
98. Zhang S, Wang X, Wise MJ, He Y, Chen H, Liu A, et al. Mutations of *Helicobacter pylori* RdxA are mainly related to the phylogenetic origin of the strain and not to metronidazole resistance. *J Antimicrob Chemother.* 1 nov 2020;75(11):3152-5.
99. Gong Y, Zhai K, Sun L, He L, Wang H, Guo Y, et al. RdxA Diversity and Mutations Associated with Metronidazole Resistance of *Helicobacter pylori*. Zhou X, éditeur. *Microbiol Spectr.* 21 mars 2023;e03903-22.
100. Jenks PJ, Ferrero RL, Labigne A. The role of the rdxA gene in the evolution of metronidazole resistance in *Helicobacter pylori*. *J Antimicrob Chemother.* juin 1999;43(6):753-8.
101. Dingsdag SA, Hunter N. Metronidazole: an update on metabolism, structure–cytotoxicity and resistance mechanisms. *J Antimicrob Chemother.* 1 févr 2018;73(2):265-79.
102. Attaran B, Falsafi T, Ghorbanmehr N. Effect of biofilm formation by clinical isolates of *Helicobacter pylori* on the efflux-mediated resistance to commonly used antibiotics. *World J Gastroenterol.* 2017;23(7):1163.

103. Chopra I, Roberts M. Tetracycline Antibiotics: Mode of Action, Applications, Molecular Biology, and Epidemiology of Bacterial Resistance. *Microbiol Mol Biol Rev.* juin 2001;65(2):232-60.
104. Nishizawa T, Suzuki H. Mechanisms of *Helicobacter pylori* antibiotic resistance and molecular testing. *Front Mol Biosci* [Internet]. 24 oct 2014 [cité 24 mai 2023];1. Disponible sur: <http://journal.frontiersin.org/article/10.3389/fmolb.2014.00019/abstract>
105. Wu JY, Kim JJ, Reddy R, Wang WM, Graham DY, Kwon DH. Tetracycline-Resistant Clinical *Helicobacter pylori* Isolates with and without Mutations in 16S rRNA-Encoding Genes. *Antimicrob Agents Chemother.* févr 2005;49(2):578-83.
106. Trieber CA, Taylor DE. Mutations in the 16S rRNA Genes of *Helicobacter pylori* Mediate Resistance to Tetracycline. *J Bacteriol.* 15 avr 2002;184(8):2131-40.
107. Heep M, Rieger U, Beck D, Lehn N. Mutations in the Beginning of the *rpoB* Gene Can Induce Resistance to Rifamycins in both *Helicobacter pylori* and *Mycobacterium tuberculosis*. *Antimicrob Agents Chemother.* avr 2000;44(4):1075-7.
108. Zhao J, Zou Y, Li K, Huang X, Niu C, Wang Z, et al. Doxycycline and minocycline in *Helicobacter pylori* treatment: A systematic review and meta-analysis. *Helicobacter* [Internet]. oct 2021 [cité 24 mai 2023];26(5). Disponible sur: <https://onlinelibrary.wiley.com/doi/10.1111/hel.12839>
109. Shao Y, Lin Y, Wang B, Miao M, Ye G. Antibiotic resistance status of *helicobacter pylori* strains isolated from initial eradication patients in Ningbo, China, from 2017 to 2021. *Helicobacter* [Internet]. oct 2022 [cité 24 mai 2023];27(5). Disponible sur: <https://onlinelibrary.wiley.com/doi/10.1111/hel.12920>
110. Shao Y, Lu R, Yang Y, Xu Q, Wang B, Ye G. Antibiotic resistance of *Helicobacter pylori* to 16 antibiotics in clinical patients. *J Clin Lab Anal.* mai 2018;32(4):e22339.
111. Yang YJ, Sheu BS. Metabolic Interaction of *Helicobacter pylori* Infection and Gut Microbiota. *Microorganisms.* 16 févr 2016;4(1):15.
112. Thung I, Aramin H, Vavinskaya V, Gupta S, Park JY, Crowe SE, et al. Review article: the global emergence of *Helicobacter pylori* antibiotic resistance. *Aliment Pharmacol Ther.* févr 2016;43(4):514-33.
113. Tshibangu-Kabamba E, Yamaoka Y. *Helicobacter pylori* infection and antibiotic resistance — from biology to clinical implications. *Nat Rev Gastroenterol Hepatol* [Internet]. 17 mai 2021 [cité 25 mai 2021]; Disponible sur: <http://www.nature.com/articles/s41575-021-00449-x>

114. Shi X, Wang C, Meng F, Ma S, Xu G, Liu T, et al. Impact of insufficient doses of medications on *Helicobacter pylori* eradication: a retrospective observational study. *Postgrad Med*. 26 juill 2022;1-7.
115. Smeets LC, Kusters JG. Natural transformation in *Helicobacter pylori*: DNA transport in an unexpected way. *Trends Microbiol*. avr 2002;10(4):159-62.
116. Fernandez-Gonzalez E, Backert S. DNA transfer in the gastric pathogen *Helicobacter pylori*. *J Gastroenterol*. avr 2014;49(4):594-604.
117. Damke PP, Di Guilmi AM, Fernández Varela P, Velours C, Marsin S, Veaute X, et al. Identification of the periplasmic DNA receptor for natural transformation of *Helicobacter pylori*. *Nat Commun* [Internet]. déc 2019 [cité 28 nov 2019];10(1). Disponible sur: <http://www.nature.com/articles/s41467-019-13352-6>
118. Waskito LA, Yih-Wu J, Yamaoka Y. The role of integrating conjugative elements in *Helicobacter pylori*: a review. *J Biomed Sci*. déc 2018;25(1):86.
119. Fernandez-Perez S, Velazco G, Lenik JM, Achuo-Egbe Y, Harley J. *Helicobacter pylori* Resistance to Triple Therapy in a Multicultural Population in New York City. *Cureus* [Internet]. 25 nov 2021 [cité 4 févr 2022]; Disponible sur: <https://www.cureus.com/articles/76921-helicobacter-pylori-resistance-to-triple-therapy-in-a-multicultural-population-in-new-york-city>
120. Contreras-Omaña R, Escorcia-Saucedo AE, Velarde-Ruiz Velasco JA. Prevalence and impact of antimicrobial resistance in gastrointestinal infections: A review. *Rev Gastroenterol México Engl Ed*. juin 2021;S2255534X21000633.
121. Argueta EA, Alsamman MA, Moss SF, D'Agata EMC. Impact of antimicrobial resistance rates on eradication of *Helicobacter pylori* in a United States population. *Gastroenterology*. févr 2021;S0016508521004017.
122. Fauzia KA, Tuan VP. Rising resistance: antibiotic choices for *Helicobacter pylori* infection. *Lancet Gastroenterol Hepatol*. 13 nov 2023;S2468-1253(23)00354-0.
123. Moss SF, Shah SC, Tan MC, El-Serag HB. Evolving Concepts in *Helicobacter pylori* Management. *Gastroenterology*. 6 oct 2023;S0016-5085(23)05083-7.
124. Friedrich V, Gerhard M. Vaccination against *Helicobacter pylori* – An approach for cancer prevention? *Mol Aspects Med*. août 2023;92:101183.
125. Zhang Y, Li X, Shan B, Zhang H, Zhao L. Perspectives from recent advances of *Helicobacter pylori* vaccines research. *Helicobacter* [Internet]. déc 2022 [cité 9 janv 2023];27(6). Disponible sur: <https://onlinelibrary.wiley.com/doi/10.1111/hel.12926>

126. Schiller JT, Lowy DR. Prospects for preventing cancer with anti-microbial prophylactic vaccines. *Cell Host Microbe*. janv 2023;31(1):137-40.
127. Dieye Y, Nguer CM, Thiam F, Diouara AAM, Fall C. Recombinant *Helicobacter pylori* Vaccine Delivery Vehicle: A Promising Tool to Treat Infections and Combat Antimicrobial Resistance. *Antibiotics*. 25 nov 2022;11(12):1701.
128. Dos Santos Viana I, Cordeiro Santos ML, Santos Marques H, Lima de Souza Gonçalves V, Bittencourt de Brito B, França da Silva FA, et al. Vaccine development against *Helicobacter pylori*: from ideal antigens to the current landscape. *Expert Rev Vaccines*. 17 juin 2021;14760584.2021.1945450.
129. Fouladi M, Sarhadi S, Tohidkia M, Fahimi F, Samadi N, Sadeghi J, et al. Selection of a fully human single domain antibody specific to *Helicobacter pylori* urease. *Appl Microbiol Biotechnol*. avr 2019;103(8):3407-20.
130. Chaleshtori ZA, Rastegari AA, Nayeri H, Doosti A. Use of immunoinformatics and the simulation approach to identify *Helicobacter pylori* epitopes to design a multi-epitope subunit vaccine for B- and T-cells. *BMC Biotechnol*. 27 sept 2023;23(1):42.
131. Du C, Zhang Z, Qiao W, Jia L, Zhang F, Chang M, et al. Expression and purification of epitope vaccine against four virulence proteins from *Helicobacter pylori* and construction of label-free electrochemical immunosensor. *Biosens Bioelectron*. 15 déc 2023;242:115720.
132. Fujiki J, Schnabl B. Phage therapy: Targeting intestinal bacterial microbiota for the treatment of liver diseases. *JHEP Rep*. déc 2023;5(12):100909.
133. Souza EBD, Pinto AR, Fongaro G. Bacteriophages as Potential Clinical Immune Modulators. *Microorganisms*. 1 sept 2023;11(9):2222.
134. Ferreira R, Sousa C, Gonçalves RFS, Pinheiro AC, Oleastro M, Wagemans J, et al. Characterization and Genomic Analysis of a New Phage Infecting *Helicobacter pylori*. *Int J Mol Sci*. 17 juill 2022;23(14):7885.
135. Muñoz AB, Stepanian J, Trespalacios AA, Vale FF. Bacteriophages of *Helicobacter pylori*. *Front Microbiol*. 12 nov 2020;11:549084.
136. Luo Q, Liu N, Pu S, Zhuang Z, Gong H, Zhang D. A review on the research progress on non-pharmacological therapy of *Helicobacter pylori*. *Front Microbiol*. 17 mars 2023;14:1134254.
137. De Paepe M, Leclerc M, Tinsley CR, Petit MA. Bacteriophages: an underestimated role in human and animal health? *Front Cell Infect Microbiol* [Internet]. 28 mars 2014 [cité 25 avr

2017];4.

Disponible

sur:

<http://journal.frontiersin.org/article/10.3389/fcimb.2014.00039/abstract>

138. Elois MA, Silva R da, Pilati GVT, Rodríguez-Lázaro D, Fongaro G. Bacteriophages as Biotechnological Tools. *Viruses*. 26 janv 2023;15(2):349.
139. Seiler J, Millen A, Romero DA, Magill D, Simdon L. Novel P335-like Phage Resistance Arises from Deletion within Putative Autolysin *yccB* in *Lactococcus lactis*. *Viruses*. 31 oct 2023;15(11):2193.
140. Zhuang Z, Cheng YY, Deng J, Cai Z, Zhong L, Qu JX, et al. Genomic insights into the phage-defense systems of *Stenotrophomonas maltophilia* clinical isolates. *Microbiol Res*. janv 2024;278:127528.
141. Mason G, Footer MJ, Rojas ER. Mechanosensation induces persistent bacterial growth during bacteriophage predation. Weitz JS, éditeur. *mBio*. nov 2023;e02766-22.
142. Kumadoh D, Archer MA, Yeboah GN, Kyene MO, Boakye-Yiadom M, Adi-Dako O, et al. A review on anti-peptic ulcer activities of medicinal plants used in the formulation of Enterica, Dyspepsia and NPK 500 capsules. *Heliyon*. déc 2021;7(12):e08465.
143. Guerra-Valle M, Orellana-Palma P, Petzold G. Plant-Based Polyphenols: Anti-*Helicobacter pylori* Effect and Improvement of Gut Microbiota. *Antioxidants*. 4 janv 2022;11(1):109.
144. Ghobadi E, Ghanbarimasir Z, Emami S. A review on the structures and biological activities of anti-*Helicobacter pylori* agents. *Eur J Med Chem*. nov 2021;223:113669.
145. Yan J, Peng C, Chen P, Zhang W, Jiang C, Sang S, et al. In-vitro anti-*Helicobacter pylori* activity and preliminary mechanism of action of *Canarium album* raeusch. Fruit extracts. *J Ethnopharmacol*. août 2021;114578.
146. Arif M, Sharaf M, Samreen, Khan S, Chi Z, Liu CG. Chitosan-based nanoparticles as delivery-carrier for promising antimicrobial glycolipid biosurfactant to improve the eradication rate of *Helicobacter pylori* biofilm. *J Biomater Sci Polym Ed*. 11 janv 2021;1-19.
147. Shipa SJ, Khandokar L, Bari MdS, Qais N, Rashid MA, Haque MdA, et al. An insight into the anti-ulcerogenic potentials of medicinal herbs and their bioactive metabolites. *J Ethnopharmacol*. juill 2022;293:115245.
148. O’Gara EA, Hill DJ, Maslin DJ. Activities of Garlic Oil, Garlic Powder, and Their Diallyl Constituents against *Helicobacter pylori*. *Appl Environ Microbiol*. mai 2000;66(5):2269-73.

149. Lettl C, Schindele F, Testolin G, Bär A, Rehm T, Brönstrup M, et al. Inhibition of Type IV Secretion Activity and Growth of *Helicobacter pylori* by Cisplatin and Other Platinum Complexes. *Front Cell Infect Microbiol*. 18 déc 2020;10:602958.
150. Khan M, Khan S, Ali A, Akbar H, Sayaf AM, Khan A, et al. Immunoinformatics approaches to explore *Helicobacter Pylori* proteome (Virulence Factors) to design B and T cell multi-epitope subunit vaccine. *Sci Rep* [Internet]. déc 2019 [cité 5 nov 2019];9(1). Disponible sur: <http://www.nature.com/articles/s41598-019-49354-z>
151. Johnson BK, Abramovitch RB. Small Molecules That Sabotage Bacterial Virulence. *Trends Pharmacol Sci*. avr 2017;38(4):339-62.
152. Escaich S. Antivirulence as a new antibacterial approach for chemotherapy. *Curr Opin Chem Biol*. août 2008;12(4):400-8.
153. Hilleringmann M, Pansegrau W, Doyle M, Kaufman S, MacKichan ML, Gianfaldoni C, et al. Inhibitors of *Helicobacter pylori* ATPase Cag α block CagA transport and cag virulence. *Microbiology*. 1 oct 2006;152(10):2919-30.
154. Ménard R, Schoenhofen IC, Tao L, Aubry A, Bouchard P, Reid CW, et al. Small-Molecule Inhibitors of the Pseudaminic Acid Biosynthetic Pathway: Targeting Motility as a Key Bacterial Virulence Factor. *Antimicrob Agents Chemother*. déc 2014;58(12):7430-40.
155. Suerbaum S, Coombs N, Patel L, Pscheniza D, Rox K, Falk C, et al. Identification of Antimotilins, Novel Inhibitors of *Helicobacter pylori* Flagellar Motility That Inhibit Stomach Colonization in a Mouse Model. *Rappuoli R, éditeur. mBio*. 26 avr 2022;13(2):e03755-21.
156. Sabino YNV, Cotter PD, Mantovani HC. Anti-virulence compounds against *Staphylococcus aureus* associated with bovine mastitis: A new therapeutic option? *Microbiol Res*. juin 2023;271:127345.
157. Fabris M, Nascimento-Júnior NM, Bispo MLF, Camargo PG. Computational Strategies Targeting Inhibition of *Helicobacter pylori* and *Cryptococcus neoformans* Ureases. *Curr Pharm Des*. mars 2023;29(10):777-92.
158. Fiori-Duarte AT, de Oliveira Guarnieri JP, de Oliveira Borlot JRP, Lancellotti M, Rodrigues RP, Kitagawa RR, et al. In silico design and in vitro assessment of anti-*Helicobacter pylori* compounds as potential small-molecule arginase inhibitors. *Mol Divers* [Internet]. 8 janv 2022 [cité 3 févr 2022]; Disponible sur: <https://link.springer.com/10.1007/s11030-021-10371-8>
159. Korwar S, Morris BL, Parikh HI, Coover RA, Doughty TW, Love IM, et al. Design, synthesis, and biological evaluation of substrate-competitive inhibitors of C-terminal Binding Protein (CtBP). *Bioorg Med Chem*. juin 2016;24(12):2707-15.

160. O'Connor L, Heyderman R. The challenges of defining the human nasopharyngeal resistome. *Trends Microbiol.* mars 2023;S0966842X23000562.
161. Amangelsin Y, Semenova Y, Dadar M, Aljofan M, Bjørklund G. The Impact of Tetracycline Pollution on the Aquatic Environment and Removal Strategies. *Antibiotics.* 23 févr 2023;12(3):440.
162. Huemer M, Mairpady Shambat S, Brugger SD, Zinkernagel AS. Antibiotic resistance and persistence—Implications for human health and treatment perspectives. *EMBO Rep* [Internet]. 3 déc 2020 [cité 18 avr 2023];21(12). Disponible sur: <https://onlinelibrary.wiley.com/doi/10.15252/embr.202051034>
163. Bengtsson-Palme J, Kristiansson E, Larsson DGJ. Environmental factors influencing the development and spread of antibiotic resistance. *FEMS Microbiol Rev* [Internet]. 1 janv 2018 [cité 18 avr 2023];42(1). Disponible sur: <https://academic.oup.com/femsre/article/doi/10.1093/femsre/fux053/4563583>
164. Yong X, Tang B, Li BS, Xie R, Hu CJ, Luo G, et al. Helicobacter pylori virulence factor CagA promotes tumorigenesis of gastric cancer via multiple signaling pathways. *Cell Commun Signal.* déc 2015;13(1):30.
165. Grossman S, Fishwick CWG, McPhillie MJ. Developments in Non-Intercalating Bacterial Topoisomerase Inhibitors: Allosteric and ATPase Inhibitors of DNA Gyrase and Topoisomerase IV. *Pharmaceuticals.* 8 févr 2023;16(2):261.
166. Mendoza-Hoffmann F, Yang L, Buratto D, Brito-Sánchez J, Garduño-Javier G, Salinas-López E, et al. Inhibitory to non-inhibitory evolution of the ζ subunit of the F1FO-ATPase of *Paracoccus denitrificans* and α -proteobacteria as related to mitochondrial endosymbiosis. *Front Mol Biosci.* 2023;10:1184200.
167. Sayer JR, Walldén K, Koss H, Allan H, Daviter T, Gane PJ, et al. Design, synthesis, and evaluation of peptide-imidazo[1,2-*a*]pyrazine bioconjugates as potential bivalent inhibitors of the VirB11 ATPase HP0525. *J Pept Sci* [Internet]. 17 juin 2021 [cité 23 juin 2021]; Disponible sur: <https://onlinelibrary.wiley.com/doi/10.1002/psc.3353>
168. García-Cazorla Y, Getino M, Sanabria-Ríos DJ, Carballeira NM, de la Cruz F, Arechaga I, et al. Conjugation inhibitors compete with palmitic acid for binding to the conjugative traffic ATPase TrwD, providing a mechanism to inhibit bacterial conjugation. *J Biol Chem.* 26 oct 2018;293(43):16923-30.
169. Hilleringmann M, Pansegrau W, Doyle M, Kaufman S, MacKichan ML, Gianfaldoni C, et al. Inhibitors of Helicobacter pylori ATPase Cag α block CagA transport and cag virulence. *Microbiology.* 1 oct 2006;152(10):2919-30.

170. Shaffer CL, Good JAD, Kumar S, Krishnan KS, Gaddy JA, Loh JT, et al. Peptidomimetic Small Molecules Disrupt Type IV Secretion System Activity in Diverse Bacterial Pathogens. Norris SJ, éditeur. mBio. 4 mai 2016;7(2):e00221-16.
171. Zharova TV, Grivennikova VG, Borisov VB. F1·Fo ATP Synthase/ATPase: Contemporary View on Unidirectional Catalysis. Int J Mol Sci. 12 mars 2023;24(6):5417.
172. Li S, Liu H, Shu J, Li Q, Liu Y, Feng H, et al. Fisetin inhibits *Salmonella* Typhimurium type III secretion system regulator HilD and reduces pathology *in vivo*. Blondel CJ, éditeur. Microbiol Spectr. 11 déc 2023;e02406-23.
173. Booth SC, Smith WPJ, Foster KR. The evolution of short- and long-range weapons for bacterial competition. Nat Ecol Evol. 30 nov 2023;7(12):2080-91.
174. Casu B, Smart J, Hancock MA, Smith M, Sygusch J, Baron C. Structural Analysis and Inhibition of TraE from the pKM101 Type IV Secretion System. J Biol Chem. nov 2016;291(45):23817-29.
175. Cunha LD, Ribeiro JM, Fernandes TD, Massis LM, Khoo CA, Moffatt JH, et al. Inhibition of inflammasome activation by *Coxiella burnetii* type IV secretion system effector IcaA. Nat Commun. 21 déc 2015;6(1):10205.
176. Arya T, Oudouhou F, Casu B, Bessette B, Sygusch J, Baron C. Fragment-based screening identifies inhibitors of ATPase activity and of hexamer formation of Cag α from the *Helicobacter pylori* type IV secretion system. Sci Rep. déc 2019;9(1):6474.
177. Barati T, Haddadi M, Sadeghi F, Muhammadnejad S, Muhammadnejad A, Heidarian R, et al. AGS cell line xenograft tumor as a suitable gastric adenocarcinoma model: growth kinetic characterization and immunohistochemistry analysis. Iran J Basic Med Sci [Internet]. mai 2018 [cité 24 nov 2023];(Online First). Disponible sur: <https://doi.org/10.22038/ijbms.2018.22938.5835>
178. Backert S, Gressmann H, Kwok T, Zimny-Arndt U, König W, Jungblut PR, et al. Gene expression and protein profiling of AGS gastric epithelial cells upon infection with *Helicobacter pylori*. Proteomics. oct 2005;5(15):3902-18.
179. You YH, Song YY, Meng FL, He LH, Zhang MJ, Yan XM, et al. Time-series gene expression profiles in AGS cells stimulated with *Helicobacter pylori*. World J Gastroenterol WJG. 21 mars 2010;16(11):1385-96.
180. Moese S, Selbach M, Kwok T, Brinkmann V, König W, Meyer TF, et al. *Helicobacter pylori* Induces AGS Cell Motility and Elongation via Independent Signaling Pathways. Infect Immun. juin 2004;72(6):3646-9.

181. Jang S, Hansen LM, Su H, Solnick JV, Cha JH. Host immune response mediates changes in *cagA* copy number and virulence potential of *Helicobacter pylori*. *Gut Microbes*. 31 déc 2022;14(1):2044721.
182. Hutchings MI, Truman AW, Wilkinson B. Antibiotics: past, present and future. *Curr Opin Microbiol*. oct 2019;51:72-80.
183. O'Connor A, Liou J, Gisbert JP, O'Morain C. Review: Treatment of *Helicobacter pylori* Infection 2019. *Helicobacter* [Internet]. sept 2019 [cité 28 oct 2019];24(S1). Disponible sur: <https://onlinelibrary.wiley.com/doi/abs/10.1111/hel.12640>
184. Rossi CC, Pereira MF, Giambiagi-deMarval M. Underrated Staphylococcus species and their role in antimicrobial resistance spreading. *Genet Mol Biol* [Internet]. 2020 [cité 18 févr 2020];43(1 suppl 2). Disponible sur: http://www.scielo.br/scielo.php?script=sci_arttext&pid=S1415-47572020000300303&tlng=en
185. Schmitz FJ, Fluit AC, Gondolf M, Beyrau R, Lindenlauf E, Verhoef J, et al. The prevalence of aminoglycoside resistance and corresponding resistance genes in clinical isolates of staphylococci from 19 European hospitals. *J Antimicrob Chemother*. 2 janv 1999;43(2):253-9.
186. World Health Organization. Global action plan on antimicrobial resistance [Internet]. Geneva: World Health Organization; 2015 [cité 22 avr 2023]. 28 p. Disponible sur: <https://apps.who.int/iris/handle/10665/193736>
187. Pinzi L, Rastelli G. Molecular Docking: Shifting Paradigms in Drug Discovery. *Int J Mol Sci*. 4 sept 2019;20(18):4331.
188. Waskito LA, Yamaoka Y. The Story of *Helicobacter pylori*: Depicting Human Migrations from the Phylogeography. In: Kamiya S, Backert S, éditeurs. *Helicobacter pylori* in Human Diseases [Internet]. Cham: Springer International Publishing; 2019 [cité 14 févr 2023]. p. 1-16. (Advances in Experimental Medicine and Biology; vol. 1149). Disponible sur: http://link.springer.com/10.1007/5584_2019_356
189. Jiang X, Xu Z, Zhang T, Li Y, Li W, Tan H. Whole-Genome-Based *Helicobacter pylori* Geographic Surveillance: A Visualized and Expandable Webtool. *Front Microbiol*. 2 août 2021;12:687259.
190. Backert S, Blaser MJ. The Role of CagA in the Gastric Biology of *Helicobacter pylori*. *Cancer Res*. 15 juill 2016;76(14):4028-31.
191. Yip KM, Fischer N, Paknia E, Chari A, Stark H. Atomic-resolution protein structure determination by cryo-EM. *Nature*. 5 nov 2020;587(7832):157-61.

192. Tordai H, Leveles I, Hegedűs T. Molecular dynamics of the cryo-EM CFTR structure. *Biochem Biophys Res Commun.* sept 2017;491(4):986-93.
193. Odenbreit S. Translocation of *Helicobacter pylori* CagA into Gastric Epithelial Cells by Type IV Secretion. *Science.* 25 févr 2000;287(5457):1497-500.
194. Lind J, Backert S, Hoffmann R, Eichler J, Yamaoka Y, Perez-Perez GI, et al. Systematic analysis of phosphotyrosine antibodies recognizing single phosphorylated EPIYA-motifs in CagA of East Asian-type *Helicobacter pylori* strains. *BMC Microbiol.* déc 2016;16(1):201.
195. Schindele F, Weiss E, Haas R, Fischer W. Quantitative analysis of CagA type IV secretion by *HELICOBACTER pylori* reveals substrate recognition and translocation requirements. *Mol Microbiol.* avr 2016;100(1):188-203.
196. Hirano S. Western Blot Analysis. In: Reineke J, éditeur. *Nanotoxicity* [Internet]. Totowa, NJ: Humana Press; 2012 [cité 8 déc 2023]. p. 87-97. (Methods in Molecular Biology; vol. 926). Disponible sur: http://link.springer.com/10.1007/978-1-62703-002-1_6
197. Noone J, Wallace RG, Rochfort KD. Immunoprecipitation: Variations, Considerations, and Applications. In: Loughran ST, Milne JJ, éditeurs. *Protein Chromatography* [Internet]. New York, NY: Springer US; 2023 [cité 8 déc 2023]. p. 271-303. (Methods in Molecular Biology; vol. 2699). Disponible sur: https://link.springer.com/10.1007/978-1-0716-3362-5_15
198. de Mesy Bentley KL, Galloway CA, Muthukrishnan G, Echternacht SR, Masters EA, Zeiter S, et al. Emerging Electron Microscopy and 3D Methodologies to Interrogate *Staphylococcus aureus* Osteomyelitis in Murine Models. *J Orthop Res Off Publ Orthop Res Soc.* févr 2021;39(2):376-88.
199. Gulati NM, Torian U, Gallagher JR, Harris AK. Immunoelectron Microscopy of Viral Antigens. *Curr Protoc Microbiol.* juin 2019;53(1):e86.
200. Hammonds J, Wang JJ, Yi H, Spearman P. Immunoelectron Microscopic Evidence for Tetherin/BST2 as the Physical Bridge between HIV-1 Virions and the Plasma Membrane. *PLoS Pathog.* 5 févr 2010;6(2):e1000749.
201. Peddie CJ, Genoud C, Kreshuk A, Meechan K, Micheva KD, Narayan K, et al. Volume electron microscopy. *Nat Rev Methods Primer.* 7 juill 2022;2:51.
202. Lee A, O'Rourke J, De Ungria M, Robertson B, Daskalopoulos G, Dixon M. A standardized mouse model of *Helicobacter pylori* infection: Introducing the Sydney strain. *Gastroenterology.* avr 1997;112(4):1386-97.
203. Ansari S, Yamaoka Y. Animal Models and *Helicobacter pylori* Infection. *J Clin Med.* 31 mai 2022;11(11):3141.

Remerciements

J'aimerais remercier le laboratoire Baron pour m'avoir permise de faire mon doctorat au sein de leur laboratoire et plus particulièrement, Christian Baron, mon superviseur, Flore Oudouhou qui m'a formée pour continuer le projet et Benoit Bessette pour son soutien lors de la prise en main du projet. J'aimerais également remercier Vijay Verma Taylor pour sa collaboration sur la partie in vitro du projet et le laboratoire Nanci pour leur soutien en microscopie électronique. Je voudrais enfin remercier l'université de Montréal et le département de biochimie et médecine moléculaire pour leur accueil.

J'aimerais aussi remercier tous les organismes subventionnaires sans lesquels le projet n'aurait pas pu être réalisé ainsi que tous nos collaborateurs.

En complément, je voudrais remercier mon jury de thèse pour leur participation.

Un spécial merci à Fabienne et Daniel Morin, pour leur soutien tout au long de mes études. Il en est de même pour mes amis et collègues au doctorat Melis, Manjari, Thulaj, Nasrin et Janaina pour leurs soutiens et conseils.

Sources et Permission d'utilisation des figures

A. Figure 1

Les images de microscopie confocale ont été réalisées par Claire Morin au laboratoire Baron.

Les images de microscopie électronique ont été réalisées par Claire Morin au laboratoire Nancy.

B. Figure 3

Citation: Sheedlo MJ, Ohi MD, Lacy DB, Cover TL (2022) Molecular architecture of bacterial type IV secretion systems. PLoS Pathog 18(8): e1010720. https://doi.org/10.1371/journal.ppat.1010720
Editor: Christoph Dehio, University of Basel, SWITZERLAND
Published: August 11, 2022
This is an open access article, free of all copyright, and may be freely reproduced, distributed, transmitted, modified, built upon, or otherwise used by anyone for any lawful purpose. The work is made available under the Creative Commons CC0 public domain dedication.
Funding: This work was supported by NIH AI118932 (TLC, MDO), CA116087 (TLC), AI039657 (TLC), AI164651 (MDO), and the Department of Veterans Affairs (I01BX004447)(TLC). The funders had no role in study design, data collection and analysis, decision to publish, or preparation of the manuscript.
Competing interests: The authors have declared that no competing interests exist.

C. Figure 4

Le schéma de la structure du SST4 a été réalisée par Claire Morin en utilisant le logiciel Biorender (<https://www.biorender.com/>)

La structure de Caga provient de Yeo *et al*, 2001, (<https://doi.org/10.2210/pdb1G6O/pdb>), disponible sur <https://www.wwpdb.org/>.